Diss. ETH NO. 17115

ENZYMATIC CARBON-CARBON BOND FORMATION INTEGRATED WITH SMB SEPARATION

A dissertation submitted to

ETH ZURICH

for the degree of

Doctor of Sciences

presented by

STEFAN KLAUS MAKART
Dipl. Bot. University of Zurich

born 30.12.1973

citizen of Gempen (SO)

accepted on the recommendation of
Prof. Dr. Sven Panke, examiner
Prof. Dr. Marco Mazzotti, co-examiner
Prof. Dr. John M. Woodley, co-examiner

2007

Abstract

Aldolases constitute a class of biotechnologically promising enzymes that can catalyze the stereoselective formation of carbon-carbon bonds. However, their wider application on a process scale has been hampered as they mostly suffer from an unfavorable position of the reaction equilibrium.

Continuous chromatography, realized as simulated moving bed (SMB), has matured into a reliable and frequently used process option in biotechnology and the pharmaceutical industry over the last years. The high resolution power of continuous chromatography should make it well suited for the purification of products from complex reaction mixtures.

The integrated operation of a SMB unit and an enzyme reactor is proposed in this thesis, as this should theoretically enable to obtain 100 % yield from a thermodynamically limited reaction. The product can be continuously removed while the remaining substrates can be recycled.

The formation of L-*allo*-threonine from glycine and acetaldehyde, catalyzed by the serine hydroxymethyltransferase GlyA from *Escherichia coli*, is used as a model reaction to explore this concept of an integrated process. The enzyme can be functionally categorized as a glycine-dependent aldolase, which introduces two new chiral centers in the product. GlyA was produced in fed-batch fermentations of *E. coli* JM101(pESM3), achieving a yield of 120 mg recombinant protein per gram cell dry weight. This high expression level allowed the direct use of cell free extract in an enzyme membrane reactor (EMR) for the continuous production of L-*allo*-threonine. The stability and activity of the enzyme, with regard to the content of organic co-solvent in the reaction medium, was investigated. A kinetic model was proposed and the according kinetic parameters were estimated for purely aqueous and 20 % methanol-containing reaction medium. The experimental data agreed well with the model, which allowed the development of a suitable model for the EMR.

For the chromatographic separation, a suitable stationary phase was identified that is capable of separating the main components of the reaction mixture, the amino acids glycine and threonine. The separation takes place under enzyme-compatible conditions, i.e. in aqueous buffer at neutral pH, with minor content of organic co-solvent. Experimental SMB runs were performed using the selected stationary phase. High purities were achieved, both in the extract and raffinate outlet stream, indicating the overall feasibility for the integrated process concept.

Zusammenfassung

Aldolasen bilden eine Klasse biotechnologisch vielversprechender Enzyme, welche die stereoselektive Bildung von Kohlenstoff-Kohlenstoff Bindungen katalysieren können. Deren weitverbreitete industrielle Anwendung wird jedoch behindert durch eine ungünstige Position des Reaktionsgleichgewichtes.

Kontinuierliche Gegenstromchromatographie, basierend auf Simulated Moving Bed (SMB) Technologie, hat sich in den letzten Jahren zu einem zuverlässigen und häufig genuzten Prozess in der Biotechnologie und der pharmazeutischen Industrie entwickelt. Die hervorragende Trennleistung der kontinuierlichen Gegenstromchromatographie prädestiniert sie für die Trennung komplexer Reaktionsgemische.

In dieser Arbeit wird der integrierte Betrieb einer SMB-Anlage und eines Enzymreaktors vorgeschlagen, da dies theoretisch eine hundertprozentige Ausbeute in einer thermodynamisch limitierten Reaktion erlaubt. Das Produkt kann kontinuierlich abgezogen und die verbleibenden Substrate zurückgeführt werden.

Die Bildung von L-*allo*-Threonin aus Glycin und Acetaldehyd, katalysiert durch GlyA, einer Serin-Hydroxymethyltransferase aus *Escherichia coli*, wurde als Modellreaktion ausgewählt zur Untersuchung diese Konzepts des integrierten Prozesses. Funktionell kann das Enzym als eine Glycin-abhängige Aldolase bezeichnet werden, welche im Produkt zwei neue chirale Zentren einführt. GlyA wurde in gefütterten Satzkulturen von *E. coli* JM101(pESM3) produziert, wobei eine Ausbeute von 120 mg rekombinantem Protein pro Gramm Zelltrockenmasse erreicht wurde. Dieses hohe Niveau der Überexprimierung erlaubte den direkten Gebrauch des zellfreien Extrakts in einem Enzym-Membranreaktor (EMR) zur kontinuierlichen Produktion von L-*allo*-Threonin. Die Stabilität und Aktivität des Enzyms wurde untersucht in Bezug auf den Gehalt an organischem Lösungsmittel im Reaktionsmedium. Ein Modell für die Kinetik wurde aufgestellt und die entsprechenden Parameter dazu wurden bestimmt, sowohl für rein wässriges als auch 20 % Methanol enthaltendes Reaktionsmedium. Die gute Übereinstimmung der experimentellen Daten mit den Modelldaten ermöglichte die Erstellung eines Modells für den EMR.

Eine stationäre Phase konnte gefunden werden, welche für die Trennung der Hauptkomponenten des Reaktionsgemischs, den Aminosäuren Glycin und Threonin, geeignet ist. Die Trennung erfolgt unter enzymkompatiblen Bedingungen, d.h. in gepufferter Lösung bei neutralem pH mit einem geringen Anteil organischen Lösungsmittels. Mit der ausgesuchten stationären Phase wurden experimentelle SMB-Versuche durchgeführt. Die

hohen Reinheiten, welche sowohl im Extrakt als auch im Raffinat erreicht werden konnten, deuten auf die Durchführbarkeit des integrierten Prozesses hin.

Table of Contents

1 Introduction

1.1 General introduction

Biotransformation is today a widely accepted technique in the pharmaceutical and fine chemical industry, for example in the production of drug intermediates [145]. Biocatalysis also receives attention in the development of sustainable technologies for bulk chemicals in the chemical industry. The frequently encountered chemo- and regioselectivites of enzymes as well as high stereoselectivities leading to enantiopure products are attractive features of biotransformation [147]. Product examples range from amino acids, carbohydrates, steroids to bulk chemicals like acrylamide [95; 161]. On the other hand, the widespread application of biotransformation is still hampered by several limitations such as the availability of the biocatalyst, a frequently narrow substrate spectrum, and a limited process stability [147]. Furthermore, many promising applications suffer from product inhibition or an unfavorable position of the reaction equilibrium, which is the topic of this thesis.

1.2 Chirality

A molecule is called chiral when it is not superimposable on its mirror-image [150]. Typically, a carbon atom that is attached to four different groups is the stereogenic center of the molecule. The two existing mirror image forms of such a molecule are called enantiomers and they exhibit essentially identical physical properties, with the exception of the rotation of polarized light. Molecules containing n stereogenic center can exist in up to 2^n different stereomeric forms. The stereoisomers that are not mirror-images of each other are called diastereomers, their physical properties differ from each other [150]. The topic in this work is the diastereospecific production of L-*allo*-threonine, one of the four stereoisomers of threonine (Fig. 1.1).

Due to their different three-dimensional configuration, enantiomers can differ in their chemical and hence in their biological activity, which led to new guidelines for the production of pharmaceutical drugs promoting the use of chiral drug molecules in enantiopure form [45]. Hence, the production of single stereoisomers gained increasing attention in the pharmaceutical industry. Some of the motives to produce optically pure materials are: (i) biological activity may be associated to only one enantiomer; (ii) enantiomers can have very

different activities of which one may be unwanted; (iii) improved cost-efficacy; (iv) improved activity of the pure enantiomer over the racemate due to antagonism [34].

There are mainly two production routes to enantiomerically pure products: (i) kinetic and dynamic kinetic resolution and (ii) asymmetric synthesis.

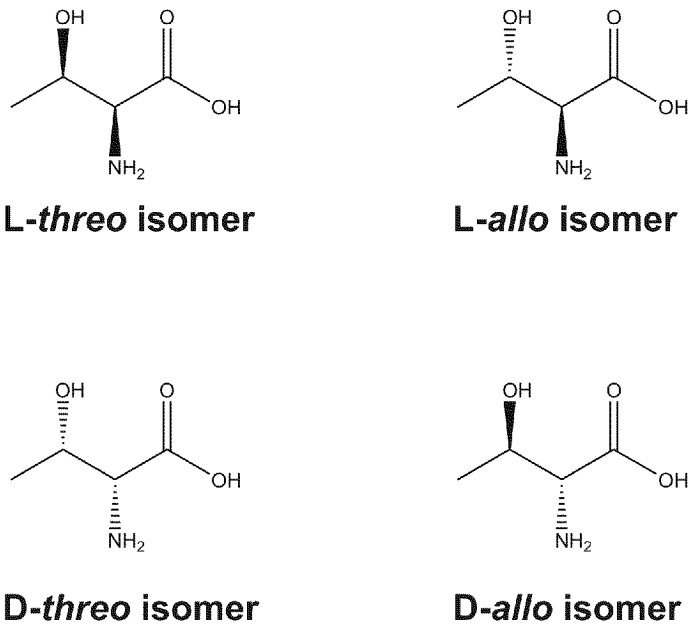

Fig. 1.1: The four stereoisomers of threonine. L-*threo* and D-*threo*, as well as L-*allo* and D-*allo* threonine form pairs of enantiomers; whereas L-*threo* and L-*allo*, respectively D-*threo* and D-*allo* threonine form pairs of diastereomers.

1.3 Asymmetric carbon-carbon bond formation

The stereoselective formation of carbon-carbon bonds is a key topic in today's synthetic organic chemistry [147]. The aldol reaction, the addition of an enolate donor to a carbonyl acceptor, has attracted much attention, as it is one of the most powerful tools in organic chemistry [106]. Chemical synthesis routes, which mimic biochemical methods and broaden the substrate acceptance, represent an extended area of research [106]. Enzymes applied in biocatalytic C-C bond forming reactions are aldolases, transaldolases, transketolases [17] and hydroxynitrile lyases [42](Fig. 1.2).

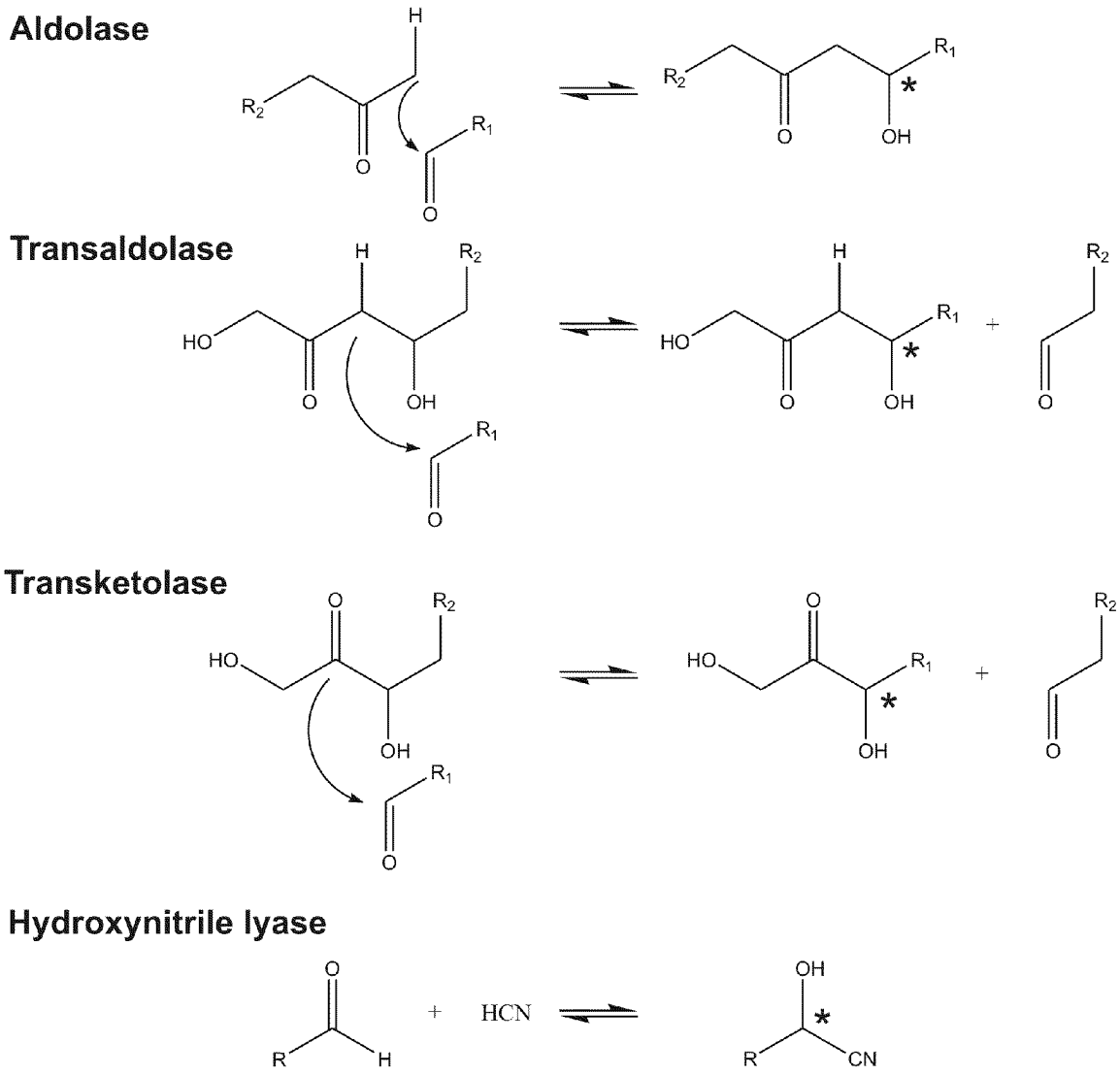

Figure 1.2: Enzymes frequently used for carbon-carbon coupling, the newly formed stereogenic centers are marked by asterisks (Adapted from [17; 42]).

A major advantage of C-C bond formation using aldolases over the chemical methods is the possibility to work without the need of protection groups. Consequently, aldolases are already applied on industrial scale [96; 128]. Aldolases can be ordered in groups according to their natural donor substrates (Fig. 1.3). The capability of aldolases to accept a broad spectrum of unnatural acceptor substrates makes them particularly interesting for asymmetric synthesis. On the other hand, many of the attractive reactions for synthetic purposes suffer from an

unfavorable position of the thermodynamic equilibrium, leading to incomplete use of the substrates. A further difficulty in aldolase catalyzed reactions is the similarity of substrate and product, complicating the downstream processing. The application of *in situ* product removal techniques [105] could limit the aforementioned problems in aldolase processes. In this thesis, the integration of continuous chromatography, as an on line product recovery tool, with the enzymatic reaction is proposed.

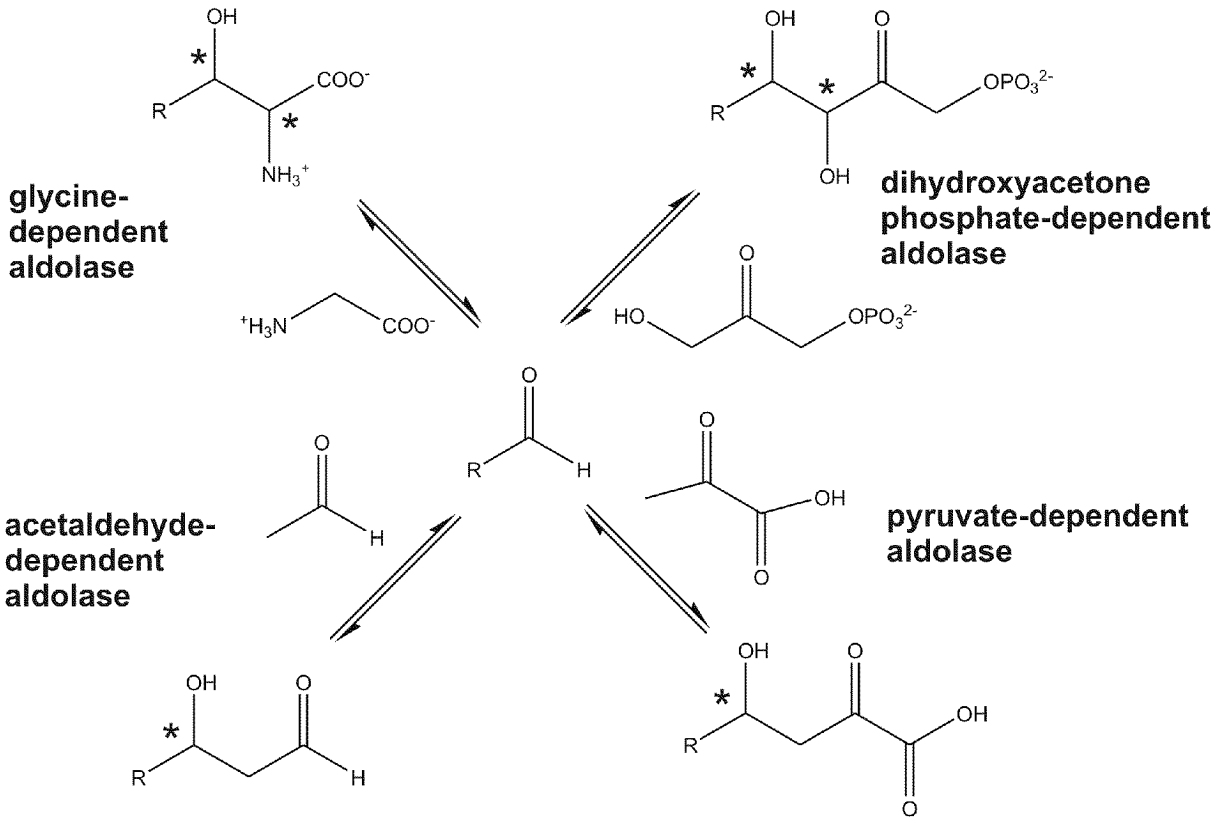

Fig. 1.3: The four main groups of aldolases, classified according to their natural donor substrate, the newly formed stereogenic centers are marked by asterisks (adapted from [155]).

1.4 Continuous chromatography

Chromatography is widely used as analytical and preparative tool. Continuous chromatography has been used in the oil and sugar industry over the last 3 decades and is nowadays gaining more and more attraction in the pharmaceutical and fine chemical industry. The concept of continuous chromatography is mostly realized as simulated moving bed (SMB). This technology allows the efficient separation of biotechnological products in the downstream processing [149].

1.5 The scope of this thesis

The enzyme GlyA, a serine hydroxymethyltransferase from *Escherichia coli*, is investigated regarding the formation of L-*allo*-threonine from the substrates glycine and acetaldehyde. The enzyme can functionally be described as a glycine-dependent aldolase. The discussed aldolase catalyzed reaction displays all characteristics for biotransformations as mentioned previously: the diastereoselective C-C bond formation leads to β-hydroxy-α-amino acids of considerable interest as precursors for more complex molecules in the pharmaceutical industry, but the reaction suffers from thermodynamic limitation. In addition, the excellent diastereoselectivity of the reaction is kinetically controlled, which means that the formation of a product mix of high diastereomeric excess is favored at the beginning of the reaction, but towards long reaction times, the reaction moves towards the thermodynamically determined and less favorable diastereomeric excess. This adds a further incentive to quickly remove the product from the reaction mixture and to maintain the reaction conditions for kinetic control. The integration with a simulated moving bed to continuously remove the product and return the remaining substrate should theoretically drive the reaction to completion.

Chapter 2 discusses the advantages of the integration of biotransformation and continuous chromatography. Different strategies to achieve the integration will be explored. The constraints that have to be taken into account and some general guidelines for the design of integrated processes are described.

Chapter 3 addresses the availability of the biocatalyst and describes the recombinant overproduction of the aldolase in fed-batch fermentations applying the AlkS/P_{alkB}-expression system.

In chapter 4, the enzyme kinetics of the aldolase are described, with respect to the integration with continuous chromatography. The enzyme was used for the continuous production of L-*allo*-threonine in an enzyme membrane reactor.
Chapter 5 describes the implementation of a SMB separation for glycine and threonine under conditions suitable for the integrated process.
Chapter 6 presents a summary and presents an outlook, discussing the further steps for the technical realization of the integrated process at lab-scale.

Chapters 2 to 5 can be treated as independent studies and contain therefore the corresponding introduction and conclusions.

2 Integrated operation of continuous chromatography and biotransformations for the generic high yield production of fine chemicals

Stefan Makart*, Matthias Bechtold*, Matthias Heinemann, Sven Panke

* The authors contributed equally to this work.

SM contributed chapters 2.1, 2.3.2, 2.3.3 and 2.4.1

also published in J Biotechnol 124:146-162 (2006)

Abstract

The rapid progress in biocatalysis in the identification and development of enzymes over the last decade has enormously enlarged the chemical reaction space that can be addressed not only in research applications, but also on industrial scale. This enables us to consider even those groups of reactions that are very promising from a synthetic point of view, but suffer from drawbacks on process level, such as an unfavourable position of the reaction equilibrium. Prominent examples stem from the aldolase-catalyzed enantioselective carbon-carbon bond forming reactions, reactions catalyzed by isomerising enzymes, and reactions that are kinetically controlled. On the other hand, continuous chromatography concepts such as the simulating moving bed technology have matured and are increasingly realized on industrial scale for the efficient separation of difficult compound mixtures - including enantiomers – with unprecedented efficiency. We propose that coupling of enzyme reactor and continuous chromatography is a very suitable and potentially generic process concept to address the thermodynamic limitations of a host of promising biotransformations. This way, it should be possible to establish novel *in situ* product recovery processes of unprecedented efficiency and selectivity that represent a feasible way to recruit novel biocatalysts to the industrial portfolio.

2.1 Introduction

Biocatalysis has become a workhorse in the chemical industry for the production of pharmaceutical intermediates [161; 177]. In particular, reactions with enzymes from the classes 1 (redox enzymes) and 3 (hydrolases) have been exploited. The most prominent reasons for this are ease of access to starting materials and enzymes. In particular the latter point has undergone some drastic improvements over the last 15 years due to a variety of developments, such as [i] large genome-scale [43] and metagenomic sequencing programs [175]; [ii] the screening of large metagenomic expression libraries [102]; [iii] constantly increasing abilities of tailoring enzymatic properties to specific needs (such as improved enantioselectivity or process stability [132]), and [iv] recombinant enzyme production. These facilitate drastically the potential transition of new biocatalytic concepts from the stage of fundamental chemical research to application in industrial processes [50; 54].

With the enzyme sourcing problem reduced, process considerations come more and more into focus, addressing such important questions as suitable cofactor regeneration protocols [158; 177], or reactions in non-conventional media [80; 86].

Thus, we can pose now the question whether by smartly coupling biocatalytic and process engineering steps we can design *generic* process schemes that extend our arsenal of industrial biocatalysis. One such area could be, for example, reactions whose yield is limited by thermodynamic constraints, which might require carrying out biocatalysis and product removal in one unit at the same time. A prominent example is isomerase catalyzed reactions. Usually, in such reactions the operator is left with a potentially difficult to process mixture of starting material(s) and product(s). In addition, in order to achieve decent yields on an expensive starting material (in reactions involving at least two starting materials), the cheaper starting material is often applied in (large) excess, adding to the difficulty of purification. Consequently, such reactions have remained largely unexplored on preparative level. A general process option to increase the yield could recruit entire new groups of enzyme with already proven synthetic merit to the preparative fine chemist's tool-box. This would include such exciting areas as the manufacturing of saccharides and enantioselective formation of C-C bonds, but also more established product groups such as amino acids. In particular enzymes from the classes 4 (lyases) and 5 (isomerases), which are frequently used in these groups of reactions, suffer from an unfavourable position of the reaction equilibrium [52], but also many hydrolase-catalyzed kinetically controlled synthetic reactions face essentially the same problem [174; 178].

An obvious solution to the problem is to selectively remove the product immediately or shortly after its formation from the reactor. This can be achieved, for example, by separating the compound mix in a continuous chromatograph, removing the product, and returning the remaining starting material to the reactor (Fig. 2.1.). Depending on the type of reaction, both operations could even be carried out in one reactor (see below). The required continuous chromatography has emerged over the last decade as an excellent and industrially viable process option for the separation of a wide range of product mixtures in two or more fractions [70]. Chromatography's high resolution power provides also a unique opportunity to accommodate the fact that (bio)catalysts frequently do not change the physicochemical properties of a molecule by much, usually rendering work-up of mixtures difficult. Furthermore, continuous chromatography considerably reduces the eluent consumption and product dilution compared to traditional batch chromatography schemes, making it a much more attractive procedure [55; 117; 119; 163; 164].

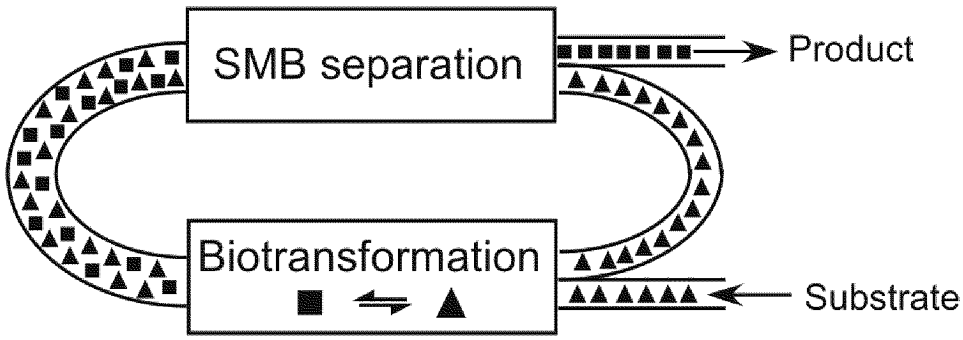

Figure 2.1: Concept of an on-line coupling of continuous chromatography and biotransformation.

Obviously, such a coupled operation of a continuous chromatography installation and an enzyme reactor creates a set of constraints for the applicable conditions. This extends at least to the choice of eluent (which is at the same time the reaction medium of the enzyme reactor), which leads to the question of suitable column materials (stationary phases) in the chromatography unit. In this work, we will explore the feasibility of coupling continuous chromatography and enzyme reactors based on previous experiences. We will first discuss possible configurations that combine biotransformation and chromatographic separation and analyze them in terms of for which types of enzyme-catalyzed reactions they might be used.

Next, we will discuss the most prominent enzyme classes that suffer from an unfavourable position of the reaction equilibrium. Finally, the continuous operation of a chromatographic unit requires particularly robust stationary phases (SPs) to be used in the chromatography columns. On the other hand, the material must be suitable to separate the most likely product classes with enzyme compatible eluents (Fig. 2.1). Thus, we investigate in the subsequent part whether there are materials that comply with both requirements. Based on these three elements, we will give some guidelines on how promising biotransformation processes for specific thermodynamically limited reactions can be realized in the future.

2.2 Biocatalysis integrated with continuous chromatography

2.2.1 The principle of continuous chromatography

Continuous chromatography has so far been most successfully realized as simulated moving bed technology (SMB). This technology is best understood as a hypothetical true countercurrent chromatography (TCC) (Fig. 2.2a). TCC is characterized by the countercurrent movement of a liquid and a solid phase. The two inlet flows (eluent make-up and feed) and the two outlet flows (raffinate and extract) are dividing the process into four distinct zones. Separation takes place in zone II and III, and regeneration of liquid and solid phase takes place in zone IV and I. The flow ratio (ratio of velocities) between liquid and solid phase has to be set such that the less retained compound is moving in direction of the liquid phase and is collected at the raffinate port while the more retained compound spends more time adsorbed on the solid phase and moves in the direction of the solid phase, so that it can be collected at the extract port. The fluid flow velocities in the zones can be controlled by the inlet and outlet volumetric flows.

Obviously, the technical realization of such a system is rather difficult, because of the required continuous movement of the solid phase. Therefore, the concept is realized as a simulated moving bed (SMB). In the scope of this discussion only a brief outline of the most important features is presented. A typical SMB consists of 4 to 24 columns that are connected in an annular alignment by multi-way valves. The true countercurrent movement of liquid and solid phase is simulated by periodically switching the inlet and outlet flows from column to column in the direction of the fluid flow. Consider for the sake of simplicity a 4-column SMB (Fig. 2.2b) with one column in each zone and a mixture of species A and B dissolved in the applied eluent entering the SMB between zone II and III at the beginning of a cycle; the

weaker retained species A reaches the outlet of zone III first. Before B reaches the end of zone III, the in- and outlets are switched in the direction of the fluid flow, so the zones are moved by one column in the direction of fluid flow. This translates into a hypothetical movement of the columns (i.e. the SP) in the direction opposite to the fluid flow.

Analogously to TCC, port switching moves the more retained compound from zone III to zone II and eventually to zone I, where complete desorption takes place and pure B can be collected at the extract port between zone I and II. Pure A can be recovered continuously from the raffinate port between zone III and IV, while in zone IV residual A is adsorbed in order to achieve a complete regeneration of the solvent. Possible SMB operating points can be easily derived by application of the triangle theory [111], which requires only the adsorption isotherms, which in turn can be obtained easily from HPLC runs.

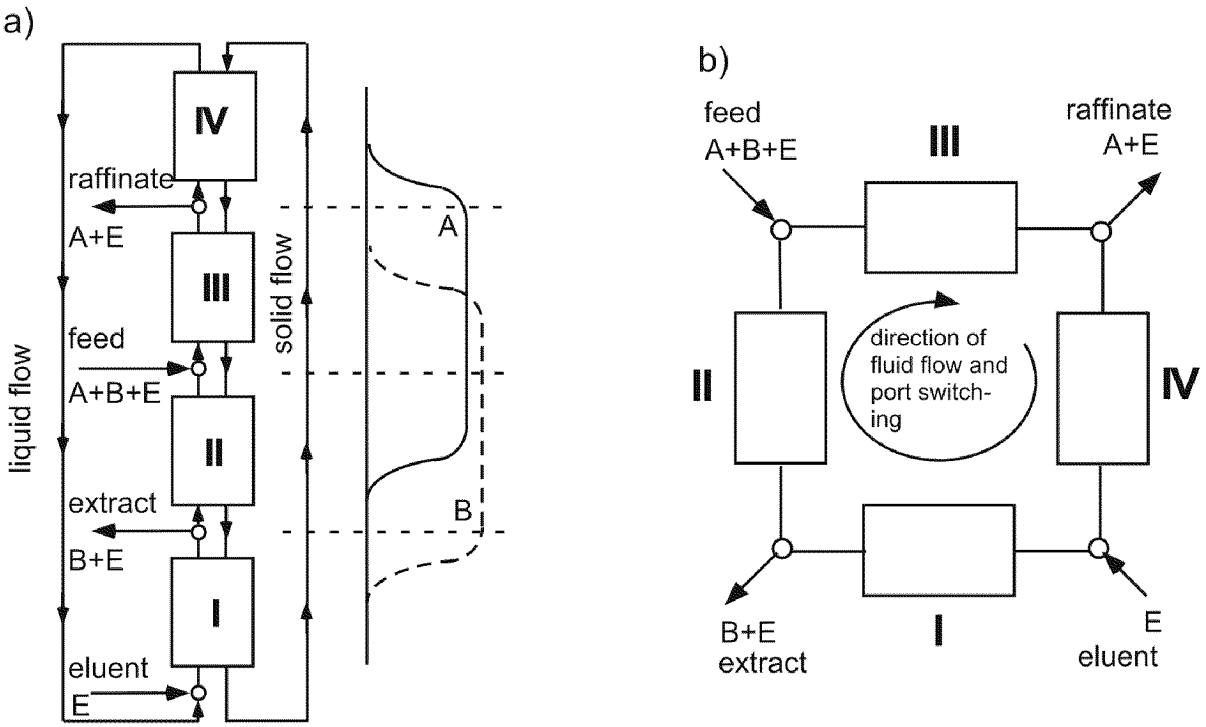

Figure 2.2: (a) Schematic diagram of a four-zone true countercurrent chromatography (TCC) unit consisting of four countercurrent chromatography columns with the corresponding axial concentration profile for a binary separation. (b) Schematic diagram of a four zone SMB, the experimental counterpart of a TCC with four columns. (A) less retained compound; (B) more retained compound; (E) eluent.

2.2.2 Continuous chromatographic bioreactor concepts

When such a continuous chromatography unit is now connected to an enzyme reactor, the potentially improved yield gained by the coupling of the two process steps has to be paid for by a decrease in the degrees of operational freedom as separation and reaction need to be operated under identical process conditions (Fig.2.1). There are basically three ways to achieve the coupling of biochemical reactions and continuous chromatography, which vary in the degrees of freedom in operation and design.

Simulated Moving Bed Reactor (SMBR):

The basic operating concept of an SMBR (Fig. 2.3a) is analogous to that of an SMB. The enzyme is simply added throughout the SMB unit, either to the SP in immobilized form or to the mobile phase in soluble form. Consequently, starting material can be continuously converted in all sections of the SMBR. Consider a thermodynamically limited reaction of type A to B and C. Species A is added to the SMBR in the feed flow and is enzymatically converted to B and C. Species B and C are separated from each other due to their different adsorption behaviour. This separation prevents the backward reaction and enables complete conversion of A. Species B and C can be collected at the extract and raffinate port, respectively, in high purity. Ideally the retention of A should be between that of B and C [100]. Separation and reaction are not separated in time and space, constituting a high degree of integration. On the other hand, the number of operation points that would be feasible were the SMB operated without reaction is much reduced because reaction kinetics and equilibrium have to be taken into account [100]. Obtainable productivities at complete separation and complete conversion are generally decreased in comparison to a purely separative SMB [162]. The few realized model processes combining biotransformation and SMB technology are almost exclusively based on the SMBR concept (Table 2.1) with reactions leading to at least two products. In earlier works, the SMBR was investigated as a two zone SMBR without the zones for regenerating eluent and SP [3; 7; 8; 151; 152]. Regeneration of the SP was accomplished by decoupling the last column of the extract zone (equivalent to zone II of Fig. 2.3a) and eluting the strongly adsorbed compound with fresh eluent. Regeneration of the eluent was omitted and the complete effluent from the raffinate zone (SMB zone III) was collected (open loop arrangement). The enzymes were dissolved in the mobile phase in all

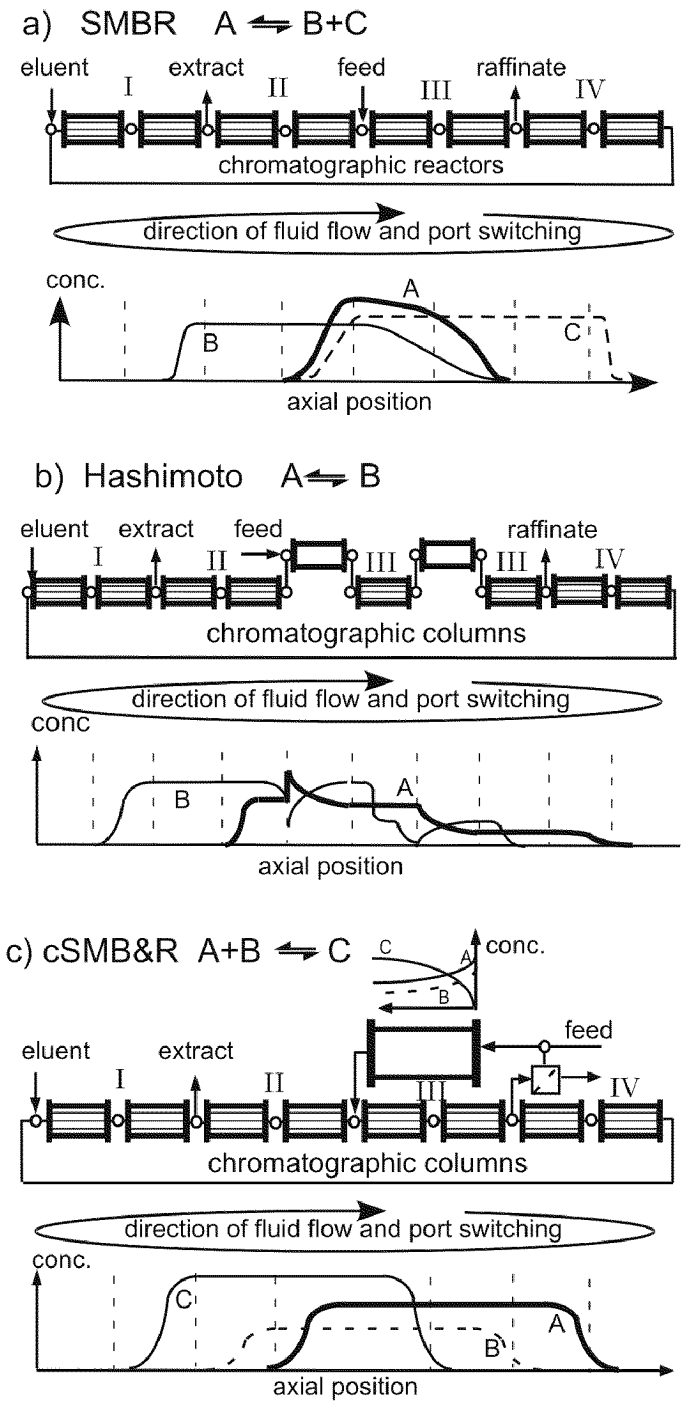

Figure 2.3: (a) Simulated moving bed reactor (SMBR) with axial concentration profile of substrate A and products B and C. (b) Hashimoto process with axial concentration profile of substrate A and product B. (c) Coupled SMB and bioreactor (cSMB&R) with axial concentration profile of substrates A and B and product C. Striped rectangles: chromatography columns. Empty rectangles: enzyme reactors.

these cases. Rather than thermodynamic limitations, the model reactions addressed product inhibition and reaction selectivity. It was shown that the applied concept required only 34-72% of the amount of enzyme needed in a corresponding conventional batch reactor of the same productivity [152]. Later, the concept was further developed into a closed-loop four zone SMBR by Azevedo and Rodrigues [6].

This concept was also used for overcoming thermodynamic limitations in lipase catalyzed esterifications [114]. Mensah and Carta [114; 115] realized a simplified SMBR, consisting of only one zone of several columns, constituting the separation and reaction zone. Two thirds of the SP on a weight basis consisted of immobilized lipase, the rest of ion exchanger material. The alcohol and acid, dissolved in hexane, were fed to the first column, which was periodically removed by elution with pure alcohol in order to recover the adsorbed water separately. The column was then added to the separation and reaction zone at the last position. Later, a three zone SMBR was applied in an open loop arrangement that omitted only the solvent regeneration zone [113]. Hexane and the alcohol were used as eluent, whereas the acid was added with the feed. Water accumulation on the immobilized enzyme was reduced by removing the water at the extract port. Both concepts keep water adsorption on the immobilized enzyme below a threshold value and thus prevent product hydrolysis.

The Hashimoto Process

In order to prevent reactions from occurring in all SMB zones, a partial disintegration of separation and reaction is required. The enzymatic reaction is then no longer distributed throughout the SMB, but localized in enzyme reactors that are fixed to specific SMB zones (e. g. zone III) while the columns are switched from zone to zone [59] (Fig. 2.3b). The advantage of such an alignment in comparison to an SMBR can easily be understood from a thermodynamically limited reaction of type A to B. The weaker retained species A moves with the mobile phase and is step-wise converted to species B in the reactors present in zone III. This process concept creates the possibility to install reactors only in those SMB zones, where reaction is advantageous. In zones where enriched product is present (zone I and II), enzyme reactors would only promote the backward reaction counteracting the conversion and resolution achieved before. Theoretically, the fraction of not converted A could be collected at the raffinate port and recycled to the feed flow in order to increase the product yield [15].

Table 2.1
Biotransformation combined with SMB

Educt	Product	Enzyme	Stationary phase	Concept	Eluent	Performance	Remarks	Reference
Sucrose	Glucose fructose	Invertase	CEX. KorelaV70C Polystyrene resin (Ca^{2+} form)	SMBR 12 columns	Water	Complete conversion 16 kg sugar/m^3 SP/day purities >95%	Product inhibition	Akintoye et al. 1991
Lactose	Galactose glucose	Lactase	CEX Dowex 50WX4 Polystyrene resin (Ca^{2+} form)	SMBR 12 columns	Water	Complete conversion 0.6 kg sugar/m^3 SP/day purities glucose >95%; galactose >77%	Product inhibition	Shieh and Barker, 1996
Sucrose	Dextran fructose	Dextran-sucrase	CEX Purolite PCR563 Polystyrene resin (Ca^{2+} form)	SMBR 12 columns	Water	Complete conversion purities fructose >99%; dextran >92%	Prevention of fructose acting as acceptor	Barker et al. 1992, 1993
Starch	Maltose dextrin	Maltogenase	CEX KorelaV70C Polystyrene resin (Ca^{2+} form)	SMBR 12 columns	Water	60% conversion > 3 kg sugar/ m^3 SP/day purities maltose >95%; dextrin >93%	Product inhibition	Shieh and Barker, 1995
Glucose	Fructose	Immobilized glucose isomerase	Y zeolite (Ca^{2+} form)	Hashimoto 16 chromat. columns 7 enzyme columns	Water	Purity fructose > 52%	Yield beyond equilibrium	Hashimoto et al. 1983
Propionic acid Isoamyl alcohol	Isoamyl propionate water	Immobilized Lipozyme IM	CEX Dowex HCR-W2 Polystyrene resin (Na^{+} form)	SMBR 3 columns	Hexane Isoamyl-alcohol	26.4 kg ester/ kg SP/day	Yield beyond equilibrium/ enzyme inactivation	Mensah and Carta, 1999
Propionic acid 2-ethyl-1,3-hexanediol	Ester water	Immobilized Lipozyme IM	CEX Dowex HCR-W2 Polystyrene resin (Na^{+} form)	SMBR 5 columns	Hexane 2-ethyl-1,3-hexanediol	~3 kg ester/ kg SP/day	Yield beyond equilibrium/ enzyme inactivation	Meissner and Carta, 2002
Sucrose Lactose	Lactosucrose glucose (byproduct fructose)	β-fructofuranosidase	CEX Amberlite CR-1310 Polystyrene resin (Na^{+} form)	SMBR 12 columns	0.1 mM NaCl	70% conversion but hydrolysis of product at raffinate port	Yield beyond equilibrium	Kawase et al. 2001
Sucrose	Glucose fructose	Invertase	CEX Monosphere 99 Polystyrene resin (Ca^{2+} form)	SMBR 12 columns	Buffer pH 4.5 (acetic acid/ Ca-acetate)	complete conversion 170 kg /m^3 SP/day purities >90%	Product inhibition	Azevedo and Rodrigues, 2001

Realized model processes combining SMB and biotransformation. The problems addressed were mostly product inhibition, low equilibrium yield or enzyme inactivation. The process concepts are described in detail in the text. CEX: cation exchanger.

Experimentally, this concept was used for the production of high fructose syrup. The enrichment of fructose beyond equilibrium was established by the stepwise conversion of glucose in the bioreactors present in zone III while the more retained fructose could be collected at the extract port. Since in the realized process alignment no regeneration of the mobile phase was implemented (no zone IV), considerable amounts of residual glucose could reach the fructose outlet and thus limit the achievable purities [59].

On-line coupling of SMB and reactor (cSMB&R)

In this concept, SMB and bioreactor constitute two separate units interconnected by a loop. The SMB continuously separates product and starting material leaving the bioreactor. Considering for example a thermodynamically limited biochemical reaction of type A to B, the starting material A is recycled from one port of the SMB unit to the bioreactor while the product B can be collected at the other effluent flow ideally completely separated from A. Thus theoretically 100% yield can be achieved. In SMB operation, generally dilution of the compounds to be separated occurs with respect to the feed concentrations. Since the effluent flows are usually higher than the feed flow only a fraction of the volume of the effluent can be recycled for continuous operation. This needs to be compensated for by e.g. nanofiltration resulting in a concentration of the residual starting material before recycling. In cSMB&R reaction and separation are decoupled as far as possible, establishing a broad range of possible applications.

Although the cSMB&R concept has – to the best knowledge of the authors - never been experimentally realized, various authors have compared the potential performance of the cSMB&R concept by model based simulations to other process concepts. For the glucose/fructose isomerisation, the Hashimoto process was superior compared to a cSMB&R process with respect to eluent consumption for fructose contents in the range of 45-65% [59]. At higher fructose purities application of the cSMB&R concept would prove advantageous [59]. This result was extended by later work, where the SMBR, an cSMB&R-Hashimoto hybrid and an cSMB&R process were compared, again for glucose/fructose isomerisation [15]. The SMBR process appeared to be the most advantageous for fructose purities smaller than 65%, the cSMB&R-Hashimoto hybrid process for purities between 65%-95%, and the cSMB&R for purities >95%. The fact that highest purities can be obtained from the cSMB&R configuration, can be easily explained by the fact that in SMBR for equilibrium reactions of type A to B the backward reaction is constantly catalyzed (the enzyme being present throughout the reactor). This way, high productivity at high purities is prevented. Due to the

continuous recycling of residual glucose in the cSMB&R process, the best performance in terms of productivity can be obtained at very high purities.

In summary, it becomes clear that coupled continuous reaction and chromatographic separation systems have addressed mostly food-related biotransformations that suffered form product inhibition and so far have not played a major role for fine-chemical purposes, and in particular have not addressed thermodynamically limited reactions in considerable depth. On the other hand, even the rather limited set of examples from various application areas already indicates that such integrated process concepts represent unique options to drive reactions to complete conversion by realizing a highly selective *in situ* product recovery. Their potential for producing products at high purities and decent productivities makes them particularly attractive for the fine chemical field with pharmaceutical applications in mind.

Next, we will investigate the scope of the opportunity with respect to the interesting catalysts that would benefit from a combined enzyme reactor/SMB operation.

2.3 Accessible enzyme classes

As the structure of the catalyzed reactions (one or more products) has obviously an impact on the most advantageous configuration of the coupled enzyme reactor/SMB, it appears useful to arrange the type of enzyme reactions according to number of reactants involved:

2.3.1 Reactions of type A to B

The easiest reactions that can be considered for integrated operation with a continuous chromatography installation are those that convert a starting material A into a product B, i.e. isomerases, epimerases, or racemases (Table 2.2). Most of the reactions catalyzed by this group have starting materials and products of very similar Gibbs' energy of formation, resulting in equilibrium positions that leave mixtures of substrate and product. The most prominent model system here is the conversion of glucose to fructose by a D-xylose isomerase (see above) to produce high fructose corn syrup [60]. From a fine chemical point of view, this reaction might not be the most interesting one, but it serves well to illustrate the potential of the concept for another set of isomerase-catalyzed reactions that open access to interesting ketoses via the corresponding aldoses whose chemistry is much better developed [60]. Here, quite a range of interesting isomerases is available, including D-xylose isomerases for the synthesis of iminoalditol-based glycosidase inhibitors [60],

Table 2.2

Overview of accessible enzyme classes in combination with SMB

Enzyme (example)	**Reaction**	**EC number**	**Requirements**
Isomerases - D-xylose-isomerase		5.3.1.5	Mn^{2+}, Mg^{2+}, Co^{2+}
Epimerases - D-tagatose-3-epimerase		5.1.3.X	None
Racemases - amino acid racemase		5.1.1.10	PLP
Pyruvate-dependent aldolases - N-acetylneuraminic aldolase	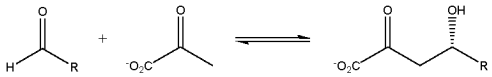	4.1.3.3	None
Glycine-dependent aldolase - L-threonine aldolase	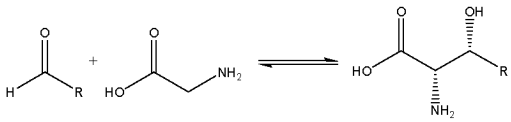	4.1.2.5	PLP
Glycosidases - β-glucosidase	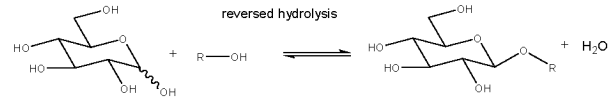 reversed hydrolysis 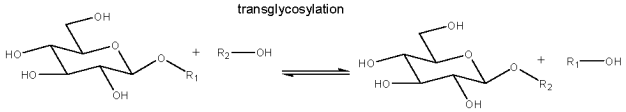 transglycosylation	3.2.1.X	Mg^{2+}, Na^{+}
Transketolase	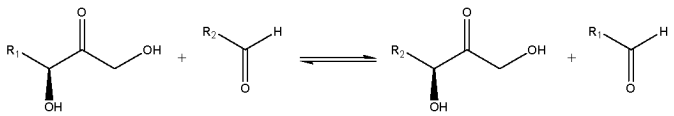	2.2.1.1	Mg^{2+}, TPP
Transaminases - L-aspartate aminotransferase	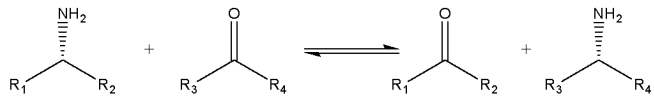	2.6.1.X 2.6.1.1	PLP
Kinetically controlled reactions - penicillin acylase	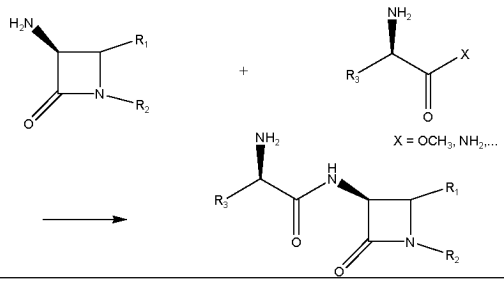 X = OCH_3, NH_2,...	3.5.1.11	None

PLP: pyridoxal phosphate; TPP: thiamine diphosphate.

L-fucose and L-rhamnose isomerase for the production of rare sugars such as L-lyxose [53], and L-arabinose isomerase to produce D-tagatose as a potential bulk sweetener [76].

The epimerases represent another interesting set of enzymes that interconvert either different aldoses or different ketoses into each other. In particular D-tagatose-3-epimerase offers access to a number of rare D-sugars e.g. D-sorbose [66] and the potential bulk sweetener D-psicose [169].

Racemases (Table 2.2) catalyze the interconversion of enantiomers and are therefore potentially of particular interest in fine chemistry. In the context of integrated processes, they might allow a novel perspective on the relationship between the number of directly accessible enantiomers and the number of required enzymes. For example, the classic resolution routes to amino acids usually start from racemic amino acid intermediates that are then enantioselectively hydrolyzed. Direct access to either one of the enantiomers with 50% yield requires two enzymes, one for each enantiomer. Getting to 100% yield requires a third enzyme, the racemase (or a suitable alternative chemical procedure). Using a combination of a racemase and a continuous chromatography system, only one enzyme would be required to access both enantiomers in a theoretical yield and enantiomeric excess of 100% from the same installation (Fig. 2.4).

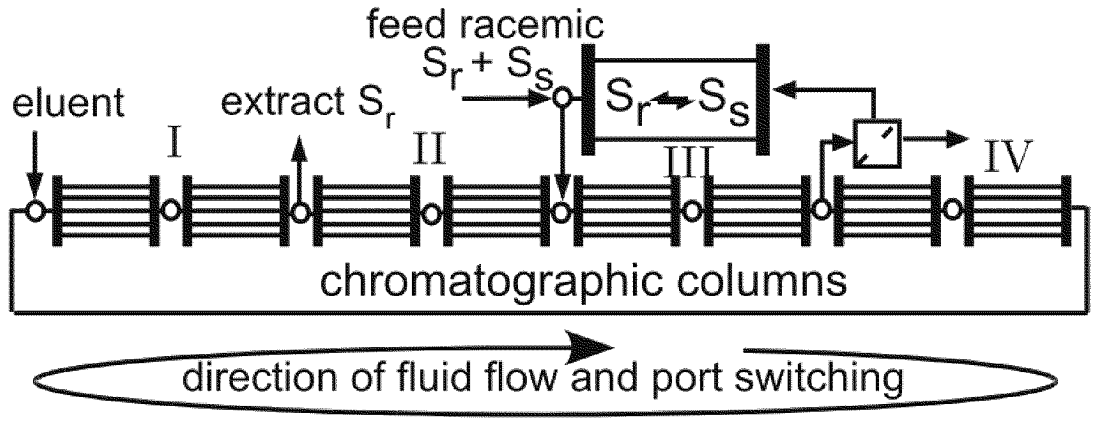

Figure 2.4: Process scheme for the production of enantiopure compounds by the integrated operation of chiral SMB and a racemase reactor. S_r: *R*-enantiomer; S_s: *S*-enantiomer.

Racemases have already found their way into industrial catalysis [110; 146] in order to remove some of the 50% yield limitation in classical resolution processes of activated amino acid intermediates. A number of racemases that operate on amino acids directly (rather than their derivatives) have been reported [146], indicating that this product group might be as well accessed directly by integrated operations rather than via activated intermediates. Other efforts to develop racemases for biotransformations have mainly focused on racemases acting on α-hydroxy carbonyl derivatives such as mandelic acid [146].

2.3.2 Reactions of type A+B to C

Lyases are important in fine chemistry due to their capacity of enantioselective C-C bond formation. In the group of aldolases, a typically essential donor substrate reacts with one of a variety of possible acceptor aldehydes. Consequently, aldolases are organized along the essential donor into dihydroxyacetonephosphate- (DHAP), acetaldehyde-, pyruvate-, or glycine-dependent aldolases. The latter two aldolase classes (Table 2.2) catalyze many highly interesting reactions with unfavourable reaction equilibria. One important example here is the conversion of pyruvate and *N*-acetyl-D-mannosamine (ManNAc) to *N*-acetylneuraminic acid by the pyruvate-dependent *N*-acetylneuraminic aldolase. This reaction is of interest for the production of, for example, neuraminidase inhibitors such as Relenza (Glaxo Smith Kline). As the manufacturing of ManNAc from *N*-acetylglucosamine is also challenging, only relatively dilute substrate mixtures are applied and the product is quite heavily contaminated with substrates (K_{eq}=28.7 M^{-1} at 25°C) [84]. A number of approaches have been followed to address the problem, all involving an excess of pyruvate to drive the reaction [13; 84; 107]. As this behaviour is a general property of the pyruvate-dependent aldolases for the production of 2-ketoaldonic acids, the removal of pyruvate as an end-of-pipe treatment received considerable attention [107; 184]. This example illustrates clearly the underlying problems of this specific enzyme class.

The same problem is encountered in the manufacturing of β-hydroxy-amino acids with glycine-dependent aldolases (Table 2.2). Here, threonine aldolases represent a synthetically interesting group of enzymes because they have the potential for selective production of diastereomerically complete sets of β-hydroxy-amino acids (theoretically consisting of 4 enzymes for all 4 stereochemically possible permutations of the C_α and C_β atom of an amino acid). Although the enzyme set is not (yet) complete [98], the industrial potential for these enzyme is already clear [87; 97].

Furthermore, there is strong evidence that glycine-dependent aldolases that are reported as indifferent to the configuration at C_β are in fact diastereoselective to a considerable extent, but the diastereomeric excess suffers from extended reaction times because the kinetically preferred isomer has time to be converted until the diastereomerically more unfavourable thermodynamic equilibrium has been reached [78] (see also below – note that this behaviour does not make these enzymes of the A + B to C + D type, because for the reverse reaction the enzyme requires only C or D, not both). We will address this behaviour in the next paragraph in more detail.

2.3.3 Reactions of type A+B to C+D (+E)

This type contains mostly hydrolase reactions, for many of which it would be interesting to reverse hydrolysis, as it is done in lipase catalyzed synthesis in organic media. One prime example for a reaction that requires an aqueous medium and would therefore potentially benefit a lot from the enzyme reactor/SMB concept is the alkylation of glycosides with glycosidases. Although these enzymes catalyze *in vivo* the hydrolysis of glycosides, they are heavily explored as biocatalysts in the synthetic direction as well, either in reverse hydrolysis or in transglycosylation [174]. For reverse hydrolysis, by adding alcohols as glycosyl acceptors to the aqueous reaction medium and thus reducing the water activity in the reaction mixture considerably ($a_w \leq 0.4$), promising yields up to >60% (for the acceptor) can be obtained [26; 176] which make this a potentially highly attractive class of reactions for integrated processing.

Transketolases catalyze *in vivo* the reversible transfer of a two-carbon ketol unit from a ketose to an aldose. Synthetically, they open the door to the manufacturing of commercially interesting enantiomerically pure diols and triols with D-*threo*-stereochemistry [170] and have attracted a lot of interest because a promising way to overcome the problem of equilibrium position is available: By using hydroxypyruvic acid (HPA) as ketol donor, CO_2 is produced and this drags the reaction theoretically to completion [28]. However, HPA is expensive, and the ability to substitute this ketol donor by one of a host of others that are accepted by transketolases might very much broaden the interest in this class of enzymes [14].

A similar strategy has been applied for transaminases that can be used to produce for example unnatural amino acids from the corresponding α-keto acids [2; 46]. Using L-aspartate as the amino donor, oxaloacetate remains which spontaneously decarboxylates to pyruvate and thus prevents the reverse reaction. Again, removing the requirement for a particular amino-donor

might broaden the utility of this class of enzymes. However, in both of the above examples, a one- (transketolases) or two-(transaminases) compound mix at the end of the reaction would need to be exchanged for a complex four-compound-mixture that would need to be suitably separated by the continuous chromatographic system.

In a number of interesting biocatalytic reactions of this class, the composition of the product mixture varies over time, i.e. first a kinetically controlled product is formed before after longer residence times in the reactor the product mixture approaches the thermodynamically most favourable composition. In fact, this has already been briefly discussed for threonine aldolases (see above). However, kinetically controlled syntheses play also an important role with hydrolases that are used in synthetic direction. In transglycosylation, a disaccharide (or any other "activated" glycoside) is used as a glycosyl-donor in the synthesis of substituted glycosides. This allows to accelerate the reaction considerably (relatively to the above discussed reverse hydrolysis), but bears the problem that water can act as a nucleophile in the enzymatic reaction as well and can cause the donor or the product to hydrolyze, thus creating an undesired dead-end product [174]. The same strategy is followed in the manufacturing of semisynthetic antibiotics, where an activated side-chain is coupled to the β-lactam-nucleus using a penicillin acylase. Again, either the activated side chain or the product might be hydrolyzed in the presence of the enzyme [178]. Obviously, a strategy that limits the time of exposure of the reactants to the enzyme and allows the selective removal of the "sensitive" product from the mixture should increase the yield (calculated based on either the activated donor or the desired nucleophile).

In summary, there is a large variety of enzymes available that have already proven their merit in terms of chemical utility but face intrinsic processing problems because of the position of the corresponding reaction's equilibrium. Consequently, it appears that there is ample motivation to investigate process concepts to exploit their synthetic power. Conceptually, they fall in two classes: reactions that lead to only one product and reactions that lead at least to two products. In terms of product, most examples address sugars and sugar-like compounds, and amino acids and their derivatives. The required separations cover separations of entirely different molecules, of stereoisomers, or of enantiomers. Consequently, a large variety of product groups would need to be separated on the SMB. Next, we will analyze whether the SP materials that are currently available are likely to be sufficient to address these diverse tasks.

2.4 Stationary phases

Due to the integrated operation of enzyme reactor and chromatographic separation unit, possible SPs have to comply with a number of requirements: if an organic solvent has to be added to the eluent, its fraction should be low enough to permit efficient enzyme function, and eluent pH should be adjusted to close to neutral conditions including buffering when necessary. Another point is that enzyme reactions will require buffering or at least some salt addition to adjust the pH properly. This can have important effects on the separation characteristics of the SP. Consequently, we need to investigate the different materials with respect to their behaviour in eluents with a high water content and (close-to) physiological pH.

2.4.1 Potential stationary phases for coupled enzyme reactor/SMB operation

Non-chiral stationary phases

Non-chiral SPs can be applied for most of the potential applications of the coupled enzyme reactor/SMB concept, because the separation task does not involve the separation of enantiomers form each other. For these separations, reversed-phase silica is the most widely used packing materials in preparative chromatography [108]. In its important C_{18}- and C_8-form, it is mostly applied for preparative separations of weakly basic or polar compounds, but cannot tolerate pure aqueous eluents as the alkyl chains bonded to the silica core would collapse. However, this is no issue as long as the enzyme used for biotransformation tolerates a minor content of organic solvents, which is frequently the case. On the same note, the slightly acidic conditions that are preferred to counter the alkaline susceptibility of the material are typically not a problem for biotransformation.

Ion-exchange materials are commonly used in the analysis of amino acids and are also good SPs for preparative applications. The group of Yonemoto separated glutamic acid and valine by continuous chromatography [79] and also a ternary mixture of glutamic acid, valine, and leucine [48] on a cation-exchange resin in the Na^+ form using sodium acetate buffer (pH 5) as eluent. Wu and co-workers separated a mixture of the amino acids tryptophan and phenylalanine in SMB using PVP resin (poly-4-vinylpyridine cross-linked) and water [186].

Also for the separation of saccharides, ion-exchange is among the most suitable techniques for preparative chromatography due to size exclusion and ligand-exchange effects [180]. Strong acid-type polystyrene/divinylbenzene-based cation-exchangers in Ca^{2+} form were already used in continuous chromatography for the separation of fructose, glucose and

sucrose in water with 0.5 g/l $CaCl_2$ [65], of fructose and dextran in water [32], and of glucose and fructose in an SMBR in a calcium acetate buffer at pH 4.5 [6]. Zeolites are an attractive alternative for the separation of sugars as was demonstrated for glucose and fructose with Ca^{2+} exchanged Y zeolites in an SMB with water as eluent [30; 59].

Chiral stationary phases

When the enzyme reactor/SMB concept is applied to racemases, enantiomers need to be separated from each other. Given the importance of chirality in pharmaceutical chemistry, it is obvious that this is an important potential application. However, there has been no integrated operation of enzyme reactor and chiral SMB before, so there is hardly any information about the behaviour of chiral SPs under enzyme-compatible conditions.

Polysaccharide SPs are considered the workhorse for chiral separation on both analytical and preparative scale due to the broad range of applicable molecules [197] and an outstanding saturation capacity of up to 100 mg/g chiral SP [47]. They can be operated in reverse mode with water contents up to 90% (manufacturer's information), however sufficient interaction with the SP requires neutral analytes as solvation of ionic analytes presumably prevents proper interaction with the SP. Hence, for the separation of basic and acidic compounds pH adjustment or addition of a counterion for ion pair formation is required. Furthermore the interactions in chiral discrimination of polysaccharides SPs are considered to be less efficient in highly polar aqueous eluents such as water [168] Other preparatively applicable chiral SPs include tartardiamide chiral SPs, SPs with low molecular-mass chiral selector (i.e. Brush type, Pirkle type) and polyacrylamide chiral SPs. Those SPs show saturation capacities of approximately 1-20 mg/g CSP and are stable in reverse and normal phase, but are usually operated in normal phase mode [5; 47].

Another broadly applicable class of preparative chiral SPs that received considerable attention over the last years is macrocyclic glycopeptide bonded phases that are reported to show good separation characteristics for a variety of compounds, in particular amino acids, when employing aqueous eluents [187]. For example, baseline resolution of racemic methionine was obtained on an analytical teicoplanin-based SP column employing pure water as solvent [12].

The different types of chiral SPs are complementary and frequently mutually exclusive in their separation characteristics. A screening of 55 different enantiomeric pairs employing different polysaccharide and macrocyclic glycopeptide chiral SPs revealed that - except for

two - all enantiomeric pairs could be separated with five compounds being only separated on the macrocyclic glycopeptide chiral SPs and 17 only on the polysaccharide chiral SPs [4]. Next to these fundamental considerations, selection criteria for the best SP include separation efficiency, mechanical stability at elevated pressure and chemical stability [70]. However little specific information is documented for these issues.

Table 2.3
Overview of potentially suitable preparative stationary phases for a potential integration with enzyme reactions

Stationary Phase	**Accessible compounds**	**Applicable enzyme compatible eluents**	**Potential accessible enzyme reactions**
Reversed phase silicas (C18)	Water soluble, non-polar or weak polar	Aqueous buffer, 10% organic modifier required	L-aspartate aminotransferase, penicillin acylase, N-acetylneuraminic aldolase, transketolase
Ion-exchanger (Organic polymers, zeolites)	Charged molecules, sugars	Aqueous buffer	β-glucosidase D-xylose isomerase, D-tagatose-3-epimerase, L-threonine aldolase, L-aspartate aminotransferase, transketolase
Macrocyclic Glycopeptides*	Amino acids, carboxylic acids, β-lactams	Aqueous buffer usually containing >20% organic modifier	Amino acid racemase

* only preparative chiral stationary phase yet applied with high water systems

In summary, it is clear that sufficient materials are available to select SPs for coupled enzyme reactor/SMB operation for the most interesting product classes (Table 2.3). Of course, this very general statement has to be verified in each specific case, because it is based on some rule of thumb assumptions about enzyme behaviour in the presence of low amounts of organic solvents.

2.5 Guidelines

In the sections above, we have analyzed the available reactor configurations for coupled enzyme reactor/SMB operation, the chemical opportunities that could be addressed by such a concept, and in how far proper SP material is available so that novel processes might indeed be realized. We will now try to accommodate the separate points into some design guidelines.

2.5.1 Choice of process configuration

The Hashimoto process requires the most complex process control of the three investigated configurations due to additional equipment such as reactors, valves etc. Furthermore, the purities that can be obtained for thermodynamically limited reactions are generally lower than in SMBR and cSMB&R configuration due to the cascade-like arrangement of reactors and separators. Recycling concepts (e.g. Hashimoto-cSMB&R hybrids) for residual substrate might increase the product yields for the Hashimoto process. However the additional equipment expenses and design complexity will only in very exceptional cases justify an application in coupled enzyme reactor/ SMB operation.

For the remaining two concepts - SMBR and cSMB&R – selection depends on the applied type of reaction. The SMBR concept is most advantageous for reactions forming two different molecules, e.g. the A and B to C and D, or A to B and C type, that is for reverse hydrolysis of glycosides, transketolase- and transaminase-catalyzed reactions. Due to the rather long residence times in the SMBR combined with the instantaneous separation of substrate(s) and products, complete conversion can usually be achieved for thermodynamically limited reactions. At the same time, the products are separated to high purities at decent productivities. When applying the SMBR concept to reactions that lead to only one product, the permanent back-reaction throughout the whole unit interferes with high product purity, so the concept is less suitable. Similarly, in batch reactive chromatography (e.g. a single column equipped with both catalyst and adsorbent) this would translate to a considerable contamination of the product elution profile with substrate. Furthermore, there is considerable loss of enzyme if this is added to the eluent.

On the other hand reactions resulting in the formation of only a single product, e.g. A to B, or A and B to C are preferably carried out in a cSMB&R. This covers aldolases and isomerases, epimerases, and racemases. Here the product can be rapidly removed from the enzyme reactor and the starting material is recycled to the enzyme reactor. This leads to high purities, theoretically 100% yield, and short residence times in the enzyme reactor, making this a

suitable configuration for kinetically controlled reactions. However as dilution of the compounds is common in SMB operation - especially for the extract - an additional concentration device for the starting material might be necessary adding to the process costs and complexity. Nevertheless, there is strong motivation to explore this configuration.

2.5.2 Choice of stationary phase

The choice of the appropriate SP mostly depends of the product class to separate. Considering the enzymes shown in Table 2.2, most products will have sugar-like or amino acid-like characteristics. This narrows down selection of materials to ion-exchangers or zeolites for sugars and sugar-like compounds and adsorbers or ion-exchangers for amino acids (Table 2.3). A wide range of these materials have already been applied successfully in preparative applications as described above.

Furthermore, enzyme reactions commonly take place in buffered systems and sometimes require the presence of cofactors (Table 2.2). Simple salts are mostly used as buffer, whereas cofactors might vary from divalent cations like Mg^{2+} to larger molecules like pyridoxal phosphate (PLP). The presence of these compounds may strongly influence separation characteristics especially if ionic interactions are governing the retention of the compounds to be resolved. This, for example, excludes the use of anion-exchangers for enzymes requiring PLP as cofactor, as PLP carries a double negative charge and would therefore be strongly retained on anion exchanger.

Still, given the many materials that are available to realize the different separation tasks, it appears likely that coupled enzyme reactor/SMB will be a very versatile concept to address a broad variety of different reactions. However, many of the potential materials have not been tested under enzyme compatible conditions yet, so care has to be taken here.

2.5.3 Economics

SMB units require high investments but on the other hand offer a high degree of automation. Hence, with increasing scale the plant costs' contribution to the total costs generally decreases while stationary and mobile phase costs dominate. Strube and co-worker have calculated the cost distribution for SMB separation of fructose and glucose (100% purity) on a 20'000 to 200'000 t/a scale and the production of an enantiopure drug on a 1 to 5 ton/a scale. The costs for the non-chiral SP employed in the sugar separation are negligible, while about two thirds of the total costs are generated by solvent costs (water in this case). For chiral separations, the costs for the SP make a considerable contribution to the total costs but still solvent costs are

the major cost driver [163]. Desirable productivities for chiral SMB as rule of thumb are 0.3 kg enantiomer per kg CSP per day [120] and reported SMB applications with chiral polysaccharide SPs realize a productivity of 0.5 to 1.5 kg/kg CSP/day [47].
Such productivities can be translated roughly into separation prices per kg of product that have to be added specifically to the enzyme catalysis step. For the production of enantiopure naproxen on 100 t/a scale by SMB separation of the racemic mixture, the separation costs were calculated to be up to 31 $/kg assuming a productivity of 1 kg/kg CSP/day. With increasing productivity the manufacturing costs decrease drastically e.g. via 10 $/kg at 2 kg/kg CSP/day down to 3 $/kg at 5 kg/kg CSP/day [20]. With the ongoing improvements made in SMB operation (e.g. Varicol [104], PowerFeed [198], ModiCon [148]) as well as in the development of new powerful SPs such productivities should be achievable and thus costs reduced.

2.6 Conclusions

The advances in biotechnology allow us to consider a whole new range of enzymes for industrial-scale fine chemistry. Some of these novel opportunities – such as those enzymes that catalyze thermodynamically limited reactions - require novel processing concepts. Realizing such concepts by integrating continuous chromatography as SMB and enzyme reaction appears to be a very attractive option – the SMB concept is sufficiently mature, financially attractive, and flexible for this purpose, and enzyme-compatible stationary phases/eluent systems are likely to be found for many of the potential biocatalytic opportunities. We suggest that there will be many applications of this technology in the near future.

3 Characterization of the AlkS/P_{alkB}-expression system as an efficient tool for the production of recombinant proteins in *Escherichia coli* fed-batch fermentations

Stefan Makart, Matthias Heinemann, Sven Panke

also published in Biotechnol Bioeng 96:326-336 (2007)

Abstract

The availability of suitable, well-characterized, and robust expression systems remains an essential requirement for successful metabolic engineering and recombinant protein production. We investigated the suitability of the *Pseudomonas putida* GPo1-derived AlkS/P_{alkB} expression system in strictly aqueous cultures. By applying the apolar inducer dicyclopropylketone (DCPK) to express green fluorescent protein (GFP) from this system in *Escherichia coli* and analyzing the resulting cultures on single cell level by flow cytometry, we found that this expression system gives rise to a homogeneous population of cells, even though the overall system is expected to have a positive feed-back element in the expression of the regulatory gene *alkS*. Overexpressing *E. coli*'s serine hydroxymethyltransferase gene *glyA*, we showed that the system was already fully turned on at inducer concentrations as low as 0.005% (vol/vol). This allows efficient mass production of recombinant enzymes even though DCPK concentrations decreased from 0.05% to 0.01% over the course of a fully aerated cultivation in aqueous medium. Therefore, we elaborated the optimum induction procedure for production of the biocatalytically promising serine hydroxymethyltransferase and found volumetric and specific productivity to increase with specific growth rate in glucose-limited fed-batch cultures. Acetate excretion as a result of recombinant protein production could be avoided in an optimized fermentation protocol by switching earlier to a linear feed. This protocol resulted in a production of a final cell dry weight concentration of 52 g L^{-1}, producing recombinant GlyA with a maximum specific activity of 6.3 U mg^{-1} total protein.

3.1 Introduction

Suitable recombinant expression systems are a fundamental prerequisite for the overproduction of recombinant proteins, for example for therapeutic or biocatalytic purposes [31], or for rational metabolic engineering [71]. The production of recombinant proteins has become standard practice within the last decades. To improve the yield, a wide variety of host and expressions systems and fermentation regimes have been developed and successfully implemented [68]. Nevertheless, *E. coli* remains an attractive recombinant host with cell dry weight (CDW) concentrations as high as 148 g L^{-1} CDW [82] and 145 g L^{-1} CDW [64] and a variety of expression systems available. However, disadvantages remain with frequently applied model *E. coli* expression systems, such as expensive and toxic inducers (e.g. isopropyl-β-thiogalactoside (IPTG) in the LacI/P_{lacZ}-system [36]), catabolite repression which makes the use of glucose as carbon source in mineral media difficult (e.g. the LacI/P_{lacZ} [166] or the PrpR/P_{prpB} expression system [91]), the requirement for dedicated strains (as for the T7 system [165] or the GalR/$P_{galP\text{-}2}$ system [116]) or - on process level - difficult induction procedures (such as heat induction for $C_{I857}/\lambda P_L P_R$ system [27]). Moreover, some well established expression systems – LacI/P_{lacZ} and AraC/P_{araB} - can display bistable rather than graded expression behaviour: upon induction they can produce two subpopulations of cells, one fully induced and the other not at all [74; 124; 154]. Although the expression response on population level appears to be increasing with the inducer concentration, this reflects on single cell level only the increase of one population over the other [74; 124]. This property has been attributed to an autocatalytic behaviour of these systems, as the inducers – lactose and thio-methylgalactoside for the *lac* or arabinose for the *ara* system - also induce the expression of a transporter gene which in turn facilitates the entry of the inducer into the cell [24; 124]. To allow truly graded responses, these systems require inducers not depending on transporter gene expression for membrane crossing, such as IPTG [74], or decoupling of the regulation of the expression of the transporter gene from the actual expression system [72; 73].

Here, we characterize another expression system, the AlkS/P_{alkB} system originally derived from *Pseudomonas putida* GPo1 [172; 173], for biotechnological purposes in strictly aqueous media. AlkS senses the presence of alkanes and induces the expression of genes from its cognate promoter P_{alkB} [81], but also from its own promoter P_{alkS2} [23]. Natural inducers of the system are *n*-alkanes (C_6 to C_{12}) [56; 172], but the system can also be induced by the ketone

DCPK [56; 159], which is well water soluble and less volatile. These inducers do not require transport proteins to enter the cell. The AlkS/P_{alkB} system has been successfully applied for whole-cell biocatalysis in two-liquid phase cultures, where an additional organic phase could serve as a reservoir for the inducer *n*-octane at rather high concentrations, which would otherwise be quickly stripped from strictly aqueous cultivations [21; 22; 126; 127]. The various parts of the system have been assembled into a series of convenient and self-sufficient expression vectors [126; 156], which can be freely exchanged between *E. coli* strains without additional strain engineering efforts. The strength of the promoter is comparable to the strong *tac* system, and it is tightly shut in the uninduced situation [126; 127]. Carbon catabolite repression – although present in the wild-type – does not occur in *E. coli* [157; 195]. First efforts to extend the expression system into protein production in *E. coli* in aqueous systems involved the production of oxygenases: One part, StyA, of a two-component styrene monooxygenase, StyAB, was produced, but to relatively low cell densities [123]. Other proteins were a two-component xylene oxygenase, the membrane protein part of which had a major impact on the host physiology [101], and a chlorobenzene dioxygenase [190; 191] which was used for concomitant biotransformations and the toxic effects of the product interfered with the cultivation.

In order to explore the more general suitability of the AlkS/P_{alkB} expression system for metabolic engineering or protein production purposes in aqueous systems, we characterized the response of the expression system to different inducer concentrations and whether the culture is homogeneously induced, and subsequently elaborated an optimized induction protocol for the overproduction of enzymes for biocatalysis. To prevent additional interference of the synthesized protein with cell physiology, we overproduced an intracellular *E. coli* protein with promising potential as a biocatalyst: GlyA, a serine hydroxymethyltransferase, which is a functional member of the group of glycine-dependent aldolases [155].

3.2 Materials and methods

3.2.1 Chemicals

All chemicals were either from Sigma-Aldrich Chemie GmbH (Buchs, Switzerland) or Roth (Reinach, Switzerland) unless mentioned otherwise. Restriction enzymes were from New England Biolabs (Beverly, MA USA).

3.2.2 Strains and plasmids

Relevant strains and plasmids used in this study are listed in Tab. 3.1. Standard cloning procedures were performed as described [139]. Helper plasmid pSPZ4 was constructed by digestion of pSPZ3 with *Pac*I and *Bam*HI and ligation to a polylinker 5'TAACCTAGGGGCGCGCC 3' and 5'GATCGGCGCGCCCCTAGGTATAAT 3' maintaining the *Pac*I site inside *alkS* next to an *Avr*II and an *Asc*I site. To eliminate an additional *Nde*I site on pSPZ4, site-directed mutagenesis was performed (CATATG changed to CATAAG) using the QuikChange XL Site-Directed Mutagenesis Kit from Stratagene (Amsterdam, The Netherlands), yielding pSPZ4ΔN, which facilitates future cloning procedures. The *glyA* gene was amplified by PCR from *E. coli* W3110 genomic DNA, adding on the 5' end an *Eco*RI and *Nde*I site and on the 3' end a *BamH*I site. The PCR product was cloned into pSPZ1(+) as an *Eco*RI/*BamH*I fragment. The *glyA* gene was removed from the resulting plasmid pESM1 as a *BamH*I/*Nde*I fragment and inserted into equally digested plasmid pSPZ2Not, resulting in pESM2. From there, a *Pac*I/*Asc*I fragment covering the 5' part of *alkS** (the star indicates an *alkS* gene in which an internal *Nde*I site has been silently mutated [126]) and the *glyA* gene was excised and inserted into pSPZ4ΔN, where it reconstituted the *alkS** gene. This resulted into the functional expression plasmid pESM3.
Plasmid pGEM-7Zf(+) was digested with *Nsi*I/*Eco*RI and ligated to a polylinker consisting of the oligonucleotides: 5' TCATATGGTCGACGGATCCAAGCTTCACGTGCTCGAGGGCG CGCCG 3' and 5' AATTCGGCGCGCCCTCGAGCACGTGAAGCTTGGATCCGTCGACC ATATGATGCA 3'. This linker was excised as *Nde*I/*Asc*I fragment and ligated into equally digested pESM3 to yield pESM5, a vector containing the AlkS/P_{alkB} expression system and a multiple cloning site.

A mutation was introduced into the *gfpuv* gene in order to eliminate its internal *Nde*I restriction site without altering the amino acid sequence using the QuikChange XL Site-Directed Mutagenesis Kit. The mutated *gfpuv* gene was amplified by PCR, flanking the gene with *Nde*I and *Asc*I restriction sites, which enable the cloning into *Nde*I/*Asc*I digested pESM3, resulting in vector pESM7.

Table 3.1: Bacterial strains and plasmids

Strain or plasmid	Characteristics	Source or reference
E. coli strains		
W3110	F^-, λ^-, IN(*rrnd-rrnE*)1	Gentic Stock Center, Yale University, USA
DH5α	*supE*44 Δ*lac*U169 (Φ80 *lacZ* ΔM15) *hsdR*17 *recA*1 *endA*1 *gyrA*96 *thi*-1 *relA*1	Gentic Stock Center, Yale University, USA
XL10-Gold	Tet^rΔ (*mcrA*)*183 Δ*(*mcrCB-hsdSMR-mrr*) 173 *endA*1 *supE*44 *thi*-1 *recA*1 *gyrA*96 *relA*1 *lac* Hte [F' *proAB lacI*^{q}Z ΔM15 Tn*10* (Tet^r) Amy Cam^r]	Stratagene
JM101	*SupE thi* Δ(*lac-proAB*) F' [*traD*36 *proAB*$^+$ *lacI*^{q} *lacZ* ΔM15]	New England Biolabs (Beverly, MA USA)
Plasmids		
pGEM-7Zf(+)	*lacZα*, phage f1ori, Ap^r	Promega
pGFP*uv*	pUC, *lacZ*, *gfpuv*, Ap^r	Clontech
pSPZ1(+)	pGEM-7Zf(+) with a new polylinker, Ap^r	Panke et al. 1999
pSPZ2Not	pUC18 derivative with *alkBp* and T4 transcriptional terminator, Ap^r	Panke et al. 1999
pSPZ4	pBR322 derivative with incomplete *alkS** and a polylinker, Km^r	This study
pSPZ4ΔN	Same as pSPZ4, but *Nde*I site deleted, Km^r	This study
pESM1	pSPZ1(+) containing *glyA*, Ap^r	This study
pESM2	pSPZ2Not containing *glyA*, Ap^r	This study
pESM3	AlkS expression vector, containing *glyA*, Km^r	This study
pESM4	pGEM-7Zf(+) with a new polylinker, Ap^r	This study
pESM5	AlkS expression vector with a new polylinker, Km^r	This study
pGFP*uv*ΔN	Same as pGFP*uv*, but GFP- internal *Nde*I site deleted, Ap^r	This study
pESM7	AlkS expression vector, containing *gfpuv*ΔN	This study

3.2.3 Induction experiments

The induction experiments with *E. coli* XL10 (pESM7), addressing homogeneous expression from the AlkS/P_{alkB} expression system, were performed in LB medium, supplemented with 50 μg mL^{-1} kanamycin at 30°C. Cells were taken from a common preculture, inoculated into 50 mL cultures and grown to an OD_{600} of 0.3 prior to induction with DCPK to concentrations specified in the text. Cells were collected after 4 h by centrifugation, washed with phosphate buffered saline (PBS), centrifuged again, and resuspended in PBS. Prior to the analysis, the cells were diluted to an OD_{600} between 0.05 and 0.1 in PBS and filtered through a 50 μm pore size sieve (Partec GmbH, Münster, Germany). Flow cytometry was performed on a Becton Dickinson FACS Aria (BD Biosciences, San Jose, CA USA) flow cytometer with an emission wavelength of 488 nm and a 530/30 nm wavelength band pass filter. Each sample was processed at a rate between 12 and 15'000 events s^{-1} and 200'000 events were analyzed.
Induction experiments with *E. coli* JM101 (pESM3) expressing *glyA*, addressing the potential of the expression system for protein production, were performed in M9* medium [126] containing 5 g L^{-1} glucose, 1 mL L^{-1} of trace element solution US [126] and supplemented with 5 mg L^{-1} thiamine. Cells were grown in a common preculture at 30°C and then diluted to an OD_{600} of 0.1 into 50 mL cultures, where they were induced at an OD_{600} of 0.3 by the addition of DCPK to concentrations specified in the text. Cells were harvested 6 h after induction by centrifugation and stored at –20°C until determination of enzymatic activity.
All concentrations reported for DCPK refer to a volume to volume ratio.

3.2.4 Fed-batch fermentations

The defined mineral medium used for precultures of the fermentation and the fed-batch fermentations themselves contained (g per liter): glucose, 10 (5 for the preculture medium); $(NH_4)_2HPO_4$, 3.0; $MgSO_4*(7H_2O)$, 0.7; KH_2PO_4, 10; Na_2HPO_4, 1.5; $CaCl_2*(2H_2O)$, 0.03; citric acid, 1.0; thiamine, 0.02; kanamycin, 0.05; and trace element solution TES, 7 mL. The pH was adjusted to 7.0 by the addition of 10 N NaOH. TES contained (g per liter): $CaCl_2*(2H_2O)$, 2.28; $FeSO_4*(7H_2O)$, 10; $ZnSO_4*(H_2O)$, 1.4; $MnSO_4*(H_2O)$, 0.38; $CuSO_4*(5H_2O)$, 1; $MoO_4Na_{2*}(2H_2O)$, 0.5; $Na_2B_4O_7*(10H_2O)$, 0.23; 35% HCl 10 mL. The feeding solution contained (g per liter): glucose, 500; $MgSO_4*(7H_2O)$, 20; thiamine, 0.2; and TES 6 mL. Glucose, $MgSO_4$ and $CaCl_2$ were autoclaved separately, while the trace element solution, thiamine and kanamycin were added by sterile filtration. For fermentations, the

strains were taken from a glycerol stock stored at -80°C and plated on LB_{Km} agar. Some colonies were then transferred to an $M9_{Km}$ agar plate with glucose and incubated over night at 37°C to ensure maintenance of *E. coli* JM101's F-plasmid that carries the proline synthesis genes. A single colony from such a plate was used to inoculate 4 mL LB_{Km} which was then incubated for 12 h at 37°C. 2.5 mL of the LB_{Km} culture were used to inoculate 100 mL of the preculture medium. This seed culture was incubated for 11 h at 30°C and used then for the inoculation of the reactor. All fermentations were carried out in a 5 L Biostat A bioreactor (Sartorius BBI Systems GmbH, Melsungen, Germany) with a starting volume of 3 L. When the glucose in the medium was depleted, the feeding solution was added exponentially following the equation (adapted from [92]):

$$Feed(t) = \left(\frac{\mu_{set}}{Y_{X/S}} + m \right) C_{X0} \frac{V_0}{C_S} e^{\mu_{set} t} \qquad \text{Eq. 3.1}$$

where *Feed* (in L h^{-1}) is the feeding rate, μ_{set} (h^{-1}) is the desired specific growth rate, $Y_{X/S}$ (g g^{-1}) is the cell yield on carbon substrate (assumed to be 0.5 for glucose), m (0.04 g g^{-1} h^{-1}) is the specific maintenance coefficient [133], C_{X0} (g L^{-1}) is the cell dry weight concentration at the beginning of the feed, V_0 (L) is the liquid volume in the reactor at the start of the feed, C_S (g L^{-1}) is the concentration of glucose in the feeding solution, and t (h) is the time that has elapsed since the start of the feed. To maintain a dissolved oxygen value of above 20% of saturation, first the stirrer speed and then the aeration rate were increased to maximum values of 1200 RPM and 2 volume per volume per minute (vvm), respectively. After that, the feed regime was changed from exponential to linear when the dissolved oxygen concentration reached below 20% or an accumulation of acetate in the fermentation broth was detected as specified in the text. Temperature, pH and oxygen saturation were measured online. The pH was maintained at 7.0 by the automatic addition of 25% (wt/vol) NH_4OH or 1 M H_2SO_4. Foaming was suppressed by the initial addition of 5 mL L^{-1} 20% polypropylenglycol (PPG 2000). The fermentation parameters were controlled by the Micro DCU 300 control unit and the MFCS/win 2.0 software package of Sartorius BBI Systems.

3.2.5 Off-line analytical procedures

Growth was monitored by measuring the optical density at 600 nm. Cell dry weight (CDW) was determined by centrifuging 1.5 mL of cell suspension in preweighed 2 mL Eppendorf tubes, washing, and re-centrifuging, drying at 95°C for at least 24 h and then transferring into

a desiccator and cooling to room temperature. Glucose, acetate and ammonia concentrations were determined by enzymatic test-kits (R-Biopharm, Darmstadt, Germany). DCPK concentration in the medium was determined by HPLC on a Prontosil Eurobond C18 124 x 4.0 mm column (Bischoff Chromatography, Leonberg, Germany) using a gradient from 15% to 40% (vol/vol) acetonitrile in water over 12 minutes with detection at 210 nm on a Merck Hitachi LaChrom HPLC system.

For determination of GlyA activity, samples were resuspended in buffer G (20 mM Tris (pH 8.0) containing 10 mM dithiothreitol (DTT)). Cell walls were disrupted by grinding with glass beads in a mixer-mill (Retsch, Haan, Germany) for 90 seconds at a frequency of 30 Hz. Cell debris was removed by centrifugation at 10'000 g for 10 min. Total protein concentration was measured using the Bradford assay from BioRad (Hercules, CA USA) against BSA as standard and analyzed by SDS-PAGE. The activity of the serine hydroxymethyltransferase was quantified using 3-phenylserine as substrate and the assay was performed as described [171].

For determination of inclusion bodies and estimating the amount of recombinant protein produced, frozen cell pellets were resuspended in 50 mM sodium phosphate buffer (pH 7.0) to OD_{600} = 20-30 and disrupted in a French press. Soluble and insoluble fractions were separated by centrifugation for 30 min at 40'000 g and 4°C and further analyzed by SDS-PAGE. Purification of GlyA was performed on an Äkta prime system (GE Healthcare, Uppsala, Sweden). 100 µl of the soluble fraction were loaded on an anion exchange column (1 ml HiTrap Q FF, GE Healthcare, Uppsala, Sweden) equilibrated with buffer G. Elution was carried out with an increasing KCl gradient in buffer G. GlyA eluted at a KCl concentration of 250 mM.

3.3 Results

3.3.1 Adaptation of the expression system

We wanted to investigate the AlkS/P_{alkB} expression system for its capacity to produce a homogeneously induced culture of recombinant *E. coli* cells and its suitability for metabolic engineering and recombinant protein production in strictly aqueous systems. Therefore, we adapted the pSPZ-series of expression vectors [126] for direct insertion of recombinant genes as *Nde*I/*Asc*I fragments and inserted a variant of the *gfp* gene [33] and *E. coli*'s *glyA* gene encoding a functional threonine aldolase [78] (Fig. 3.1).

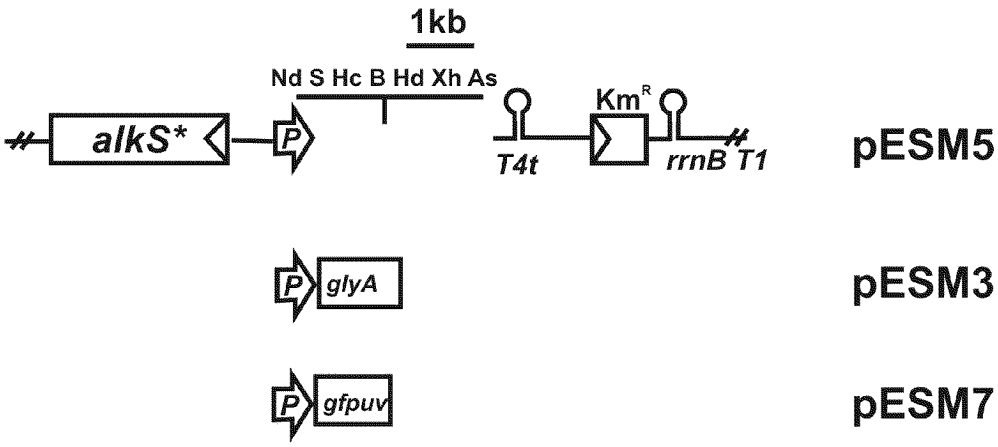

Figure 3.1: Structures of the central genetic elements used. All plasmids are medium-copy pBR322 derivatives. Plasmid pESM5 contains the AlkS/P_{alkB} expression system and a multiple cloning site. In plasmid pESM3, *E.coli*'s *glyA* gene, and in pESM7, the *gfpuv* gene are under control of the P_{alkB} promoter. Abbreviations: As, *Asc*I; B, *Bam*HI; Hc, *Hinc*II; Hd, *Hin*dIII; Nd, *Nde*I; S, *Sal*I; Xh, *Xho*I.

3.3.2 Homogeneous expression of GFP

To examine the homogeneity of the expression response of recombinant *E. coli* cells to induction by DCPK, the synthesis of the GFPuv protein under control of the AlkS/P_{alkB} expression system was analyzed by flow cytometry (Fig. 3.2). Cells were induced by different concentrations of DCPK and analyzed for their GFPuv level after 4 h (which is sufficient for full induction under conditions of unlimited growth [126]). The level of GFPuv increased from the situation without induction via 0.001% DCPK to 0.05% DCPK and did not further increase with the inducer concentration. At those DCPK concentrations that are relevant for typical production processes ($\geq$ 0.01%, see below), only one population of cells could be observed in all three induced situations. Furthermore, the strength of the induction was a function of the inducer concentration. Clearly, the response had a reduced variance when the inducer concentration became higher.

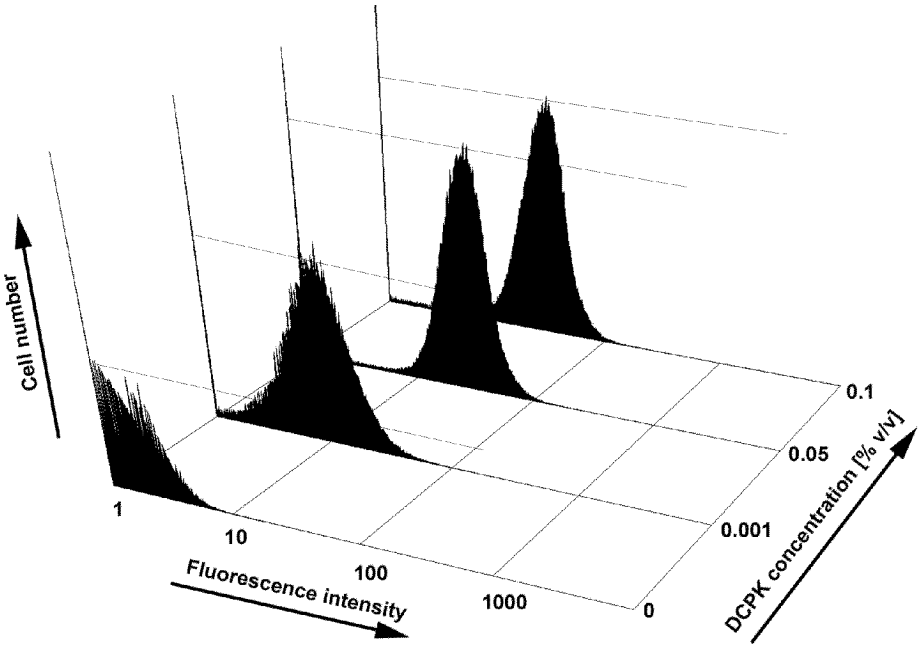

Figure 3.2: Histogram showing the number of cells and their fluorescence intensity against the concentration of the inducer DCPK. Cells were analyzed by flow cytometry 4 h after addition of DCPK.

3.3.3 Expression of serine hydroxymethyltransferase

Functional expression of GlyA in *E. coli* JM101 (pESM3) was verified in shake flasks with mineral medium and glucose as the sole carbon source and the inducer concentration varying from 0.001 to 0.1%. 6 hours after induction with 0.05% DCPK, far more than 20% of the total cell protein was GlyA as estimated from SDS-PAGE (see Fig. 3.3), resulting in specific activities in the order of 2 U mg^{-1} of total protein. However, 5-10% of the recombinant protein were found in the insoluble fraction (data not shown). Increasing the DCPK concentration further did not result in an increase of specific activity, but in a decreased cell dry weight concentration. On the other side, the addition of as little as 0.001% DCPK resulted in the overexpression of *glyA*, although to a lower level. Induction with 0.005% gave a similar expression level as with 0.05% (Fig. 3.3), confirming the results obtained with GFPuv. From these results, it appeared that the AlkS/P_{alkB} expression system was fully turned on above DCPK concentrations of 0.005%.

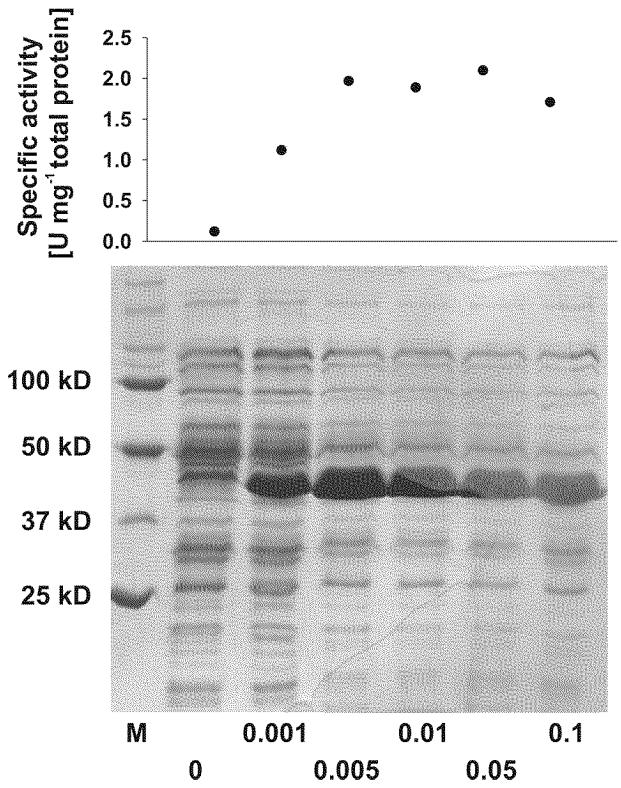

Figure 3.3: Specific activity of GlyA as a function of the inducer concentration and corresponding SDS-PAGE. Cells were harvested 6 h after induction. (M: marker; 0-0.1: concentration of added DCPK in %).

3.3.4 DCPK concentration decrease during fermentation

Considering the results from above, we investigated the behavior of the inducer concentration in fully aerated cultures of *E. coli*. After the addition of 0.05% DCPK to a fed-batch culture of plasmid-free *E. coli* JM101, a concentration drop over time was indeed observed (Fig. 3.4). At an airflow of 1.5 vvm, the concentration of DCPK decreased continuously to 0.01 % over 11 hours. At this concentration, the AlkS/P_{alkB} expression system is still fully induced according to the previous shake flask experiments (Fig. 3.3). As can be seen from Fig. 3.4, this result was confirmed by a number of subsequent cultivations of *E. coli* JM101 (pESM3), expressing *glyA*. The patterns of DCPK concentrations were similar for all these fermentations, indicating that the decrease in DCPK concentration was not due to any plasmid encoded function. This was further supported when an experiment was performed under the same conditions as for the fermentations but without inoculation: the DCPK concentration decreased in a very similar fashion (Fig. 3.4).

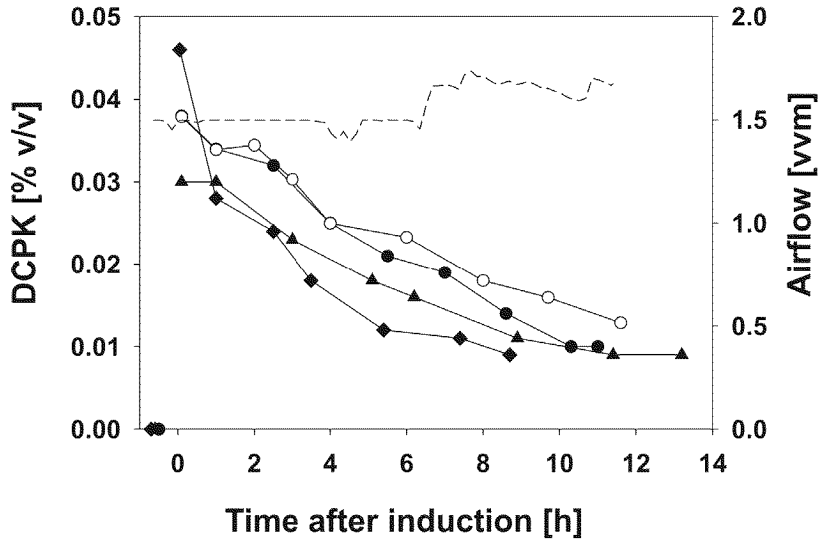

Figure 3.4: Decrease of the DCPK concentration in the fermentation broth. Samples from three different fermentations of *E. coli* JM101: (●) plasmid-free, DCPK addition at growth rate $\mu = 0.15\ h^{-1}$; dashed line: corresponding airflow into the reactor in vvm; (▲) containing plasmid pESM3, induction at growth rate $\mu = 0.15\ h^{-1}$; (◆) containing plasmid pESM3, induction at growth rate $\mu = 0.2\ h^{-1}$; (○) from fermentation without inoculation (lines drawn only to show trend).

3.3.5 Fed-batch cultivations with induction at different growth rates

An often applied method of operation for the production of recombinant proteins is the induction of the expression system towards the end of the fermentation, with optimized variations adapted to the particular needs of the specific process and product [142; 196]. This way, a high cell density can be achieved before induction and the resulting additional metabolic burden, which for example reduces the risk of plasmid loss [88]. However, at such a late stage of fermentation, the specific growth rate is already rather low, often even below $0.05\ h^{-1}$, due to the difficulties in supplying enough oxygen. Most of the energy consumption of the cells then goes into maintenance [142] and the additional request of protein production results in further stress. To elucidate the effect of the growth rate on recombinant protein expression employing the AlkS/P_{alkB} expression system, cells were induced during fed-batch fermentations at different specific growth rates of 0.05, 0.15, and $0.2\ h^{-1}$.

3.3.6 Volumetric productivity as a function of specific growth rate

In Fig. 3.5, time profiles of the cell dry weight concentration and of the specific activity of the recombinant GlyA are shown for fermentations with different predefined specific growth rates μ_{set}. Within the first few hours after induction, the cells produced the recombinant enzyme more rapidly at a higher growth rate. The maximum specific activity at the slow specific growth rate of 0.05 h^{-1} was 5.5 U mg^{-1} total protein after 19.6 hours of induction at a cell dry weight of 26.9 g L^{-1}. This fermentation at a low specific growth rate received a second addition of DCPK 9.4 hours after the first one to increase the inducer concentration again to 0.05 % (Fig. 3.5a). The maximum specific activity value increased slightly when μ_{set} was increased to 0.15 h^{-1}, to 5.9 U mg^{-1} total protein at a cell dry weight of 29.2 g L^{-1} after 11.4h (Fig. 3.5b), and reached its maximum value at the highest growth rate examined, μ = 0.2 h^{-1}, when 6.4 U mg^{-1} total protein was reached 7.4 hours after induction at a cell dry weight of 30.1 g L^{-1} (Fig. 3.5c). From this data, and by comparing the specific production rates (Fig. 3.8), induction at a high growth rate should be most favorable.

3.3.7 Acetate and glucose concentrations during fermentations

Acetate and glucose concentrations during fed-batch fermentations are shown in Fig. 3.6. The increase in concentration of acetate during the initial batch phase was expected as a result of overflow metabolism. However, we observed a second increase of acetate concentration up to 1.3 g L^{-1} during cultivation after the cells were induced at specific growth rates μ = 0.2 or 0.15 h^{-1}. We therefore performed control fermentations with either *E. coli* JM101 or *E. coli* JM101 (pESM5). No accumulation of acetate could be observed after the addition of 0.05% DCPK to the plasmid-free *E. coli* JM101 fermentation (μ_{set} = 0.15 h^{-1}), excluding any toxic or stress inducing effects of DCPK on *E. coli* as the cause of acetate formation. Plasmid pESM5 contains the functional AlkS/P_{alkB} expression system, but no recombinant gene is under the control of the P_{alkB} promoter. The addition of 0.05% DCPK to a culture of *E. coli* JM101 harboring pESM5 (μ_{set} = 0.17 h^{-1}) did not provoke excretion of acetate either. In the fermentation with induction at low specific growth rate μ = 0.05 h^{-1}, initially no acetate formation could be observed, whereas after a second pulse of DCPK at a later stage of cultivation, also in this case the cells began to form acetate. Following the accumulation of acetate in the induced cultivations at specific growth rates of either 0.15 or 0.2 h^{-1}, also the accumulation of glucose in the medium could be observed (Fig. 3.6b). Changing the feed

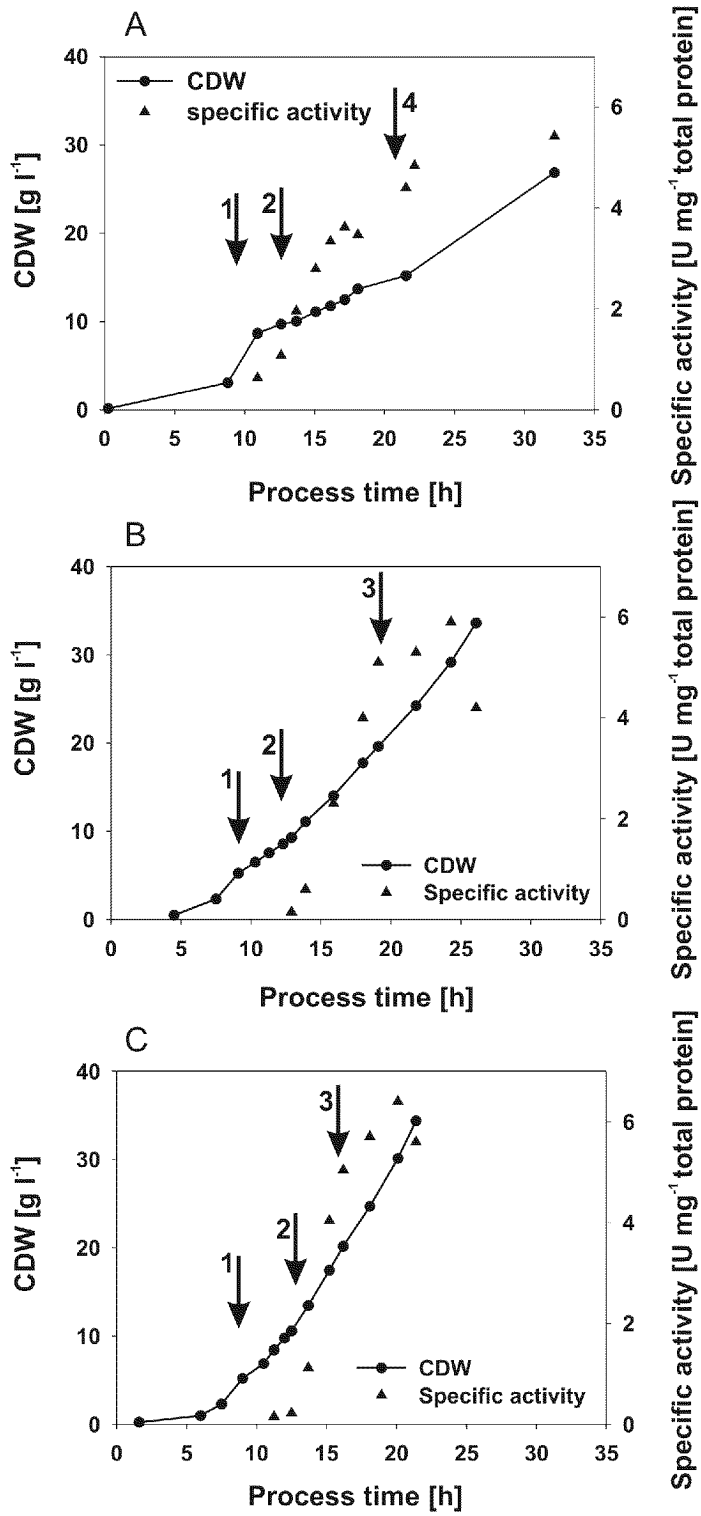

Figure 3.5: Fed-batch cultivations of *E. coli* JM101 (pESM3) showing the time course of the cell dry weight concentration and the specific activity of GlyA. Induction was performed at different specific growth rates. a) growth rate 0.05 h^{-1}; b) growth rate 0.15 h^{-1}; c) growth rate 0.2 h^{-1}. Arrows: (1) start of exponential feed; (2) induction with 0.05 % DCPK; (3) setting feed linear; (4) second addition of 0.05 % DCPK.

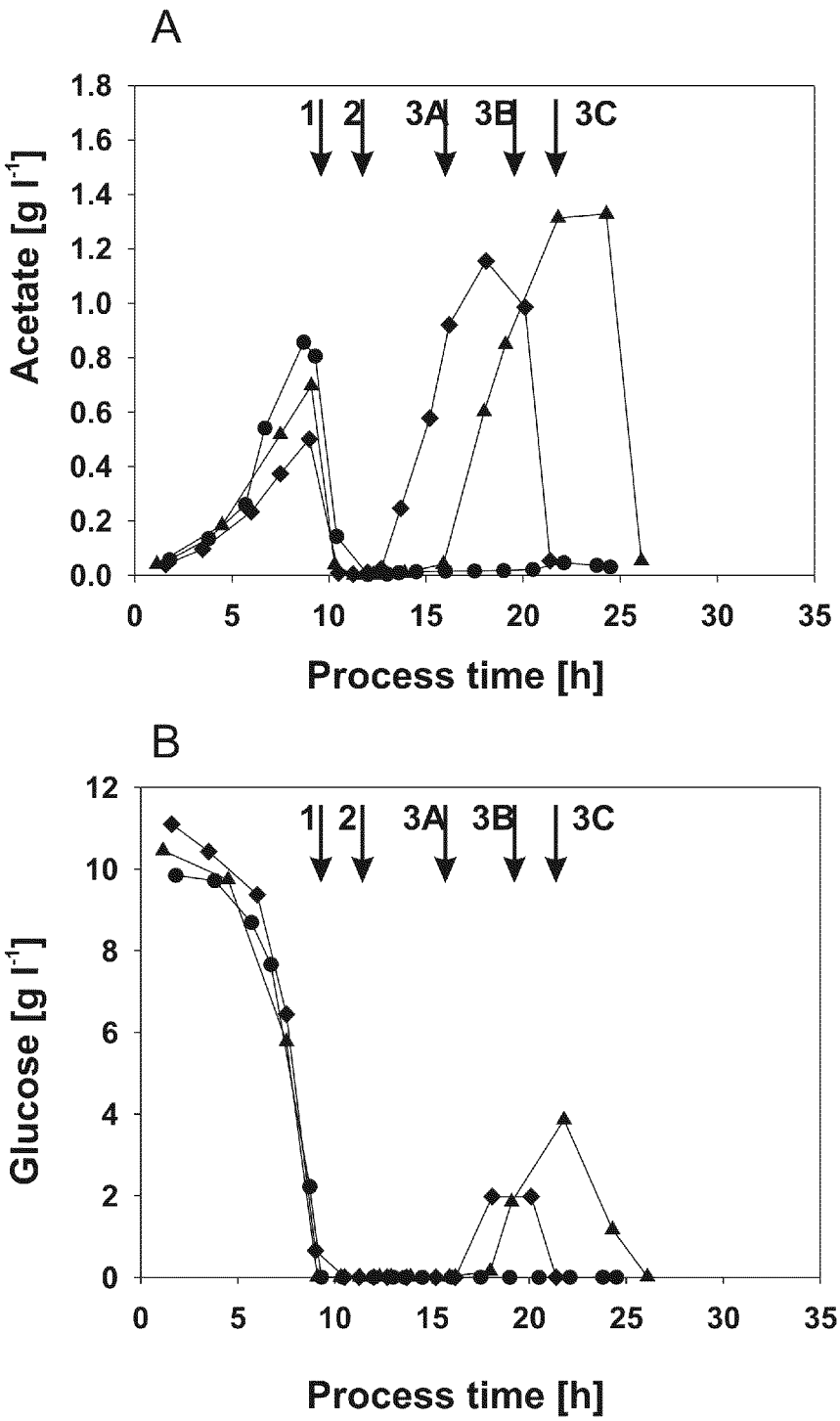

Figure 3.6: Time profile of the acetate and glucose concentrations of fed-batch fermentations of *E. coli* JM101 (●) plasmid-free, DCPK addition at growth rate $\mu = 0.15\ h^{-1}$; (▲) containing plasmid pESM3, induction at growth rate $\mu = 0.15\ h^{-1}$; (◆) containing plasmid pESM3, induction at growth rate $\mu = 0.2\ h^{-1}$. Arrows: 1) start of exponential feed; 2) addition of 0.05 % DCPK; 3) setting feed linear, A) at $\mu = 0.2\ h^{-1}$, B) at $\mu = 0.15\ h^{-1}$, C) at $\mu = 0.15\ h^{-1}$, plasmid-free.

regime from exponential to linear caused a concentration drop of glucose as well as acetate in the fermentation broth. The glucose accumulation was not observed in the control experiments, neither with plasmid-free nor pESM5 containing cells.

3.3.8 Recombinant protein production with an optimized protocol

Based on the previous results, we performed an optimized fermentation (Fig. 3.7), considering the constraints of sufficient oxygen supply and avoiding the formation of acetate after induction. In the fed-batch phase, the cells were grown at a growth rate of 0.2 h^{-1} up to a cell density of 20 g L^{-1} before induction with 0.05 % DCPK. The feed was maintained exponential for one more hour and then, as oxygen transport capacity of the reactor reached its maximum, set to linear. After 9.5 h of linear feed, a final cell dry weight of 51.7 g L^{-1} was reached, resulting in a final specific activity of 5.2 U mg^{-1} total protein, whereas the maximum specific activity of 6.3 U mg^{-1} total protein was observed 6.5 h after induction at a cell dry weight of 41.6 g L^{-1}. The specific production rate, however, dropped very fast as can be seen in Fig. 3.8. The amount of produced recombinant protein has been estimated to be 120 mg per gram CDW. The specific activity of GlyA decreased at elongated fermentation times, most probably because of some proteolytic activity of the stressed cells as the growth rate steadily decreased because of the linear feed. Only a minor part of the recombinant protein was found in the insoluble fraction due to aggregation (data not shown).

3.4 Discussion

The AlkS/P_{alkB} expression system has the potential to overcome several drawbacks associated with current recombinant expression systems, such as carbon catabolite repression, strain dedications, or complex or difficult to control induction procedures. However, it has been designed for preparative applications in two-liquid phase cultivations [126] where a second organic phase could serve as a reservoir for the required apolar inducer [21; 22; 126; 127]. In this work, we investigated its suitability for metabolic engineering or protein production purposes in strictly aqueous systems. First we addressed the question whether the system would produce a monostable or a bistable ("all or none" [24]) expression response, as this would interfere with the usefulness of the system for metabolic engineering purposes [90]. It has been shown that a positive feed-back characteristic of the expression system is a

necessary – though not sufficient – requirement for bistable expression behaviour [10; 124]. In the AlkS/P_{alkB} system, such a characteristic is potentially introduced by induction of *alkS* expression by the activated gene product itself, which has been confirmed in a *Pseudomonas* background [23]. Consequently, bistable behaviour cannot a priori be excluded.

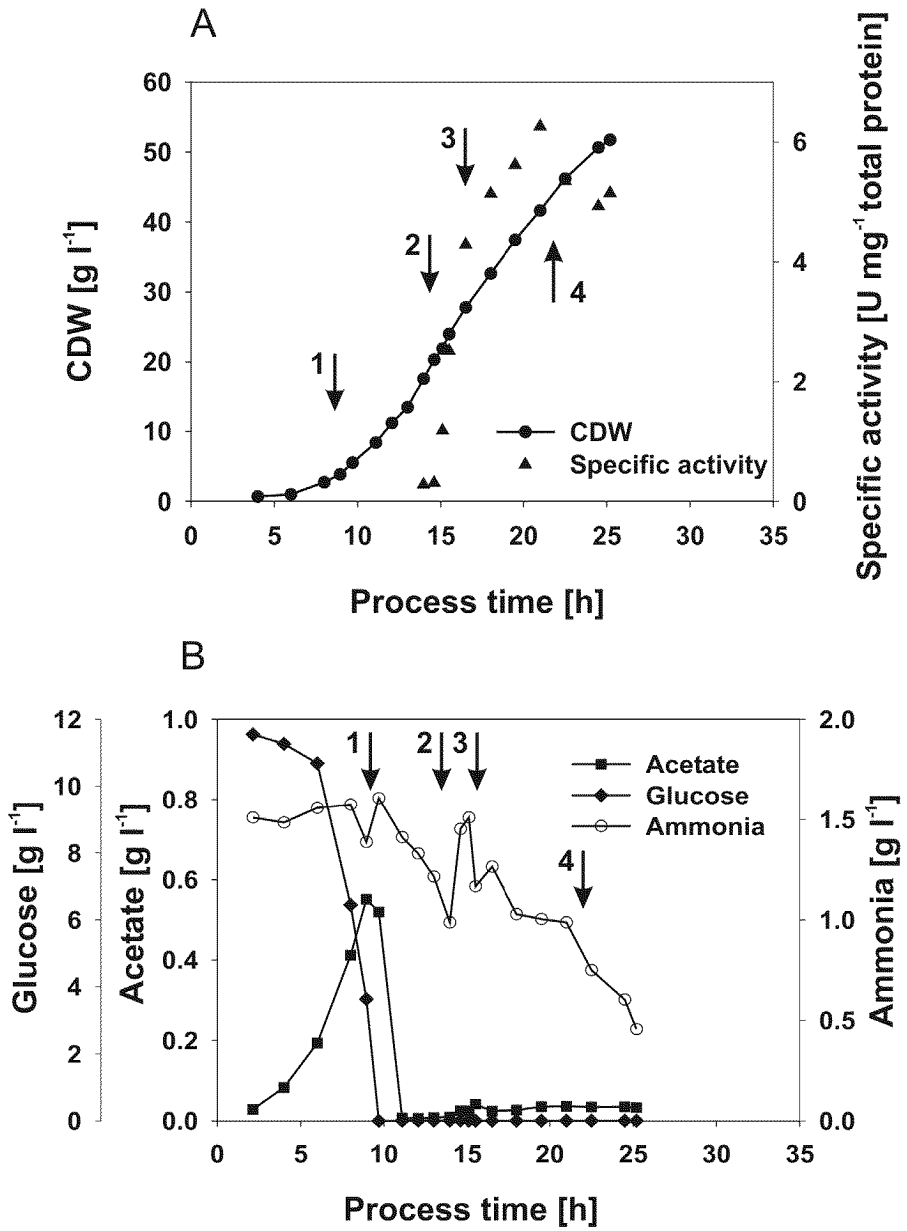

Figure 3.7: Fed-batch cultivation of *E. coli* JM101 (pESM3) with induction at optimized conditions. a) Time course of cell dry weight and specific GlyA activity. b) Time profile of the corresponding glucose, acetate and ammonia concentrations in the fermentation broth. Arrows: 1) start exp. feed (μ_{set} = 0.2 h^{-1}); 2) induction with 0.05 % DCPK; 3) setting feed linear; 4) reduced linear feed.

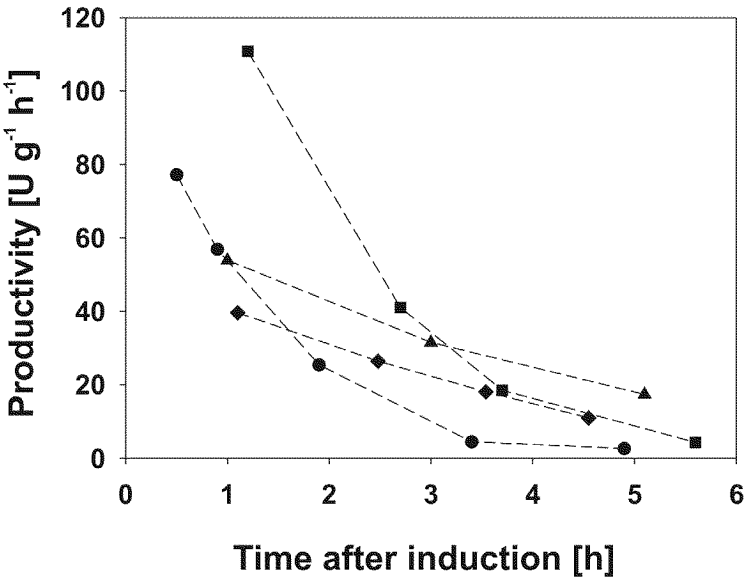

Figure 3.8: Specific GlyA production rates in fermentations of *E. coli* JM101 (pESM3) with induction at different specific growth rates. (■) at growth rate 0.2 h^{-1}; (▲) at growth rate 0.15 h^{-1}; (◆) at growth rate 0.05 h^{-1}; (●) optimized fermentation.

However, when single cells producing GFPuv under AlkS/P_{alkB} control were analyzed for fluorescence, we found only one population of cells over the range from 0.001 to 0.1 % of inducer, suggesting that the specific parameters of the AlkS/P_{alkB} expression system in *E. coli* – such as the extent of the autocatalytic behaviour of the *alkS* expression and potential AlkS cooperative behaviour at P_{alkB}, maximal activity of activated AlkS, and ratio of activities of induced over non-induced state - do not result in bistable behaviour [10; 24; 124]. As the translational apparatus is thought to be saturated at full induction, pre-translational sources of fluctuation hardly matter anymore, in particular differences in plasmid copy number per cell of pBR-type plasmids [167]. This could explain the reduced variance at higher inducer concentrations (Fig. 3.2).

The fluorescence analysis also indicated that the AlkS/P_{alkB} expression system operates already at full expression at relatively low inducer concentrations of 0.05%. Taking additionally into account the *glyA* expression data (Fig. 3.3), this value is as low as 0.005%. Consequently, it will be very difficult to operate this expression system in *E. coli* in another fashion than fully expressed. Considering the concentration drop of the inducer over one cultivation from 0.05 to 0.01% (Fig. 3.4), it will be rather cumbersome to implement control

systems that allow maintaining the inducer concentration at a level required for sub-maximal expression. Consequently, in order to exploit the AlkS/P_{alkB} system for metabolic engineering purposes, future work will need to expand the inducer concentration window to elicit intermediate expression responses, most probably by re-designing *alkS* expression.

On the other hand, the fact that the system is already fully turned on above DCPK concentrations of 0.005 % and no DCPK-toxicity effects were observed up to concentrations of 0.05 %, there is a considerable range over which the concentration of the relatively volatile DCPK can drop in aerated cultivations before the expression level is affected. This indicates that the AlkS/P_{alkB} expression system might be useful for the mass production of proteins where full induction of the system is normally the experimental method of choice anyway.

When comparing the maximum specific GlyA activities obtained from shake flask or from fed-batch cultivations, the GlyA activities from the shake flask experiments were around three-fold lower. But by looking at the specific production rates, calculated to be 280 U g^{-1} h^{-1} in the shake flask, the results indicate a possible advantage of induction at a high specific growth rate of 0.32 h^{-1}. However, also the formation of inclusion bodies was observed in shake flasks, contributing to – but not fully explaining - the lower specific activity.

The problem of producing inactive forms of GlyA was no longer present – or at least significantly reduced - when we investigated mass-production of the enzyme in fed-batch cultivations with respect to suitable patterns of induction (Fig. 3.5). It is known that the activity and the concentration of components of the cellular protein synthesis machinery show a direct relation to the actual growth rate [118], for instance, the number of ribosomes and the fraction of functioning ribosomes is increasing with increasing growth rate [193; 194]. This suggests that, as a general rule, recombinant protein production is most efficient at higher growth rates. However, simulations suggested that the optimum growth rate for maximum expression of a cloned gene in recombinant microorganisms is also depending on the stability of the recombinant product [89]. Furthermore, other factors than the expression system such as the stress situation and the proteolytic activity affect the efficiency of recombinant protein production [118]. The literature provides studies that found no correlation between growth rate and protein production [58; 153], whereas others found a distinct optimum for the specific growth rate [44; 62; 134] or a maximum production rate at a high growth rate [29; 141; 142].

As the fundamental reasons for these different observations remain unclear, the influence of the specific growth rate needs to be determined. We limited our investigations to a maximum specific growth rate of 0.2 h^{-1} as formation of acetate is a well-known phenomenon for *E. coli*

cultures at growth rates between 0.17 h^{-1} [82] and 0.23 h^{-1} [136], which should be avoided because of its inhibitory effect on growth and on product formation [69]. Furthermore, our reactor system showed a K_La of roughly 250 h^{-1} at high cell densities (data not shown), which indicates that it is difficult to maintain a growth rate larger than 0.2 h^{-1} for longer than 4 h or one generation time, which we considered the minimum time period to follow the development of the specific GlyA activity.

Our experiments confirmed that induction at a higher growth rate indeed is advantageous for the production of GlyA as a higher specific activity could be achieved in an even shorter time frame than in cultivations with induction at a low growth rate (Fig. 3.5). However, the production rate at the highest growth rate showed a sharp drop within the first 4 h after induction, whereas at low growth rates, a smoother decline was observed (Fig. 3.8). We also observed a strong increase in acetate formation after the cells were induced. The data suggest that this depended on recombinant protein production alone as no acetate was detected in the control fermentations: neither the addition of DCPK to a cultivation of *E. coli* JM101 (Fig. 3.6a) nor to a fermentation of *E. coli* JM101 (pESM5) (vector without a gene expressed from the P_{alkB} promoter; data not shown) resulted in additional acetate formation. This excluded the metabolic burden of the plasmid replication alone [11] and any stress induced by DCPK directly as the main cause for acetate formation.

Acetate formation after induction also depended on the growth rate: at a growth rate of 0.2 h^{-1}, the cells started earlier with acetate excretion than at a growth rate of 0.15 h^{-1}. A simple explanation might be that the stress induced by the expression of recombinant proteins led to a reduction in the specific growth rate and the glucose consumption rate [122], so that the glucose feed rate no longer matched the actual growth rate of the cells, however, we cannot completely exclude accompanying cell lysis. This would have led to an increase of the glucose concentration in the fermentation broth, a typical prerequisite for acetate formation. In the optimized fermentation, acetate formation was avoided by changing the feed regime to linear one hour after induction. This way, we exploited at least in the beginning, the high capacity of the cell for recombinant protein production, stemming from the high pre-induction specific growth rate, and at the same time avoiding the discrepancy between feed rate and the glucose uptake rate of the cells (Fig. 3.7).

In this contribution, we addressed expression behavior of the AlkS/P_{alkB} system and the development of a suitable production strategy in recombinant *E. coli* strains. This system unites an attractive number of suitable properties for recombinant expression systems, such as

the independence from carbon catabolite repression, the availability of self-contained vectors, a truly inducer concentration-dependent behavior, and a cheap inducer. The volatility of the inducer and the small window of useful inducer concentrations will make the adjustment of expression states below full induction cumbersome and need to be addressed in the future. Finally, the only moderate final cell dry weight yield achieved in the current fermenter system would require further optimization of the mixing regime or switching to oxygen enriched air to increase oxygen transfer.

In summary, we could demonstrate that the AlkS/P_{alkB} system is an efficient system for the recombinant production of enzymes, for example for the serine hydroxymethyltransferase GlyA, that has shown much potential in diastereoselective carbon-carbon bond formation [78; 137].

Acknowledgments

This work was supported by a grant to S. Makart from the ETH.

We are indebted to E. Niederer from the Central Laboratory for Flow Cytometry of the Institute of Biomedical Engineering, ETH and University of Zurich for help with the flow cytometer.

4 Towards preparative asymmetric synthesis of β-hydroxy-α-amino acids: L-*allo*-threonine formation from glycine and acetaldehyde using recombinant GlyA

Stefan Makart, Matthias Bechtold, Sven Panke

submitted for publication

Abstract

The diastereospecific formation of L-*allo*-threonine, catalyzed by the serine hydroxymethyltransferase GlyA form *Escherichia coli*, was studied with regard to the application in integrated processes with continuous chromatography as *in situ* product recovery tool. The design of such an integrated process relies on a suitable description of enzyme stability and kinetics under relevant process conditions. Therefore, the effects of addition of organic co-solvents – methanol and acetonitrile – to the reaction mixtures on activity, stability, and diastereoselectivity were investigated. A series of progress curves from batch reactions at 35°C in 50 mM sodium phosphate buffer pH 6.6 and 50 mM sodium phosphate buffer pH 6.6 in 20% methanol was used to estimate the respective kinetic parameters for an appropriate kinetic model.

The experimental data agreed well with a kinetic model for a bi-uni reaction mechanism and a pseudo-equilibrium assumption. The model was then applied in order to simulate the performance of the enzyme in an enzyme membrane reactor (EMR) and gave an excellent agreement with the corresponding experimental data. A space time yield of 227 g L^{-1} d^{-1} was achieved in a continuous running EMR without loss of enzyme activity over 120 h of operation.

4.1 Introduction

The stereospecific formation of carbon-carbon bonds is of great importance in current organic synthesis. Next to chemical synthesis routes, biocatalysis provides attractive alternatives with aldolases, transaldolases and transketolases, and hydroxynitrile lyases [17]. In particular aldolases have received a lot of attention for applications in biocatalysis [140]. They catalyze a reversible aldol reaction of a ketone or aldehyde donor and an aldehyde acceptor, and are usually highly specific for the donor substrate but flexible with respect to the acceptor group [155]. In addition, their ability to generate new stereocentres makes them an attractive tool for asymmetric synthesis [42]. Aldolases are now widely used, both in academic research as well as in industrial applications. Dihydroxyacetone phosphate (DHAP)-dependent aldolases constitute the most prominent group [140] and have found widespread use e.g. in the synthesis of iminocyclitols (azasugars) [39; 40]. However, their application is limited by the difficult access to the required donor DHAP [140]. The acetaldehyde-dependent 2-deoxyribose-5-phosphate aldolase can perform sequential aldol reactions [49], which can be exploited in the synthesis of statins [35; 54; 128]. The pyruvate-dependent *N*-acetylneuraminic acid aldolase has attracted much attention for the synthesis of sialic acids [77; 84; 107] up to industrial scale [96]. NeuAc aldolases have been furthermore engineered for the synthesis of influenza A sialidase inhibitors similar to zanamivir [185].

However, despite their great potential for asymmetric synthesis and the wealth of promising applications, the implementation of aldolases in industrial biocatalysis is hampered as many of these reactions exhibit an unfavorable position of the thermodynamic equilibrium [51; 52]. This leads to - an economically rarely feasible - incomplete use of starting materials. Furthermore, the comparatively long reaction times that are frequently encountered in aldolase processes can provoke negative effects on the stereoselectivity of the reactions, especially in the formation of diastereomers, where a favorable diastereomeric excess in the initially kinetically controlled reaction might be reduced when the reaction approaches thermodynamic control [78]. Different strategies are available to address the problem of an unfavorable thermodynamic equilibrium: (i) shifting the equilibrium by changing the temperature, (ii) increasing yield on the more expensive substrate by increasing the concentration of the cheaper substrate; and (iii) increasing yield by *in situ* product recovery (ISPR) [105]. Rapid product removal would be especially desired to preserve an initially favorable diastereomeric excess.

However, continuous ISPR can be very difficult to realize as the substrate and product in aldolase reaction have frequently very similar properties and consequently require a highly efficient separation process that furthermore is compatible with the enzyme operation. Our group explores the on-line coupling of enzyme reactors with continuous chromatographic processes such as simulated moving bed (SMB) [Chapter 2]. This approach requires the same solvent for the enzymatic reaction and the chromatographic separation process. To provide the required selectivity in the separation, the addition of – in chromatographic processes - commonly used organic solvents such as methanol and acetonitrile to the reaction buffer has to be considered. However, the presence of small amounts of organic solvents can cause major changes in enzyme catalytic activity and stability [25] and thereby influence the efficiency of the overall process. In order to design such an integrated process, a suitable and reliable description of the enzyme kinetics under appropriate reaction conditions is required.

In this study, we investigated the behavior of GlyA, a serine hydroxymethyltransferase from *Escherichia coli* that requires pyridoxal-5-phosphate (PLP) as a cofactor and can functionally be classified as a glycine-dependent aldolase. It catalyzes the synthesis of β-hydroxy-α-amino acids with two new chiral centers, such as L-*allo*-threonine, from glycine and an aldehyde, such as acetaldehyde (Fig. 4.1). The reaction does not depend on phosphorylated substrates, and model substrates are readily available. In the growing amino acid market [93], the β-hydroxy-α-amino acids form an important class of compounds as naturally occurring amino acids or as components of complex compounds with interesting biological properties, such as antibiotics [67; 87; 137] or an anti-parkinsonism drug [99]. The stereoselectivity of the enzyme is absolute on the C-alpha atom, less strict on C-beta, and the diastereomeric excess decreases over time. Furthermore, the enzyme exhibits a broad substrate spectrum towards the aldehyde acceptor [78].

4.2 Experimental

4.2.1 Chemicals

All chemicals were either from Sigma-Aldrich Chemie GmbH (Buchs, Switzerland) or Roth (Reinach, Switzerland) unless mentioned otherwise. Acetonitrile (HPLC grade) was purchased from Chemie Brunwschwieg (Basel, Switzerland).

4.2.2 Enzyme

The applied enzyme was produced in fed-batch fermentations with *E. coli* JM101 (pESM3) as described previously [Chapter 3]. The harvested cells were resuspended in 50 mM sodium phosphate buffer pH 6.6 and disrupted in a high-pressure homogenizer (Haskel Hochdrucksysteme, Wesel, Germany) at a 1000 bar pressure drop over the orifice for one hour. The resulting cell free extract (CFE) containing the soluble enzyme was cleared from the cell debris by centrifugation at 30'000 g and 4°C for 30 min and stored at -80°C until further use. Total protein concentration in the CFE was 40 mg mL^{-1}.

4.2.3 Analytics

All ratios and percentages of liquid mixtures mentioned in the following refer to volume per volume.

A precolumn derivatization method was applied for the quantification of the amino acids glycine and threonine [38]. For analysis, samples were diluted in 0.1 M sodium borate buffer pH 8.0 to obtain substrate or product concentrations between 0.02 and 1 mM. An aliquot of 150 µL of derivatization solution (10 mM 9-fluorenylmethoxycarbonyl chloride (FMOC-Cl) in acetonitrile) was added to 150 µL of the diluted samples, mixed and incubated at room temperature for 90 seconds. An aliquot of 150 µL of quenching solution (20 mM 1-adamantylamine (ADAM) in MeOH) was added and mixed again. Of this mix, 10 µL were injected onto a Prontosil Eurobond C18 (124 x 4.0 mm column, Bischoff Chromatography, Leonberg, Germany), mounted on a Merck-Hitachi LaChrom HPLC system, using acetonitrile as eluent A and 50 mM sodium acetate buffer pH 4.25 as eluent B with the following gradient profile: 0-3 min, isocratic 27% A; 3-12 min, gradient up to 35% A; 12-14 min, gradient up to 100% A; 14-17 min, isocratic 100% A; 17-19 min, gradient down to 27%

A; 19-22 min, isocratic 27% A; the flow-rate was set to 1.5 mL min^{-1}. Detection was done at 265 nm. Commercially available pure stereoisomers of threonine were used as references.

Acetaldehyde was quantified by precolumn derivatization with 2,4-dinitrophenylhadrazine (DNPH) [37] with detection at 365 nm on the same HPLC system as described above. The derivatization solution was prepared by dissolving 40 mg DNPH in 20 mL acetonitrile. An aliquot of 6 µL of 1 M HCl was added to 1 mL of diluted sample and mixed. Then 50 µL of derivatization solution were added, mixed and left at room temperature for 45 min. An aliquot of 10 µL was then injected onto the same column as before with isocratic elution in 60:40 acetonitrile/10 mM ammonium acetate buffer for 13 min at a flow-rate of 0.8 mL min^{-1}.

The diastereomeric excess (d.e.) of a product mixture was calculated as the ratio of the difference and of the sum of the concentrations for L-*allo*- and L-threonine.

Total protein concentration was measured using the Bradford assay [16] from BioRad (Hercules, CA) against bovine serum albumin as standard.

4.2.4 Batch reactions

Enzyme assays to assess the relative activity, stability and stereoselectivity of the enzyme for a series of different buffer/organic solvent compositions up to 30% organic solvent content were performed in 1 mL assays at 35°C. The reaction mixture contained 2 mg of total protein, 100 mM glycine, 100 mM acetaldehyde, and 40 µM PLP in 50 mM sodium phosphate buffer pH 6.6 and the respective organic solvent. Aliquots of 300 µL were removed at specific time points as specified in the text. The enzymatic reaction was stopped by the addition of 10.5 µL of 1 M HCl and the samples were centrifuged for 2 min at 13'200 g to remove residual proteins. The samples were stored at -80°C until further analysis.

For the stability experiments, the CFE was diluted in the corresponding aqueous-organic solvent mixtures and kept at a constant temperature of 25°C in a shaking water bath. After different incubation times up to 7 days, samples were subjected to enzymatic assays as described above.

Enzyme assays for kinetic studies were performed in continuously stirred 10 mL batch experiments at a constant temperature of 35°C. The kinetics were investigated in detail for 50 mM sodium phosphate pH 6.6 and for 50 mM sodium phosphate pH 6.6 in 20% methanol as reaction solvents. The reaction mixture contained furthermore 40 µM PLP and varying concentrations of substrate and CFE. The reactions were started by the addition of the second

substrate, acetaldehyde. To follow the course of the reaction, aliquots of 300 µL were periodically withdrawn and processed as mentioned above.

In this study, an enzymatic activity of 1 U is defined as the formation of 1 µmol of L-*allo*-threonine per minute.

4.2.5 Determination of kinetic parameters

We applied a model-based experimental analysis approach [109] to identify an appropriate kinetic model for enzyme catalysis. A series of progress curves, depicting the formation of L-*allo*-threonine in 10 mL batch reactions as described before, was used as dataset. The gPROMS software (Process Systems Enterprise Ltd., London, UK) was used to estimate the kinetic parameters for the supposed kinetic model (see next section) by minimizing the deviation between the experimental data and the model prediction. The estimation process is based on a maximum likelihood objective function and a constant relative variance model, with the standard deviation set to 10%.

4.2.6 Enzyme kinetic model

During the aldol reaction of glycine and acetaldehyde catalyzed by GlyA, the tightly bound co-factor PLP first activates glycine, then the aldehyde acts as the acceptor and the product is formed [42; 143]. We therefore suggest that the reaction follows an ordered bi-uni reaction mechanism. A pseudo-equilibrium assumption [135; 160] was used to derive a rate equation capable of describing the reaction. According to the pseudo-equilibrium assumption, the association and dissociation of any Michaelis complex are at equilibrium, and the reaction rate is determined by the breaking and making of covalent bonds. This can be written schematically for a general ordered bi-uni reaction as:

$$\mathrm{E} \underset{k_{-1}}{\overset{k_1 C_\mathrm{A}}{\rightleftarrows}} \mathrm{EA} \underset{k_{-2}}{\overset{k_2 C_\mathrm{B}}{\rightleftarrows}} \mathrm{EAB} \underset{k_{-3}}{\overset{k_3}{\rightleftarrows}} \mathrm{EP} \underset{k_{-4} C_\mathrm{P}}{\overset{k_4}{\rightleftarrows}} \mathrm{E} \qquad \text{Eq. 4.1}$$

Here, E represents the free enzyme, EA, EAB and EP the complexes of enzyme and substrates A and B or of enzyme and product P. This model results in the following rate equation [160], already adapted to the formation of L-*allo*-threonine from glycine and acetaldehyde:

$$-r_\mathrm{A} = \frac{\dfrac{k_\mathrm{cat}^\mathrm{f}}{K_\mathrm{mGly} K_\mathrm{mAld}} \left(C_\mathrm{Gly} C_\mathrm{Ald} - C_\mathrm{Thr} / K_\mathrm{eq} \right)}{1 + \dfrac{C_\mathrm{Gly}}{K_\mathrm{mGly}} + \dfrac{C_\mathrm{Gly}}{K_\mathrm{mGly}} \dfrac{C_\mathrm{Ald}}{K_\mathrm{mAld}} + \dfrac{C_\mathrm{Thr}}{K_\mathrm{mThr}}} C_\mathrm{E} \qquad \text{Eq. 4.2}$$

This rate equation contains three types of parameters: a catalytic constant k_{cat}^{f}; the dissociation constants of the Michaelis-Menten complexes of enzyme with glycine, acetaldehyde, and L-*allo*-threonine (K_{mGly}, K_{mAld} and K_{mThr}), and the equilibrium constant K_{eq} for the three compounds. The terms C_{Gly}, C_{Ald}, C_{Thr}, and C_E refer to the concentrations of glycine, acetaldehyde, L-*allo*-threonine, and the overall concentration of the active enzyme, which is composed of free form of the enzyme and the enzyme-reactand complexes. However, as we operated with CFE rather than with pure enzyme, C_E is given as the concentration of total protein in g L^{-1}. Additionally, the equilibrium constant K_{eq} can be derived either as a parameter from the model or calculated independently from the concentrations of the three reactands at equilibrium after long enzyme reactions:

$$K_{eq} = \frac{C_{Thr,eq}}{C_{Gly,eq} C_{Ald,eq}} \qquad \text{Eq. 4.3}$$

4.2.7 Continuous reactions and reactor model

The reactions were performed in an enzyme membrane reactor (EMR) (Julich Chiral Solutions GmbH, Jülich, Germany) with an internal volume of 10 mL, which was operated at 35°C and with an internal magnetic stirrer at 600 rpm. The reactor was equipped with a Biomax PB polyethersulfone membrane (Millipore Corporation, Bedford, MA, USA) with a cut off of 10 kDa. An HPLC pump was used to deliver reaction solvent and substrates. The substrates were kept separately to avoid chemical side reactions during storage and were mixed in the static mixer just shortly before entering the reactor. A defined amount of CFE (as specified in the text) was applied through a 6-port injection valve (GE Healthcare, Uppsala, Sweden). The reactor was then flushed with the corresponding reaction solvent for 45 min at 1 mL min^{-1} before addition of substrates was started (concentration and flow rates as given in the text). Aliquots were periodically withdrawn from the reactor outlet stream and stored at –80°C until further analysis.

To describe the enzymatic conversion in the EMR, an ideal continuous stirred tank reactor (CSTR) model was applied:

$$\frac{\partial C_i}{\partial t} = \frac{F}{V_{reactor}} (C_{i,in} - C_i) + r_{(C_i, C_E)} \qquad \text{Eq. 4.4}$$

Here, C_i represents the concentration of compound *i* in the reactor, $C_{i,in}$ the concentration of compound *i* at the inlet of the reactor, F the volumetric flow rate, $V_{reactor}$ the volume of the

EMR, and r the reaction rate as a function of the concentrations of the compounds i (see Eq. 4.2) and enzyme.

Furthermore, for a detailed prediction of the reactor performance, diffusion, and non-ideal effects upstream of the reactor (i.e. in the tubing and injection valve) had to be included. This was achieved by the implementation of an ideal mixer stage:

$$\frac{\partial C_i}{\partial t} = \frac{F}{V_{mixer}}(C_{i,in} - C_i) \qquad \text{Eq. 4.5}$$

and convective flow through a standard tubing:

$$\frac{\partial C_i}{\partial t} = \frac{F}{A_{cap}}\frac{\partial C_i}{\partial z} + D_l\frac{\partial^2 C_i}{\partial z^2} \qquad \text{Eq. 4.6}$$

with V_{mixer} as the volume of the mixer stage, A_{cap} as the mean cross section of the capillary, and a lumped diffusion coefficient D_{l}.

4.3 Results and Discussion

The serine hydroxymethyltransferase GlyA from *E. coli* catalyzes the formation of β-hydroxy-α-amino acids from glycine and an aldehyde. We will discuss the properties and the application of the enzyme for the production of L-*allo*-threonine (Fig. 4.1). The enzyme can be efficiently overproduced in *E. coli* JM101 (pESM3) during fed-batch fermentations [Chapter 3] to such an extent that allows the direct use of the CFE to study the biocatalytic formation of L-*allo*-threonine. As the reaction mixture used will be at the same time the fluid phase in the projected coupling with continuous chromatography for *in situ* product recovery [Chapter 2], we examined the enzyme properties in a series of different aqueous-organic solvent compositions. As a first step, pH 6.6 was chosen for all reaction mixtures to drastically reduce possible chemical side reactions between glycine and acetaldehyde, such as the addition of the amine to the carbonyl group by a nucleophilic attack of the former on the latter, followed by rapid proton transfer [112], that typically leads to a red colorization of the reaction mix (data not shown).

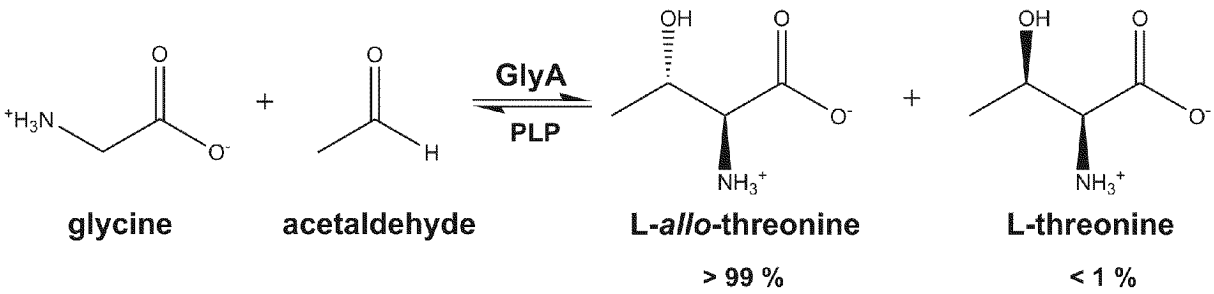

Figure 4.1: GlyA-catalyzed aldol reaction of glycine and acetaldehyde in the presence of the co-factor PLP. Stereoselectivity is absolute on the C_α-atom and less strict on C_β, but still with a strong preference for the *allo*-form.

4.3.1 Suitable reaction conditions and stability

The formation of L-*allo*-threonine was followed in batch experiments under standardized conditions either in purely aqueous reaction mixtures or in mixtures of aqueous buffer with up to 30% of methanol or acetonitrile. To estimate the relative activity of GlyA in the different reaction solvents, we determined the initial reaction rates of L-*allo*-threonine formation for a fixed set of starting concentrations (Tab 4.1). As a reference, the specific activity in 50 mM sodium phosphate buffer pH 6.6 and with 0.17 U mg^{-1} of total protein was set as 100% (Tab. 4.1). The addition of methanol to the reaction mixture drastically increased the activity, which reached a maximum at a methanol content of 20%, and did not further increase at a higher methanol content of 30%. The activity measured in the reaction mixtures containing 10 or 20% acetonitrile was slightly higher as the aqueous reference, whereas it was reduced in 30% acetonitrile. This stimulating effect of low concentrations of organic co-solvent on initial rates of enzymatic reactions has also been reported previously for other enzymes [9; 41].

Next to the specific activity in different aqueous-organic reaction mixtures, the problem of precipitating proteins or other components of the CFE in the presence of organic solvents was addressed. Precipitation was observed in reaction mixtures with 30% acetonitrile already after short reaction times. Precipitation also occurred in mixtures containing 20%, and to a lesser extent in mixtures containing 10% of acetonitrile after longer reaction times (between 4 and 20 h). Precipitation was furthermore observed in the reaction mixture containing 30% methanol after 4 h. The higher susceptibility of proteins towards acetonitrile is in accordance with the postulated higher denaturation capacity of acetonitrile compared to methanol [75]. However, as the experiments were carried out with CFE instead of purified enzyme, we cannot say if GlyA or other proteins or compounds of the CFE precipitated.

Table 4.1: Relative activity of GlyA in reaction mixtures containing different amounts of organic solvent compared to the standard reaction mixture.

Reaction mixture	**Specific activity [U mg^{-1} of total protein]**	**Relative activity [%]**
Purely aqueous	0.17	100 ± 7
+ 10% MeOH	0.24	141 ± 8
+ 20% MeOH	0.3	176 ± 9
+ 30% MeOH	0.29	171 ± 8
+ 10% ACN	0.2	118 ± 2
+ 20% ACN	0.2	118 ± 9
+ 30% ACN	0.15	88 ± 5

Reaction conditions: 2 mg total protein in 50 mM sodium phosphate buffer pH 6.6, 100 mM glycine, 100 mM acetaldehyde, and 40 μM PLP; at 35°C; averaged from three independent measurements.

It has been reported in literature that, besides a higher initial rate of transformation, enzymes also show a higher stability at low concentration of organic co-solvent [9; 41] – an effect also depending on the nature of the co-solvent [103]. The stability of GlyA in the CFE was tested for aqueous conditions and mixtures containing 10 % acetonitrile or 10 % or 20 % methanol. The CFE was incubated in appropriate buffer/organic solvent mixtures at 25°C and the activity was measured after 1, 2, 4 and 7 days (Fig. 4.2). The activity at the beginning of the experiment was set to 100%. The enzyme remained rather stable over one week and exhibited still 80% of the initial activity in the aqueous and methanol-containing mixtures. The activity in 10% acetonitrile decreased to 70% of the starting value, and precipitation was observed.

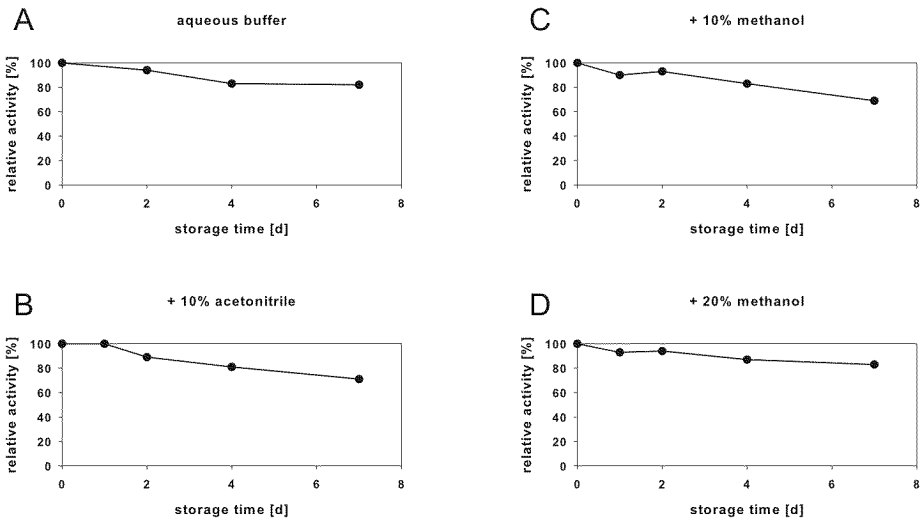

Figure 4.2: Stability of GlyA stored in different aqueous-organic solvent compositions at 25°C. 50 mM sodium phosphate buffer pH 6.6 was mixed with A) no organic solvent; B) 10 % acetonitrile; C) 10% methanol; and D) 20% methanol.

4.3.2 Diastereoselectivity

GlyA is considered to be stereoselective on the C_α atom but less strict on C_β. However, depending on the reaction conditions and on the nature of the acceptor aldehyde, the enzyme can show also considerable selectivity on C_β [78]. The reaction is initially kinetically controlled and leads to good to excellent d.e.'s, which decrease when the reaction approaches thermodynamic equilibrium. As can be seen from Tab. 4.2, the degree of the diastereoselectivity decreases also with increasing organic solvent content in the reaction mixtures at elongated reaction times. Still, the d.e. was excellent in all investigated cases as after 4 h and even after 20 h more than 90% of the produced threonine was of the *allo*-form. The diastereoselectivity in reaction mixtures of higher acetonitrile content at longer reaction times could not be determined due to precipitation of the CFE.

As consequence of these experiments, acetonitrile was no longer considered as organic co-solvent. A more detailed look into the differences of the enzyme kinetic parameters in purely aqueous reaction mixture and in reaction mixture containing 20% methanol will be given in the next section.

Table 4.2: Diastereomeric excess (d.e.) of GlyA subject to the composition of the reaction mixture.

Reaction time:	**1h**	**4h**	**20h**
Composition of reaction mixture:	**d.e. [%]**	**d.e. [%]**	**d.e. [%]**
50 mM Na_xPO_4 pH 6.6	> 98	> 98	> 90
+ 10% MeOH	> 98	> 98	> 82
+ 20% MeOH	> 98	> 96	> 82
+ 30% MeOH	> 98	> 96	> 86
+ 10% ACN	> 98	> 96	> 84
+ 20% ACN	> 98	> 96	n.d.
+ 30% ACN	> 98	n. d.	n. d.

n.d. = not determined

4.3.3 GlyA kinetic parameters in batch reactions

The kinetic parameters of GlyA were determined for two reaction mixtures: in 50 mM sodium phosphate buffer pH 6.6, and in the same buffer containing 20% methanol as co-solvent. The high diastereoselectivity of GlyA for L-*allo*-threonine, which is even maintained at longer reaction times to a considerable extent (Tab. 4.2), prompted us to adopt a simplified equation for the reaction rate (see Eq. 4.2) as the competing reaction of forming L-threonine could be neglected. We therefore assumed an ordered bi-uni reaction mechanism (Eq. 4.1). For a practical approach, a pseudo-equilibrium assumption is applied, as a relatively simple rate equation can be derived (Eq. 4.2), the validity of which can be tested in the experiments described subsequently. It is worth noting that we only like to empirically describe the reaction kinetics to such an extent that it allows the prediction of enzyme-catalyzed reactions in batch and continuous processes. However, with the applied method we cannot discriminate between different reaction models, e.g. between the pseudo-equilibrium and the pseudo-steady-state assumption [160].

The experimental data for the parameter estimation was gained from a series of batch reactions with different starting concentrations of substrates and CFE. The substrate concentrations were varied to cover a wide range, above and below the - previously roughly estimated - K_m values. The recorded progress curves of all three reaction-compounds were

used for the parameter estimation, exploiting the full range of the reaction time up to equilibrium. Independently from the estimation process, the estimated value of K_{eq} was validated by recalculation using Eq. 4.3. The respective values for K_{mThr} were taken from literature (K_{mThr} of 1.5 mM in aqueous medium [144] of 0.62 mM in medium containing organic co-solvent [78]), as they could not be determined exactly enough with the experimental data of the progress curves because the back-reaction, which is not relevant for the development of the process, was not recorded.

The estimated parameters for aqueous reaction mixtures and those containing 20 % methanol are listed in Tab. 4.3. The addition of methanol almost doubled the catalytic constant k_{cat}^{f} suggesting the addition of methanol would be advantageous for process applications. However, the addition of methanol also shifts the equilibrium of the reaction to the substrate side. The values for K_{mGly} and K_{mAld} remained approximately the same for both reaction mixtures. Errors in the experimentally measured values was accounted for by using a constant relative variance model with a standard deviation of 10% for the experimental values in the parameter estimation process, which led to the relatively large insecurity for the K_m values. Still, the description of the progress curves for substrates and product by the estimated kinetic was rather satisfactory, as can be seen in Fig. 4.3 for two example situations.

Table 4.3: Estimated kinetic parameter values for aqueous and for methanol-containing reaction solvents.

Parameter	**50 mM sodium phosphate buffer pH 6.6**		**50 mM sodium phosphate buffer pH 6.6 in 20% MeOH**		**Unit**
k_{cat}^{f}	3.4×10^{-3}	$\pm 0.20 \times 10^{-3}$	6.0×10^{-3}	$\pm 0.50 \times 10^{-3}$	mM L g^{-1} s^{-1}
K_{eq}	0.026	± 0.0016	0.013	$\pm 6 \times 10^{-4}$	mM^{-1}
K_{mGly}	25	±9.0	21.4	± 10	mM
K_{mAld}	7.1	± 2.3	8.1	± 3.2	mM
K_{mThr}	1.5[a]	n.a.	0.62[b]	n.a.	mM

[a] Taken from [144]; [b] taken from [78]. n.a.: not applicable

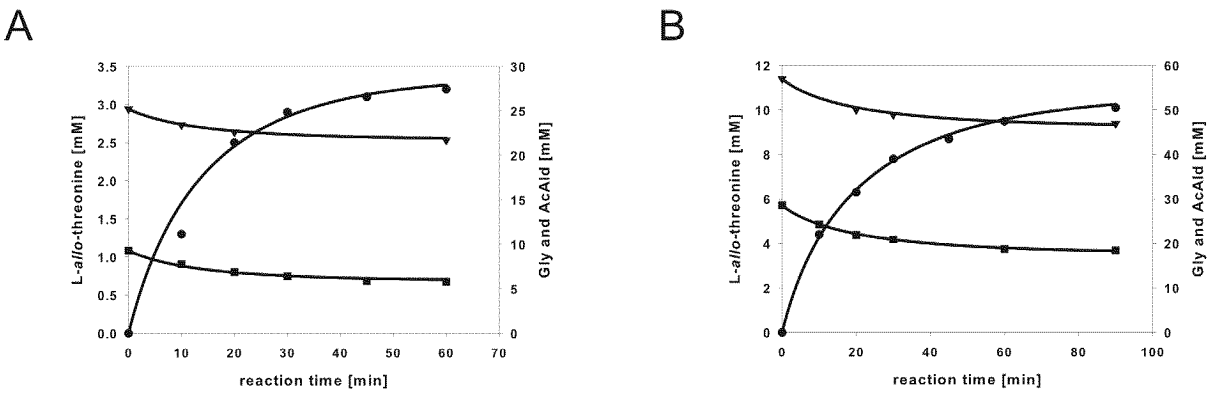

Figure 4.3: Representative overlay of simulated (lines) and experimentally determined concentrations of L-*allo*-threonine (●), glycine (■), and acetaldehyde (▼) for progress curves in batch reactions showing the accuracy of the model and estimated parameters in (A) 50 mM sodium phosphate buffer pH 6.6 and (B) with methanol added to 20 %.

4.3.4 Continuous reactions

The stability of the enzyme over one week with only minimal loss of activity (Fig. 4.2), should allow its use in free form in an EMR, which was chosen for simplicity of set-up over the theoretically more productive plug-flow reactor. The EMR is a widely established concept to study continuous biocatalytic processes, e.g. for co-factor regeneration [85; 181], formation of C-C bonds [83], or in combination with ISPR [94]. It has also been applied on an industrial scale [182; 183] and specifically with aldolases [84; 138]. The experimental set-up for the continuous formation of L-*allo*-threonine in an EMR can be seen, schematically drawn, in Fig. 4.4a. The above described kinetic model with the estimated parameters, together with a model for the CSTR, the diffusion in the tubing and the mixing (equations 4.4-6), were used to predict the performance of the reactor. The model and corresponding parameters for the fluid dynamics of the tubing, mixer and injection valve were required for an accurate prediction of the concentration profiles at the inlet of the reactor. The model of the whole setup and ideal CSTR performance was validated, without enzyme present in the EMR, by applying a feed of glycine and acetaldehyde in 50 mM sodium phosphate buffer pH 6.6 at a flow rate of 1 mL min^{-1} for 90 min, followed by flushing the reactor with 50 mM sodium phosphate buffer pH 6.6 at a flow rate of 1 mL min^{-1} for another 60 min. An overlay of the model-predicted and the experimentally measured values for glycine and acetaldehyde was in good agreement (Fig. 4.4b). To demonstrate the accuracy of the CSTR model in combination

with the completed kinetic model for the enzyme, the rectangular feed pulse of glycine and acetaldehyde was repeated with CFE added to the EMR. This experiment accounted for a wide range of concentrations of substrates and product in a time-dependent manner: from small starting concentrations up to the operation of the reactor at steady-state with continuous feed. The experiment was performed with aqueous as well as with 20% methanol containing reaction mixture. In both cases, the EMR was charged with 4 mL of CFE, corresponding to 160 mg of total protein. An overlay of the predicted and measured values of the substrate and product concentrations at the reactor outlet showed an excellent agreement for both reaction mixtures and the corresponding kinetic model (Fig. 4.4c and d).

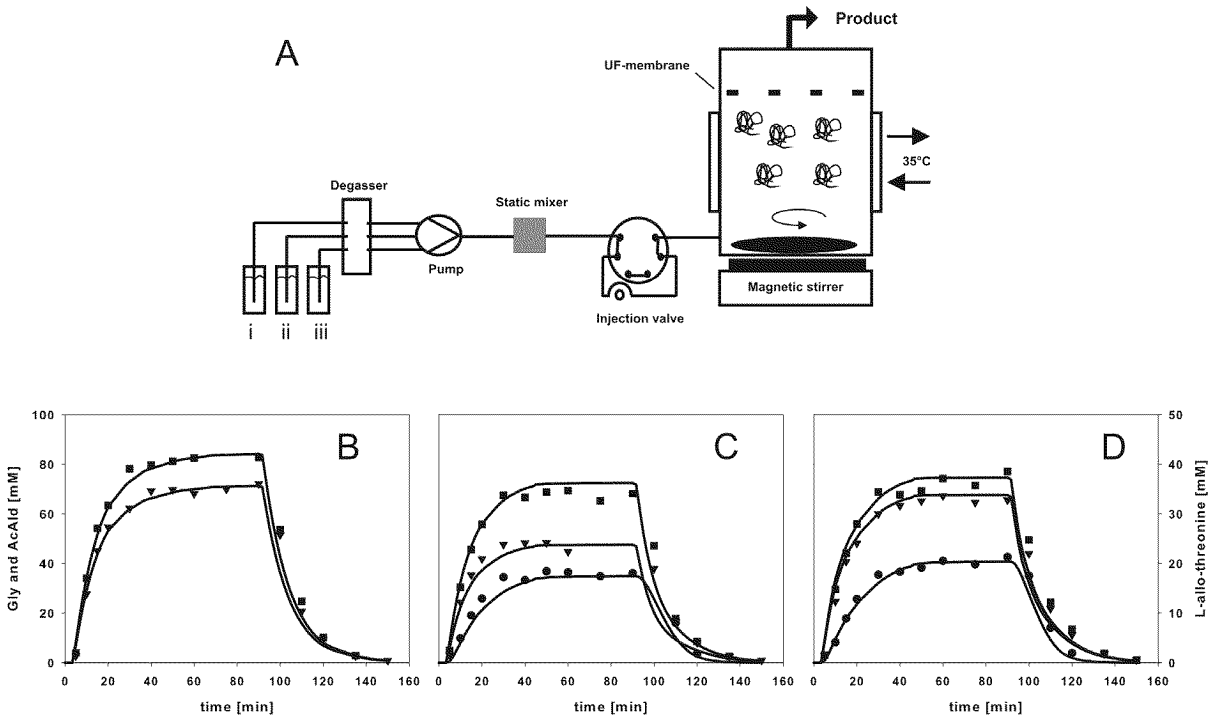

Figure 4.4: A) Experimental set-up for the continuous production of L-*allo*-threonine in an EMR. Storage bottles contain (i) reaction solvent for rinsing the reactor; (ii) glycine and PLP in reaction solvent; (iii) diluted acetaldehyde. UF: ultrafiltration. B) to D) Validation of the reactor model by applying a pulse of glycine and acetaldehyde at a flow rate of 1 mL min^{-1}. Overlay of predicted (lines) and experimental (symbols) values at reactor outlet. B) no enzyme added to the EMR; C) EMR operated with 160 mg of total protein in 50 mM sodium phosphate buffer pH 6.6; and D) as C, with methanol added to 20%. L-*allo*-threonine (●), glycine (■), and acetaldehyde (▼).

The somewhat inferior correlation of experimental and predicted values in the declining part of the curves is best explained by small imprecisions in sampling times which will have large effects on the accuracy as the slope of the concentration decrease is very steep.

A continuous production of L-*allo*-threonine was run over 120 h to demonstrate the feasibility of operating the reactor with CFE and gain more data on the stability of the enzyme under prolonged reaction conditions. In contrast to the stability test described above, the enzyme is exposed to high substrate concentrations throughout the entire process time, and the temperature has been increased by 10°C. The process was performed in 50 mM sodium phosphate buffer pH 6.6 containing 20% methanol as co-solvent and 160 mg of total protein, added to the reactor at the beginning. The organic co-solvent in the reaction mixture allowed the operation of the EMR under non-sterile conditions without the risk of fouling and thereby loss of enzyme activity. The time-course of L-*allo*-threonine, glycine and acetaldehyde at the reactor outlet can be seen in Fig. 4.5. No significant loss of enzyme activity was observed over the entire operation time of 120 h.

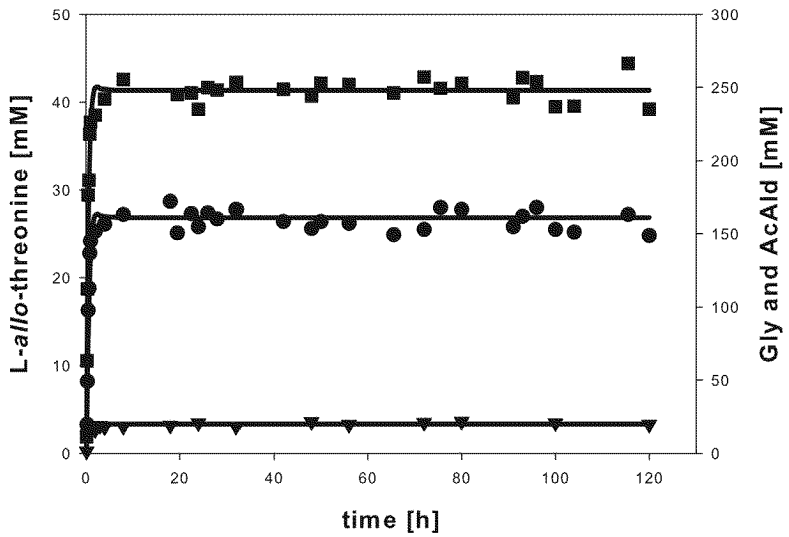

Figure 4.5: Continuous formation of L-*allo*-threonine in an EMR operated with 160 mg total protein for 120h. The reaction mixture contained (at the inlet): 50 mM sodium phosphate buffer pH 6.6 containing 20% methanol, 280 mM glycine, 50 mM acetaldehyde, and 40 µM PLP; the flow rate was set to 0.5 mL min^{-1}. Simulated (lines) and experimental values of L-*allo*-threonine (●), glycine (■), and acetaldehyde (▼) concentrations at reactor outlet.

Furthermore, a high diastereomeric excess of more than 96% was also maintained during the whole process time. Glycine was in excess over acetaldehyde to drive the reaction to the product side, however, the enzymatic reaction in the reactor did not reach equilibrium but only a steady-state due to the high flow rate (0.5 mL min^{-1}) and the corresponding short residence time of 20 min. On the other hand, a short residence time is beneficial for the diastereoselectivity as can be seen in Tab. 4.2. The process resulted in a space time yield of L-*allo*-threonine of 227 g d^{-1} L^{-1} reactor volume. As can be seen in Fig. 4.5, the CSTR model combined with the enzyme kinetic could accurately predict the performance of the reactor for reaction mixtures with 20% methanol.

4.4 Conclusions

We characterized GlyA, a glycine-dependent aldolase from *E. coli* with respect to the application in biocatalytic processes. The enzyme exhibits excellent diastereoselectivity for the formation of L-*allo*-threonine under process conditions, making it a valuable tool for asymmetric C-C bond formation. GlyA is active and fairly stable in different aqueous-organic solvent compositions, enabling the operation of integrated processes with continuous chromatography for *in situ* product recovery. We proposed an enzyme kinetic model for the aldol-reaction of glycine and acetaldehyde, catalyzed by GlyA and determined the corresponding kinetic parameters. This model was accurate enough to predict the performance of the enzyme under process conditions in an EMR, either for aqueous or 20% methanol-containing reaction mixtures. The possibility of simulating the process will facilitate the determination of feasible operation points in an integrated process.

Acknowledgments

This work was supported with a grant from ETH to S. Makart and by the Swiss national Science Foundation with a grant to M. Bechtold.

5 Separation of amino acids by simulated moving bed under solvent constrained conditions for the integration of continuous chromatography and biotransformation

Stefan Makart, Matthias Bechtold, Sven Panke

Abstract

A large number of promising enzyme reactions, such as diastereospecific carbon-carbon bond formation by aldolases, suffer from an unfavorable position of the reaction equilibrium. Combining continuous chromatography and enzymatic reactions should allow for new *in situ* or online product recovery process to achieve high reaction productivity and yield and make these biocatalysts economically more attractive. The integration implies a series of constraints on the chromatographic separation, mainly the range of applicable solvents, which are at the same time the reaction medium for the enzymatic reaction. In an integrated biocatalytic process to produce L-*allo*-threonine from glycine and acetaldehyde, the separation of the two amino acids glycine and threonine is the most important separation task. This separation was performed on a lab-scale simulated moving bed (SMB) unit. The operating conditions were designed to fulfill the requirements for the future integration with biotransformation. In particular, the choice of potential eluents was restricted to aqueous buffers with minor content of organic co-solvent at neutral pH. A suitable stationary phase was identified and the effects of added organic co-solvent to the eluent were investigated. Using the triangle theory, operating points for the SMB were derived. High purities could be obtained in the extract and raffinate outlet stream. The experimental runs indicate the feasibility of the SMB for an integrated process.

5.1 Introduction

Simulated moving bed (SMB) is a continuous chromatographic multi-column process which emerged in the 1960's in the oil industry [18; 19] and has made its way since into the pharmaceutical and fine chemicals industry [70]. SMB technology provides some advantages over batch chromatography, like the efficient continuous operation mode that leads to reduced volumes of stationary and mobile phase and results in considerable cost savings [131]. The continuous mode of operation is also more permissive to integration with additional equipment in a more complex process design [121]. Furthermore, SMB-operation is easy to scale up [120].

The on line-integration of SMB and continuous biotransformations [Chapter 2] enables a variety of applications, such as driving thermodynamically limited reactions to a theoretical yield of 100 %. Previous processes that integrated SMB technology and biotransformation mostly applied the concept of an SMB reactor (SMBR) and addressed product inhibition [3; 6; 152]. A SMBR is basically operated the same way as a conventional SMB, with the catalytic enzyme simply added throughout the unit, either in soluble form to the mobile phase or in immobilized form to the stationary phase. The SMBR concept was furthermore applied to overcome thermodynamic limitations in lipase-catalyzed esterifications in organic solvents, where removal of the by-product water allowed to increase reaction yield [113; 115]. In these cases, the enzyme was part of the stationary phase, one substrate was added with the feed and one substrate with the eluent.

We are interested in the stereoselective formation of carbon-carbon bonds by aldolases, a topic of prime importance in (bio)catalysis [17]. Though of high chemical potential, many biotransformations in this group are characterized either by the dependence on expensive starting materials [140], or by the limitation of product yield due to unfavorable reaction thermodynamics [78; 107]. Specifically, we investigate the formation of L-*allo*-threonine from glycine and acetaldehyde catalyzed by the serine hydroxymethyltransferase GlyA from *Escherichia coli* as a model reaction. The enzyme has been previously thoroughly characterized for process application [Chapter 4].

The integration of the enzyme reactor and continuous chromatography defines a series of constraints for process conditions. First of all, it restricts the range of useful eluents, which at the same time constitute the reaction medium for the biotransformation. This restricts the choice effectively to aqueous buffers with minor content of organic co-solvents [Chapter 4].

In the chosen model reaction, the prime separation task is the separation of the two amino acids glycine, present in large excess, and threonine that have very similar physicochemical

characteristics. Amino acids are commonly separated on sulfonated cation exchangers for analytical purposes [179]. On production scale, lysine has been purified from cell-free fermentation broth on cation exchangers [63]. These separations are performed under strong acidic conditions, under which the carboxy group is no longer charged and the amine group is protonated, favoring the adsorption to the cation exchanger. These conditions are usually not feasible in an integrated process with biotransformation. Reports in literature on the separation of amino acids using SMB focus mainly on the model compounds phenylalanine and tryptophan [186; 188; 189] in an unbuffered system, using water as eluent. Consequently, we investigated a novel SMB-process for the integration with aldolase reactions.

5.2 Theory

5.2.1 Adsorption isotherms

The availability of the adsorption isotherms for the compounds that are involved in the separation is fundamental for SMB-design. For the applied low feed concentrations of up to 500 mM amino acid, linear adsorption isotherms can be used for threonine and glycine:

$$q_i = H_i \cdot c_i \qquad \text{Eq. 5.1}$$

with q_i as the adsorbed solid phase concentration, c_i as the mobile phase concentration and H_i as the Henry constant of compound *i*. In the case of linear isotherms, the shape of the peaks remains symmetric and the Henry constants can be calculated from the retention times t_i^R of the compounds in the bed:

$$t_i^R = t_0\left(1+\frac{1-\varepsilon}{\varepsilon}H_i\right) \qquad \text{Eq. 5.2}$$

where t_0 is the retention time of an unretained compound in the column and ε the bed void fraction.

The axial dispersion coefficients D_i were estimated from finite injections of the compounds at different concentrations with the gPROMS software (Process Systems Enterprise Ltd., London, UK) applying the equilibrium dispersive model, which can be written for the case of linear isotherms as follows:

$$\frac{\partial c_i}{\partial t}\left(1+\frac{1-\varepsilon}{\varepsilon}H_i\right)+v\frac{\partial c_i}{\partial z}=D_i\frac{\partial^2 c_i}{\partial z^2} \qquad \text{Eq. 5.3}$$

with v as the liquid velocity. The estimation process is based on a maximum likelihood objective function and a constant variance model.

5.2.2 True moving bed (TMB) model

To easily simulate and predict the efficiency of the process, a TMB model was applied [125] with a differential mass balance of compound *i* in section *j*:

$$\frac{\partial c_{i,j}}{\partial t}+\frac{1-\varepsilon}{\varepsilon}k(q_{i,j,eq}-q_{i,j})+v_j\frac{\partial c_i}{\partial z}=D_j\frac{\partial^2 c_i}{\partial z^2} \qquad \text{Eq. 5.4}$$
$$j=1,\ldots,4$$

and includes convection for the solid phase:

$$\frac{\partial q_{i,j}}{\partial t}=u\frac{\partial q_{i,j}}{\partial z}+k(q_{i,j,eq}-q_{i,j}) \qquad \text{Eq. 5.5}$$

where q_{eq} represents the adsorbed solid phase concentration in equilibrium with the mobile phase concentration and u the velocity of the solid phase. The initial and boundary conditions, as well as the global balances were described in detail elsewhere [125].

For numerical optimization with the TMB model, a maximal yield was introduced as an objective function:

$$Y=\left[\frac{Q_R\cdot c_{Thr,raff}}{Q_D}\right]_{max} \qquad \text{Eq. 5.6}$$

together with the constraints for the desired purities:

$$Pur_{extr}=\frac{c_{Gly,extr}}{c_{Gly,extr}+c_{Thr,extr}}>0.95 \qquad \text{Eq. 5.7}$$

$$Pur_{raff}=\frac{c_{Thr,raff}}{c_{Thr,raff}+c_{Gly,raff}}>0.99 \qquad \text{Eq. 5.8}$$

5.2.3 Triangle theory

A convenient way to derive optimal operating points for the SMB is given by the triangle theory [111], that makes use of the flow rate ratios m_j in the different sections of the SMB:

$$m_j=\frac{\text{net fluid flow rate}}{\text{adsorbed phase flow rate}}=\frac{Q_j t^*-V\varepsilon}{V(1-\varepsilon)} \qquad \text{Eq. 5.9}$$
$$j=1,\ldots,4$$

where j denotes one of the typically four SMB sections, Q_j denotes the internal volumetric flow rate in section j, t^* the switch time and V the volume of a single column. In the case of

linear isotherms, the conditions for complete separation of the two compounds glycine and threonine, with $H_{Gly} > H_{Thr}$, consist of the following inequalities [111]:

$$H_{Gly} < m_1 \quad \text{Eq. 5.10}$$

$$H_{Thr} < m_2 < H_{Gly} \quad \text{Eq. 5.11}$$

$$H_{Thr} < m_3 < H_{Gly} \quad \text{Eq. 5.12}$$

$$m_4 < H_{Thr} \quad \text{Eq. 5.13}$$

The triangular projection onto the (m_2, m_3) plane shows graphically the region of complete separation, as long as the constraints on m_1 and m_4 are also respected.

For the experimental runs, the effective fluid flow rate is reduced by the extra-column dead volume in the plant, which has to be included in the calculations of the flow rate ratios m_j [129]:

$$m_j = \frac{Q_j t^* - V\varepsilon - V_j^D}{V(1-\varepsilon)} \quad \text{Eq. 5.14}$$

Where V_j^D denotes the extra-column dead volume in section j.

5.3 Material and Methods

5.3.1 Chemicals

All chemicals were either from Sigma-Aldrich Chemie GmbH (Buchs, Switzerland) or Roth (Reinach, Switzerland) unless mentioned otherwise. Acetonitrile (HPLC grade) was purchased from Chemie Brunwschwieg (Basel, Switzerland). The suppliers for the tested resin materials are listed in the Tab. A.1 of the appendix. The resin material used for the SMB, Amberlite CG-50 II, was purchased from Sigma-Aldrich Chemie GmbH.

All percentages of liquid mixtures in this text refer to a volume to volume ratio.

5.3.2 Resin screening

The suitability of the resins was tested in two different ways: either by determining isotherms in batch equilibrium experiments or by packing the material in columns and then applying finite injections of amino acid samples. All resin materials were washed with demineralized water and methanol before equilibration in sodium phosphate buffer pH 6.6 or pH 7.0.

In the batch equilibrium experiments, 2.5 mL of amino acid solution (either glycine or threonine at concentrations of 20, 50 and 100 mM in sodium phosphate buffer) were added to

100 mg of resin in test tubes. The tubes were kept in a shaking water bath at a constant temperature of 25°C until equilibrium was reached, typically after approximately 12 h. The isotherms were calculated based on the assumption that the difference in amount of amino acid in the supernatant had adsorbed to the solid phase.

Alternatively, the solid phase materials were packed in standard PEEK columns with a fixed length (150 x 7.5 mm; Omnilab, Mettmenstetten, Switzerland) after washing and equilibration. The columns were mounted on a Merck-Hitachi LaChrom HPLC system and analyzed by applying injections of 100 mM glycine or 100 mM threonine with sodium phosphate buffer pH 6.6 or pH 7.0 as eluent. The columns were kept in a column oven (Henggeler, Riehen, Switzerland) at 25°C.

5.3.3 Preparation and characterization of Amberlite CG-50 II

As described in the results section, we chose a weak cation exchanger, Amberlite CG-50 II, as the solid phase for the SMB, because it showed the best characteristics in terms of selectivity and resolution. For process applications, the resin material had first to be sieved to obtain a more even particle size distribution and to eliminate the fraction of particles smaller than 20 μm, which would otherwise clog the chromatographic columns in later steps. A sieve with a cut-off of 63 μm was applied and the particle fraction larger than 63 μm was used in the subsequent steps. Next, the material was washed extensively, first in methanol and then in 50 mM sodium phosphate buffer pH 6.6, followed by equilibration in 50 mM sodium phosphate buffer pH 6.6 with various contents of methanol as specified in the text. The material was packed in PEEK columns and tested as described in the resin screening section. Adsorption isotherms were determined by applying finite injections of glycine or threonine at different concentrations with 50 mM sodium phosphate buffer pH 6.6 and the respective methanol content as eluent at a flow rate of 1 mL min^{-1}. The stability of the columns with respect to SMB application was investigated over 10 runs of "loaded feed" treatment, which consisted of the application for 20 min of a mixture of 10 mM threonine and 40 mM glycine dissolved in the eluent, followed by flushing with eluent for 25 min. This treatment was followed by finite injections of threonine and glycine. This procedure was repeated five times to detect any potential changes in the retention times. Furthermore, a second test on the stability necessary for the application in the SMB was performed by increasing the flow rate of the eluent up to 9 mL min^{-1}, followed by a series of finite injections to ascertain the

stability of the retention times and hence the stability of the packed bed under increased pressure.

It is worth noting that several batches of resin material were sieved and used for the packing of the columns, explaining the slight differences between the data on resin characterization and the data from the SMB experiments (see below).

5.3.4 Analytics

A semi-automated precolumn derivatization method (adapted from [38; 57]) was used to determine the concentrations of the amino acids glycine and threonine in the collected samples at the extract and raffinate port using 9-fluorenylmethoxycarbonyl chloride (FMOC-Cl) as derivatization agent with detection at 262 nm on a Hewlett-Packard HP1050 system (Agilent Technologies, Palo Alto, CA, USA). Samples were diluted in 0.1 M sodium borate buffer pH 8.0. Derivatization was performed automatically by the autosampler by mixing 14 µL diluted sample and 14 µL derivatization solution (10 mM FMOC-Cl in acetonitrile) and waiting for 90 seconds before injection. An aliquot of 28 µL was injected into the HPLC onto a Prontosil Eurobond C18 (124 x 4.0 mm column, Bischoff Chromatography, Leonberg, Germany). Elution was performed as described previously [chapter 4].

Amino acid concentrations in samples containing only one amino acid could be determined by measuring the UV absorbance at 210 nm, either in a Lambda 25 UV/VIS spectrometer (PerkinElmer, Waltham, MA, USA) for the samples of the batch equilibrium experiments, or with the UV/VIS detector of the HPLC system for the column experiments.

5.3.5 Experimental set-up of SMB

A modified ÄKTAbasic 10 (GE Healthcare, Uppsala, Sweden) chromatography system was used. The system was changed into a SMB installation by the addition of some extra devices similar to a modified ÄKTAexplorer system as described in [1], i.e. a second pump module P900 (GE Healthcare) and five multi-position valves PV-908 (GE Healthcare). The original pump of the ÄKTAbasic was assigned to the desorbent and feed, whereas the extra pump was used to control the extract and the raffinate. Each pump, with a flow rate range from 0.01 to 10 mL min^{-1}, was connected to a multi-position valve. The setup for a column in the 1-2-2-1 configuration for an open loop SMB can be seen in Fig. 5.1. The 6-port manifolds and the check valves, placed between each pair of columns to assure the correct direction of the flow, were purchased from Ercatech AG (Bern, Switzerland). The dead volume of the installation

was measured and added up to V_1^D = 0.12 mL, V_2^D = 0.24 mL, V_3^D = 0.24 mL, and V_4^D = 0.12 mL in the 1-2-2-1 configuration for an open loop SMB. All devices were controlled by a specially designed "SMB strategy" [1] of the UNICORN software (GE Healthcare). The raffinate was monitored with the UV-detector of the ÄKTA system at 210 nm, while the extract was followed at the same wavelength with an additional Merck Hitachi 655A variable wavelength UV monitor, the signal was recorded using LabView software (National Instruments, Ennetbaden, Switzerland). Samples from the extract and raffinate port were withdrawn using an additional fraction collector (GE Healthcare). For the assessment of raffinate and extract purity, samples were collected at steady state over at least one cycle and averaged. Desorbent and feed were passed through a degasser (Henggeler) before entering the chromatographic system. The SMB was operated without temperature control at room temperature, in contrast to the determination of the adsorption isotherms.

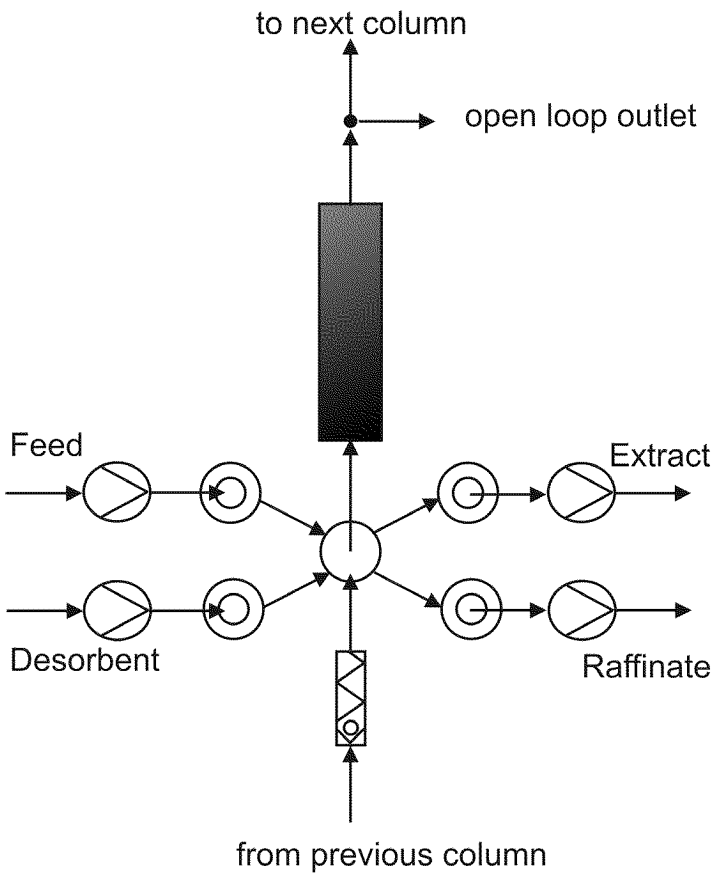

Figure 5.1: Setup for a single column in the SMB unit for an open loop configuration with 6 columns.

5.4 Results and Discussion

5.4.1 Choice of stationary phase

From an extensive qualitative screening of commercially available resins (see appendix), we identified the weak cation exchanger Amberlite CG-50 II as the most promising stationary phase for an integrated process for the enzymatic production of L-*allo*-threonine. This material showed the best selectivity and band broadening was not as pronounced as for other materials. With the material used in the reported SMB separation of amino acids, a poly-4-vinylpyridine resin [186; 188; 189], no separation of glycine and threonine was achieved (appendix, Tab. A.3). Therefore, Amberlite CG-50 II was further characterized regarding the separation of glycine and threonine under process conditions. The pI values of glycine (6.04) and threonine (5.8) are slightly lower than the pH of the eluent applied, which means that the amino acids are present in the zwitterionic form, which should lead to only weak adsorption on the resin compared to commonly applied acidic conditions [130; 192]. Despite this disadvantage, which is a direct result of the constraint of using the same solvent for enzymatic conversion as well as chromatographic separation in the integrated process, the material showed promising separation characteristics. Simulations with a TMB model, with these primary data implemented, indicated the suitability of this resin material for the application in SMB.

5.4.2 Influence of methanol content of the fluid phase on separation characteristics

It was shown that biotransformation with the GlyA aldolase is compatible with the presence of organic co-solvents in the reaction mixture [78] and chapter 4. Especially in the presence of low amounts of methanol, the initial rates of the reaction are higher than in the respective aqueous buffer. In addition, the enzyme is stable in medium containing 20 % methanol, exhibiting still 80 % of its initial activity after storage at 25°C for one week [chapter 4]. Therefore, the influence of methanol content up to 30 % in the fluid phase was investigated. The effects of added organic co-solvent on separation by ion-exchange are difficult to predict [61], hence the influence was determined experimentally.

The Henry constants of glycine and threonine at 25°C as a function of the methanol content in the fluid phase are listed in Tab. 5.1. The Henry constants increase with increasing methanol content, with a faster increase for glycine than for threonine. However, diffusion effects were

more pronounced, because the residence time is longer. This can be seen from Fig. 5.2, where the elution profiles of finite injections of glycine and threonine at different concentrations are depicted for eluent containing no methanol and 30 % methanol. The best separation was achieved with 30 % methanol in the fluid phase.

Table 5.1: Henry's constants of glycine and threonine as a function of the methanol (MeOH) content in the 50 mM sodium phosphate pH 6.6 buffer used as mobile phase.

MeOH content [%]	***H* Glycine**	***H* Threonine**
0	0.9	0.6
10	1.4	0.8
20	1.6	0.9
30	2.0	1.1

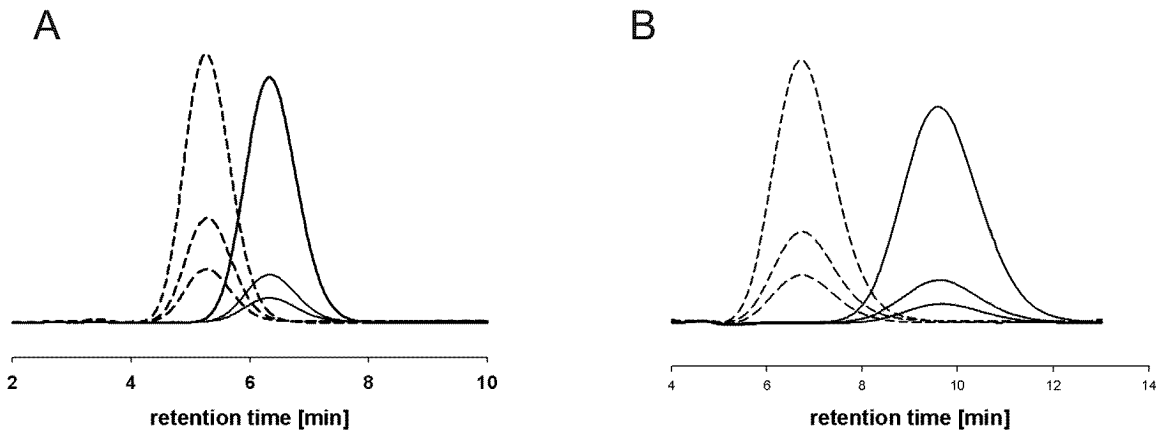

Figure 5.2: Effect of methanol content on the retention of glycine and threonine. (A) no methanol in the eluent; (B) with 30 % methanol in the eluent. Finite injections of 50, 100 and 500 mM glycine (solid lines), respectively 50, 100 and 250 mM threonine (dashed lines). The arbitrary absorption units in vertical direction are not displayed.

This data were then used in a TMB model for numerical optimization, taking the diffusion into account, with a maximal yield as the objective function. As a result of this optimization, the addition of 30 % methanol as co-solvent was identified as the most favorable eluent composition to achieve a high yield. However, at 30 % methanol-content, precipitation of the enzyme or other proteins or components of the cell free extract had been observed after 4 h reaction time [chapter 4]. In contrast, in mixtures containing 20 % methanol, no precipitation was observed, and the enzyme was remarkably stable under process conditions. Furthermore, the enzyme kinetics have been determined for reaction mixtures in 50 mM sodium phosphate buffer pH 6.6 in 20 % methanol [chapter 4], facilitating future simulations of the integrated process. Therefore, the subsequent SMB experiments were performed with 50 mM sodium phosphate buffer pH 6.6 in 20 % methanol.

5.4.3 SMB operation

All SMB experiments were performed in a 1-2-2-1 configuration for an open loop. The chromatographic columns were packed as described in the experimental part and each column was tested separately by applying finite injections of glycine and threonine. A quite even packing of the columns, which is a prerequisite for the successful SMB operation, was achieved. Standard deviation for the retention times of glycine and threonine in the different columns was less than 0.1 min. The stability of such a packed column was tested by applying a series of loaded feed treatments as well as increasing the volumetric flow rate, followed again by finite injections as described in materials and methods. No change in the adsorption behavior of glycine and threonine was observed suggesting the suitability of the columns for their use in the SMB.

Operating points for the SMB runs were derived using the triangle theory [111] as described in the theory section. A graphical display of the chosen operating points in the (m_2, m_3) plane can be seen in Fig. 5.3. The maximal flow rate for the SMB experiments was set to 5 mL min^{-1} and designated to section 1. The external flow rates were kept constant for runs A to D, while the switch time t^* was varied between 100 and 115 seconds. Within the second series of SMB runs, E to H, the external flow rates were also kept constant, while the switch time t^* was varied between 106 and 131 seconds (Tab. 5.2). The feed concentration c_i^F was 100 mM for each amino acid in all SMB runs. By keeping the flow rates constant while varying the switch time, the set of operating points builds a straight line in the (m_2, m_3) plane almost in

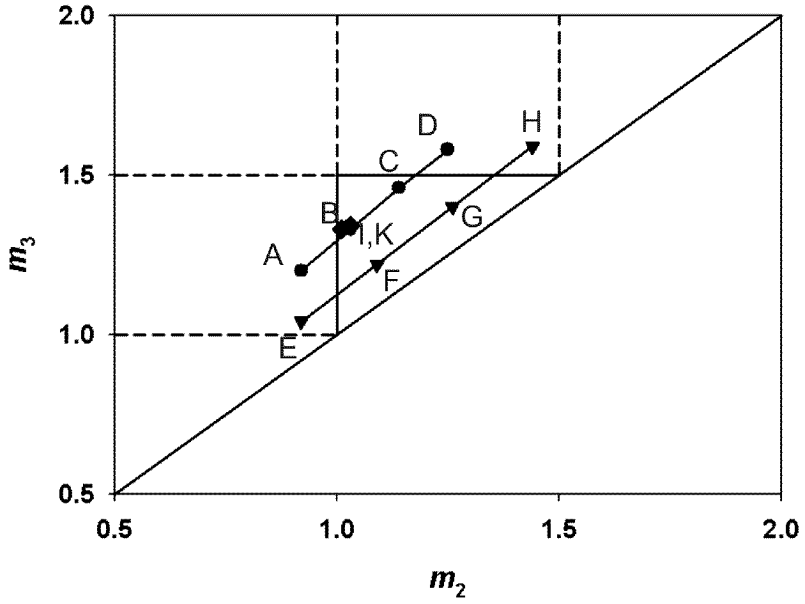

Figure 5.3: Operating points of the experimental SMB runs A to K plotted in the (m_2, m_3) plane.

Table 5.2: Operating conditions and performance of the experimental runs A to H. Column configuration in the SMB: 1-2-2-1

Run	**Flowrates [ml min^{-1}]**				***t**** **[s]**	**Operating parameters**				**Purity [%]**	
	Q_1	Q_2	Q_3	Q_4		m_1	m_2	m_3	m_4	Pur_{raff}	Pur_{extr}
A	5.0	3.97	4.49	3.46	100	1.53	0.92	1.20	0.67	98.8	96.1
B	5.0	3.97	4.49	3.46	105	1.67	1.03	1.33	0.77	99	99.3
C	5.0	3.97	4.49	3.46	110	1.81	1.14	1.46	0.86	93.5	99.5
D	5.0	3.97	4.49	3.46	115	1.95	1.25	1.58	0.96	67.9	99.6
E	5.0	3.75	3.95	2.97	106	1.7	0.92	1.04	0.5	99.5	90.8
F	5.0	3.75	3.95	2.97	114	1.92	1.09	1.22	0.63	99.8	99.4
G	5.0	3.75	3.95	2.97	122	2.15	1.26	1.39	0.77	99.7	99.5
H	5.0	3.75	3.95	2.97	131	2.4	1.44	1.59	0.92	54.5	>99.8

External flow rates for runs A to D: Q_D = 5 mL min^{-1}, Q_E = 1.025 mL min^{-1}, Q_F = 0.52 mL min^{-1}, and Q_R = 1.025 mL min^{-1}; for runs E to H: Q_D = 5 mL min^{-1}, Q_E = 1.25 mL min^{-1}, Q_F = 0.2 mL min^{-1}, and Q_R = 0.98 mL min^{-1}.

parallel to the diagonal (Fig. 5.3) [129]. The operating points were chosen such that this line crosses the region of complete separation, starting from the region of pure raffinate, through the complete separation region, to the region of pure extract [111].

The first set of experiments, runs A to D, whose operating points constituted the line further away from the diagonal (Fig 5.3), was performed at the higher constant feed flow rate of $Q_F = 0.52$ mL min^{-1} than the second set of experiments. As the feed concentration was kept constant, these runs should achieve a higher productivity than runs E to H, i.e. maximally 3.12 mmole h^{-1} of each amino acid. The effect of increasing switch times on the purities of the raffinate and extract stream can be seen in Fig. 5.4a as a function of the flow rate ratio m_2. The purity in the extract increases as expected, while the purity of the raffinate decreases from 99 % in run B to only 68 % in run D. In run A, the raffinate shows only a purity of 98.8 %, although the operating point lies in the region of pure raffinate in the (m_2, m_3) plane. This can be explained with the low flow rate ratio m_1: the value of m_1 was only 1.53, which was, considering the non-idealities of the system, too close to the Henry constant of the more retained compound glycine of 1.5. The conditions for complete regeneration of the solid phase in section 1 were no longer given leading to the reduced purity of the raffinate. Increasing m_1 in this case should increase the purity of the raffinate, as was observed for run E (see below). The purities of the extract were higher than 99 % in runs B to D. The best separation was achieved in run B, with Pur_{extr} = 99.3 % and Pur_{raff} = 99 %; in the raffinate stream, 94 % of the threonine, and in the extract stream, 92 % of the glycine fed to the SMB could be collected.

In the second set of SMB experiments, the feed flow rate was smaller, $Q_F = 0.2$ mL min^{-1}, leading to a lower productivity of the plant. However, higher purities could be achieved. The purities as a function of the flow rate ratio m_2 can be seen in Fig 5.4b, showing the expected pattern. Purities in the raffinate were higher than 99 % in runs E to G, dropping down to 54.5 % in run H. The purities of the extract were increasing from 90.8 % in run E to over 99 % in runs F to H. The best separations were achieved in runs F and G, of which the operating points are located within the region of complete separation; the recovery of threonine at the raffinate and glycine and the extract port was almost 100 %. Run E was performed with the same value for m_2 as run A, but with a higher value for m_1 and indeed showed a higher purity of the raffinate, but still was not pure. This suggested that, given by the poor efficiency of the stationary phase, one should operate the SMB with a higher flow rate ratio m_1 to ensure complete regeneration of the solid phase.

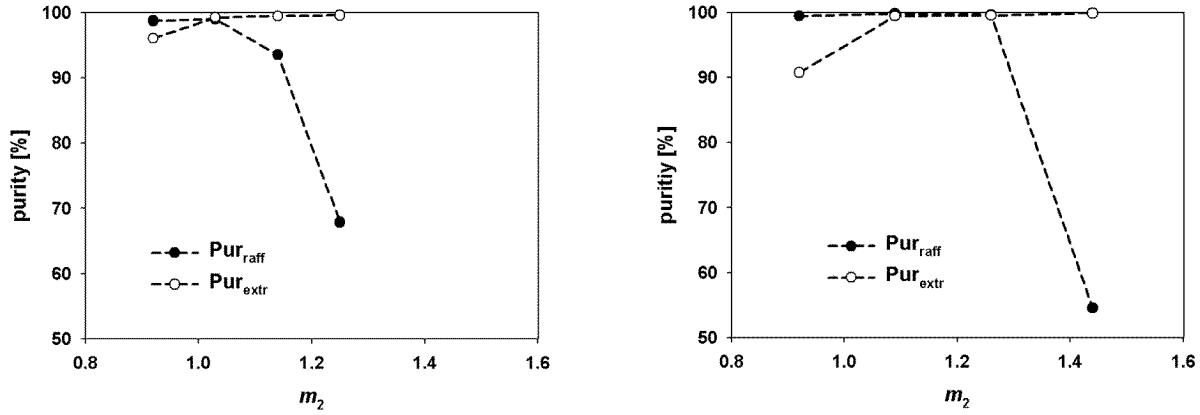

Figure 5.4: Purities of the raffinate and extract outlet streams as a function of the flow rate ratio m2. (a) runs A to D; (b) runs E to H.

It is worth noting that the m_1 values of runs A and B would be too low, respectively the m_4 values of runs C, D and H would be too large for the application in a closed loop configuration.

Two SMB experiments, runs I and K, were performed applying a feed as it would be in an integrated process at lab scale. The feed flow rate Q_F was set to 0.5 mL min^{-1} with concentrations of 250 mM glycine and 30 mM threonine, which corresponds to the outlet of the reactor in a previously performed experiment for the continuous production of L-*allo*-threonine in an enzyme membrane reactor [chapter 4]. Operating parameters are listed in table 5.3. In run K, 40 µM pyridoxal-5-phosphate (PLP) was added to the desorbent and the feed in order to show that PLP will have no negative impact on the separation process. PLP is a co-factor needed by the enzyme GlyA to catalyze the aldol reaction [78] and has to be added to the reaction mixture, therefore it will be present in the separation step. PLP carries a double negative charge at neutral pH and should therefore not be adsorbed on the cation exchanger used as resin. The purity of the raffinate in both runs, roughly 97 %, was slightly lower than expected, as the operating points are located within the region of complete separation. However, the recovery at the raffinate port of the fed threonine was more than 98 %, giving a productivity of 0.9 mmole h^{-1} threonine. The purity of the extract was as high as expected, the threonine content was below the detection limit.

The stability of the packed bed of a SMB column after its use in runs A to K, was tested by applying again finite injections of glycine and threonine under the same conditions as for the testing of the columns directly after packing. Two slight changes were observed: the retention

times of both compounds increased by approximately 3 %, and the band broadening was more pronounced. Probably, a more stringent packing procedure would improve the bed stability. The column capacity could also decrease over time because of incomplete regeneration [186], suggesting that a stringent cleaning procedure should be implemented in the integrated process.

Table 5.3: Operating conditions for SMB runs I and K.
Column configuration in the SMB: 1-2-2-1

		Run I	**Run K**
Flowrates [mL min-1]	Q_1	5.0	5.0
	Q_2	3.8	3.64
	Q_3	4.3	4.15
	Q_4	3.03	2.94
	Q_D	5.0	5.0
	Q_F	0.5	0.5
	Q_E	1.2	1.36
	Q_R	1.27	1.21
Operating parameters	m_1	1.81	1.91
	m_2	1.03	1.01
	m_3	1.34	1.33
	m_4	0.6	0.6
Switch time	t^*	110	114
Purity [%]	Pur_{raff}	96.7	97.3
	Pur_{extr}	>99.8	>99.8

5.5 Conclusions

We could show the efficient separation of amino acids, glycine and threonine, in a SMB plant at neutral pH, which is a prerequisite for the on-line coupling with biotransformation and use of the SMB as *in situ* product removal tool. Excellent separation could be achieved in experimental runs, applying an equimolar feed of glycine and threonine. The productivity of the installation, with the feed concentration applied, reached 75 mmole d^{-1} of threonine, which sums up to approximately 0.5 (kg of threonine) (kg of stationary phase)$^{-1}$ d^{-1}. Adding a further component of the enzymatic reaction, the co-factor PLP, to the system did not change the performance, confirming the suitability of the SMB separation for an integrated process.

Acknowledgments

The authors wish to thank Dr. Joachim Stadler (GE Healthcare, Freiburg, Germany) for advice in the installation of the SMB unit. We like to thank G. Caviezel and D. Strässler for their help in the resin screening. This work was supported by the ETH with a grant to S. Makart and by the Swiss national Science Foundation with a grant to M. Bechtold.

Nomenclature

c_i	concentration of species *i* [g L^{-1}] or [mM] as specified in the text
ε	bed void fraction
H_i	Henry's constant of species *I*
j	section index
m_j	flow rate ratio in section *j*
q_i	adsorbed solid phase concentration of species *i* [g L^{-1}]
Q	volumetric flow rate [mL min^{-1}]
t_0	residence time [s]
t_i^R	retention time for species *i* [s]
t^*	switch time [s]
u	solid velocity [cm min^{-1}]
v	liquid velocity [mL min^{-1}]
V	column volume [mL]
V_j^D	extra-column dead volume in section *j* [mL]

Y	yield [g L^{-1}]
Gly	glycine
Thr	threonine

6 Summary and outlook

6.1 Summary

This work described some fundamental aspects on the long way from identifying the gene of a potential biocatalyst via its production, characterization to the design of the biocatalytic process. The chosen biocatalyst was GlyA, a serine hydroxymethyltransferase from *E. coli*, which can functionally be classified as a glycine-dependent aldolase.

The second chapter explored the field of attractive enzymatically catalyzed reactions that could benefit from the integration with continuous chromatography. Some guidelines were established in order to design integrated processes straightforward and determine the proper configuration of the process for a given task.

The third chapter discussed the production of the biocatalyst. The availability of efficient expression systems is a prerequisite for the success of biotransformation. The suitability of the AlkS/P_{alkB} expression system for the production of recombinant proteins in purely aqueous fed-batch fermentations has been shown with a yield of approximately 120 mg recombinant enzyme per gram cell dry weight. Furthermore, the homogeneity of the induction response throughout the cell culture as a function of the inducer concentration was verified.

Chapter four addressed the development of a suitable process model for the enzymatic reaction for the formation of L-*allo*-threonine from glycine and acetaldehyde. A kinetic model was proposed and the kinetic parameters were estimated for purely aqueous and methanol-containing reaction mixtures. The enzyme resulted to be diastereoselective to a great extent. An enzyme membrane reactor was operated for 120 h without significant loss of enzyme activity, resulting in a space-time yield of 227 g d^{-1} L^{-1}.

In chapter five, the separation of glycine and threonine by simulated moving bed is described. A suitable stationary phase for the integrated process was identified and it was experimentally verified that the continuous chromatographic separation of amino acids at neutral pH is possible. The SMB was furthermore operated under the same conditions as expected for the integrated process.

6.2 Outlook

6.2.1 Implementation of the integrated process

For the technical realization of a (lab-scale) pilot installation of the cSMB&R, as discussed in this thesis, it is important to consider the dilution introduced by the chromatographic separation. As the excess substrate of the enzymatic reaction is recovered at the extract or the raffinate port of the SMB and returned to the enzyme reactor, this would lead over time to a continuous decrease of the substrate concentration and hence of the reactor performance. As an obvious solution, the stream of recycled substrate has to be concentrated before entering the enzyme reactor. One technical solution would be the implementation of a crossflow membrane filtration unit, capable for the continuous operation, such as the GE Sepa^{TM} CF II nanofiltration system (GE, Osmonics Labstore, Minnetonka, MN, USA).

Furthermore, the following points have to be considered:

(i) The separation studies and the SMB runs were performed using L-*threo*-threonine instead of the main product of the enzymatic reaction L-*allo*-threonine. L-*threo*-threonine, a proteinogenic amino acid available from fermentations, is easily available and cheap whereas the main product of the GlyA reaction, L-*allo*-threonine, is not (it is more than 500 times more expensive than L-*threo*-threonine). However, only minor differences in the adsorption characteristics were observed experimentally, when finite injections of L-*allo*-threonine on a single SMB column were performed. Thus, it stands to reason to use the data obtained for L-*threo*-threonine for simulations of the integrated process.

(ii) The adsorption isotherms were determined at 25°C, the SMB runs were performed at room temperature, but the enzyme membrane reactor was operated at 35°C. In the integrated process, the two units could either be operated at different temperatures, where actually only the enzyme reactor is temperature controlled and the SMB is left at room temperature. The implication on the stability of the separation will have to be determined experimentally. Alternatively, the two units could be operated at the same temperature, i.e. 35°C. However, the separation efficiency is slightly reduced at 35°, as was measured already for a single column. The impact of this effect will have to be simulated which should help defining the optimal process configuration.

(iii) So far, the SMB was discussed for the separation of two compounds, glycine and threonine (chapter five). However, the enzymatic reaction mixture is composed of four compounds (apart from the buffer-methanol mixture that constitutes the eluent): glycine and acetaldehyde as substrates, L-*allo*-threonine as the product, and the enzyme co-factor PLP. It

has been shown that the co-factor PLP has no effect on the separation. The unreacted acetaldehyde from the enzyme reactor would ideally be returned from the SMB to the reactor together with the excess glycine. However, the adsorption behavior of acetaldehyde is completely different from that of glycine. The Henry constant H for acetaldehyde with 50 mM sodium phosphate buffer pH 6.6 in 20 % methanol as eluent was calculated to be 0.3. Therefore, most of the acetaldehyde would leave the SMB at the raffinate port, while only a minor fraction would be collected at the extract port together with the glycine and returned to the reactor. Options to minimize this problem will be discussed in the next section.

Finally, the integrated process needs to be simulated, using the experimentally verified models for the enzyme membrane reactor and the SMB, including the concentration step to derive appropriate operating points.

6.2.2 Further optimization steps

As the acetaldehyde cannot be substantially recovered during the chromatographic separation - at least with the stationary phase applied - the task of achieving a high yield on acetaldehyde is left to the biotransformation part of the process. Primarily, equilibrium should be achieved in the enzyme reactor. However, the residence time in the reactor would have to increase by a factor of ten to 200 min in the described enzyme membrane reactor experiment of chapter 4 to reach at least 90 % of equilibrium. There again, a prolonged reaction time will not be beneficial for maintaining the high diastereoselectivity of the reaction. By increasing the concentration of the second substrate, glycine, the reaction could be driven to the product side. This option, for the sake of argument considered for the most favorable case of equilibrium in the reactor, could reduce the concentration of unreacted aldehyde to a negligible quantity. A possible upper limit for the glycine concentration has not yet been determined. Furthermore, in order to operate an enzyme reactor close to equilibrium at reasonable residence times, the k_{cat} of the enzyme should be increased. As the protein concentration in the enzyme membrane reactor is already quite high, a directed evolution approach to increase the specific activity of the enzyme would appear most suitable.

Furthermore, an obvious solution to improve the volumetric productivity of the reactor would be the implementation of a plug-flow reactor instead of the less productive enzyme membrane reactor, which has been chosen in chapter four because it is easier to handle in an early process design phase. The enzyme would then have to be immobilized. First experiments in this direction have already been performed (data not shown).

Finally, the use of the sodium-phosphate buffer has to be considered. On a larger scale, it raises environmental concerns because the disposal as wastewater further increases the phosphate concentration in the water leading to eutrophication. Furthermore, the phosphate is incompatible with many immobilization methods required for the plug-flow reactor concept. The proper choice of eluent, respectively reaction buffer, will be a further task in the optimization of the integrated process once all the relevant experimental data are at hand for a detailed simulation.

Appendix

Table A.1: List of the tested resin materials and their suppliers (supplementary to chapter 5).

Resin	**Type**	**Matrix/ Functional groups**	**Supplier**
Amberlite CG-120 II	SCX	Polystyrene-divinylbenzene; sulfonate	Sigma-Aldrich Chemie GmbH (Buchs, Switzerland)
Dowex 50WX8-400	SCX	Styrene-divinylbenzene; sulfonate	Sigma-Aldrich Chemie GmbH
Fractogel EMD SO_3^-	SCX	Polymethacrylate; Sulfoisobutyl-group	Merck KgaA (Darmstadt, Germany)
SP Sepharose™ FF	SCX	Cross-linked agarose; sulfopropyl-group	GE Healthcare (Uppsala, Sweden)
Source™ 15S	SCX	Polystyrene-divinylbenzene; methyl sulfonate	GE Healthcare
Capto™ MMC	WCX	Cross-linked agarose; multimodal CX	GE Healthcare
Fractogel EMD COO^-	WCX	Polymethacrylate; carboxy ethyl-group	Merck KgaA
Amberlite CG-50 II	WCX	Polymethacrylic ester-divinylbenzene; COO^-	Sigma-Aldrich Chemie GmbH
PVP Reillex 425 and 402	ADS	Poly(4-vinylpyridine)	Sigma-Aldrich Chemie GmbH
Sepabeads SP207	ADS	Brominated polystyrene	Resindion S.r.l. (Binasco, Italy)
Amberlite XAD 4	ADS	Styrene-divinylbenzene	Sigma-Aldrich Chemie GmbH
Amberlite XAD 7	ADS	Acrylic ester	Sigma-Aldrich Chemie GmbH
Amberlite XAD 1180	ADS	Styrene-divinylbenzene polyaromatic	Sigma-Aldrich Chemie GmbH
Silica Gel 100CN	ADS	Silica; $(-CCH_2)_3CN$)	Sigma-Aldrich Chemie GmbH
Amberlite XAD 761	ADS	Phenol-formaldehyde	Sigma-Aldrich Chemie GmbH

SCX strong cation exchanger; WCX weak cation exchanger; ADS adsorbent

Table A.2: list of resins tested in batch equilibrium experiments and qualitative statements on the adsorption of glycine and threonine (supplementary to chapter 5).

Resin	**Adsorption**
Sepabeads SP207	Weak
Amberlite XAD 4	Moderate
Amberlite XAD 7	Moderate
Amberlite XAD 1180	Moderate
Aminopropyl Silica Gel	Weak
Silica Gel 100CN	Weak
Duolite XAD 761	Moderate
Dowex 50WX8-400	strong

Table A.3: list of resins tested in column experiments and qualitative statements on their applicability in the integrated process (supplementary to chapter 5).

Resin	**Type**	**Applicable**	**Remarks**
Amberlite CG-120 II	SCX	yes	good selectivity
Dowex 50WX8-400	SCX	yes	good selectivity, low resolution
Fractogel EMD SO_3^-	SCX	no	Gly/Thr identical elution volumes
SP Sepharose™ FF	SCX	no	Gly/Thr identical elution volumes
Source™ 15S	SCX	no	Gly/Thr identical elution volumes
Capto™ MMC	WCX	no	Gly/Thr identical elution volumes
Fractogel EMD COO^-	WCX	no	Gly/Thr identical elution volumes
Amberlite CG-50 II	WCX	yes	good selectivity
PVP Reillex 425 and 402	ADS	no	Gly/Thr identical elution volumes

References

[1] Abel S, Bäbler MU, Arpagaus C, Mazzotti M, Stadler J. 2004. Two-fraction and three-fraction continuous simulated moving bed separation of nucleosides. J Chromatogr A 1043:201-210.

[2] Ager DJ, Li T, Pantaleone DP, Senkpeil RF, Taylor PP, Fotheringham IG. 2001. Novel biosynthetic routes to non-proteinogenic amino acids as chiral pharmaceutical intermediates. J Mol Catal B: Enz 11:199-205.

[3] Akintoye A, Ganetsos G, Barker PE. 1991. The inversion of sucrose on a semicontinuous counter-current chromatographic bioreactor-separator. Trans Inst Chem Eng 69:35-44.

[4] Anderson ME, Aslan D, Clarke A, Roeraade J, Hagman G. 2003. Evaluation of generic chiral liquid chromatography screens for pharmaceutical analysis. J Chromatogr A 1005:83-101.

[5] Andersson S, Allenmark SG. 2002. Preparative chiral chromatographic resolution of enantiomers in drug discovery. J Biochem Biophys Methods 54:11-23.

[6] Azevedo DCS, Rodrigues AE. 2001. Design methodology and operation of a simulated moving bed reactor for the inversion of sucrose and glucose-fructose separation. Chem Eng J 82:95-107.

[7] Barker PE, Ganetsos G, Ajongwen J, Akintoye A. 1992. Bioreaction separation on continuous chromatographic systems. Chem Eng J 50:B23-B28.

[8] Barker PE, Ganetsos G, Ajongwen NJ. 1993. A novel approach to the production of clinical-grade dextran. J Chem Technol Biotechnol 57:21-26.

[9] Batra R, Gupta MN. 1994. Enhancement of enzyme activity in aqueous-organic solvent mixtures. Biotechnol Lett 16:1059-1064.

[10] Becskei A, Seraphin B, Serrano L. 2001. Positive feedback in eukaryotic gene networks: cell differentiation by graded to binary response conversion. EMBO J 20:2528-2535.

[11] Bentley WE, Mirjalili N, Andersen DC, Davis RH, Kompala DS. 1990. Plasmid-encoded protein: the principal factor in the "Metabolic Burden" associated with recombinant bacteria. Biotechnol Bioeng 35:668-681.

[12] Berthod A, Liu Y, Bagwill C, Armstrong DW. 1996. Facile liquid chromatographic enantioresolution of native amino acids and peptides using a teicoplanin chiral stationary phase. J Chromatogr A 731:123-137.

[13] Blayer S, Woodley JM, Dawson MJ, Lilly MD. 1999. Alkaline biocatalysis for the direct synthesis of *N*-acetyl-D-neuraminic acid (Neu5Ac) from *N*-acetyl-D-glucosamine (GlcNAc). Biotechnol Bioeng 66:131-136.

[14] Bolte J, Demuynck C, Samaki H. 1987. Utilization of enzymes in organic chemistry: transketolase catalyzed synthesis of ketoses. Tetrahedron Lett 28:5525-5528.

[15] Borren T, Schmidt-Traub H. 2004. Comparison of chromatographic reactor concepts. Chem Ing Tech 76:805-814.

[16] Bradford MM. 1976. Rapid and sensitive method for quantitation of microgram quantities of protein utilizing principle of protein-dye binding. Anal Biochem 72:248-254.

[17] Breuer M, Hauer B. 2003. Carbon-carbon coupling in biotransformation. Curr Opin Biotechnol 14:570-576.

[18] Broughton DB. 1968. Molex: case history of a process. Chem Eng Prog 64:60-65.

[19] Broughton DB, Neuzil RW, Pharis JM, Brearley CS. 1970. The parex process for recovering paraxylene. Chem Eng Prog 66:70-75.

[20] Bruno JR. 2004. The economics of SMB. Chim. Oggi 22:32-34.

[21] Bühler B, Bollhalder I, Hauer B, Witholt B, Schmid A. 2003. Use of the two-liquid phase concept to exploit kinetically controlled multistep biocatalysis. Biotechnol Bioeng 81:683-694.

[22] Bühler B, Bollhalder I, Hauer B, Witholt B, Schmid A. 2003. Chemical biotechnology for the specific oxyfunctionalization of hydrocarbons on a technical scale. Biotechnol Bioeng 82:833-842.

[23] Canosa I, Sanchez-Romero JM, Yuste L, Rojo F. 2000. A positive feedback mechanism controls expression of AlkS, the transcriptional regulator of the *Pseudomonas oleovorans* alkane degradation pathway. Molecular Microbiol 35:791-799.

[24] Carrier TA, Keasling JD. 1999. Investigating autocatalytic gene expression systems through mechanistic modeling. J Theoret Biology 201:25-36.

[25] Castro GR, Knubovets T. 2003. Homogeneous biocatalysis in organic solvents and water-organic mixtures. Crit Rev Biotechnol 23:195-231.

[26] Chahid Z, Montet D, Pina M, Bonnot F, Graille J. 1994. Biocatalyzed octylglucoside synthesis from a disaccharide. Biotechnol Lett 16:795-800.

[27] Chao YP, Law WS, Chen PT, Hung WB. 2002. High production of heterologous proteins in *Escherichia coli* using the thermo-regulated T7 expression system. Appl Microbiol Biotechnol 58:446-453.

[28] Chauhan RP, Powell LW, Woodley JM. 1997. Boron-based separations for in situ recovery of L-erythrulose from transketolase-catalyzed condensation. Biotechnol Bioeng 56:345-351.

[29] Cheng LC, Hor LI, Wu JY, Chen TL. 2003. Effect of specific growth rate on the production of a recombinant nuclease by *Escherichia coli*. Biochem Eng J 14:101-107.

[30] Ching CB, Ho C, Hidajat K, Ruthven DM. 1987. Experimental study of a simulated countercurrent adsorption system - 5. Comparison of resin and zeolite absorbents for fructose glucose separation at high concentration. Chem Eng Sci 42:2547-2555.

[31] Choi JH, Keum KC, Lee SY. 2006. Production of recombinant proteins by high cell density culture of *Escherichia coli*. Chem Eng Sci 61:876-885.

[32] Coelho MS, Azevedo DCS, Teixeira JA, Rodrigues A. 2002. Dextran and fructose separation on an SMB continuous chromatographic unit. Biochem Eng J 12:215-221.

[33] Crameri A, Whitehorn EA, Tate E, Stemmer WPC. 1996. Improved green fluorescent protein by molecular evolution using DNA shuffling. Nat Biotechnol 14:315-319.

[34] Crosby J. 1991. Synthesis of optically active compounds: a large scale perspective. Tetrahedron 47:4789-4846.

[35] DeSantis G, Liu JJ, Clark DP, Heine A, Wilson IA, Wong CH. 2003. Structure-based mutagenesis approaches toward expanding the substrate specificity of D-2-deoxyribose-5-phosphate aldolase. Bioorg Med Chem 11:43-52.

[36] Donovan RS, Robinson CW, Glick BR. 1996. Review: Optimizing inducer and culture conditions for expression of foreign proteins under the control of the *lac* promoter. J Industr Microbiol 16:145-154.

[37] Edelkraut F, Brockmann U. 1990. Simultaneous determination of carboxylic acids and carbonyl compounds in estuaries by HPLC. Chromatographia 30:432-435.

[38] Einarsson S, Josefsson B, Lagerkvist S. 1983. Determination of amino acids with 9-Fluorenylmethyl chloroformate and reversed-phase high-performance liquid chromatography. J Chromatogr 282:609-618.

[39] Espelt L, Parella T, Bujons J, Solans C, Joglar J, Delgado A, Clapes P. 2003. Stereoselective aldol additions catalyzed by dihydroxyacetone phosphate-dependent aldolases in emulsion systems: Preparation and structural characterization of linear and cyclic iminopolyols from aminoaldehydes. Chem Eur J 9:4887-4899.

[40] Espelt L, Bujons J, Parella T, Calveras J, Joglar J, Delgado A, Clapes P. 2005. Aldol additions of dihydroxyacetone phosphate to N-Cbz-amino aldehydes catalyzed by L-fuculose-1-phosphate aldolase in emulsion systems: Inversion of stereoselectivity as a function of the acceptor aldehyde. Chem Eur J 11:1392-1401.

[41] Fernandez MM, Clark DS, Blanch HW. 1991. Papain kinetics in the presence of a water-miscible organic solvent. Biotechnol Bioeng 37:967-972.

[42] Fessner W-D. 2000. Enzymatic asymmetric synthesis using aldolases. In: Patel RN, editor. Stereoselective Biocatalysis. p 239-265.

[43] Fleischmann RD, Adams MD, White O, Clayton RA, Kirkness EF, Kerlavage AR, Bult CJ, Tomb JF, Dougherty BA, Merrick JM and others. 1995. Whole-genome random sequencing and assembly of *Haemophilus influenzae* Rd. Science 269:496-512.

[44] Flickinger MC, Rouse MP. 1993. Sustaining protein synthesis in the absence of rapid cell division: an investigation of plasmid-encoded protein expression in *Escherichia coli* during very slow growth. Biotechnol Prog 9:555-572.

[45] Food and Drug Administration. 1992. FDA's policy statement for the development of new stereoisomeric drugs. Chirality 4:338-340.

[46] Fotheringham I. 2000. Engineering biosynthetic pathways: new routes to chiral amino acids. Curr Opin Chem Biol 4:120-124.

[47] Francotte ER. 2001. Enantioselective chromatography as a powerful alternative for the preparation of drug enantiomers. J Chromatogr A 906:379-397.

[48] Fukumura T, Bhandari VM, Kitakawa A, Yonemoto T. 2000. Complete separation of ternary mixture of amino acids using continuous rotating annular chromatography with partial recycling of effluent. J Chem Eng Jpn 33:778-784.

[49] Gijsen HJM, Wong CH. 1994. Unprecedented asymmetric aldol reactions with 3 aldehyde substrates catalyzed by 2-deoxyribose-5-phosphate aldolase. J Am Chem Soc 116:8422-8423.

[50] Glieder A, Weis R, Skranc W, Pöchlauer P, Dreveny I, Majer S, Wubbolts M, Schwab H, Gruber K. 2003. Comprehensive step-by-step engineering of an (R)-hydroxynitrile lyase for large-scale asymmetric synthesis. Angew Chem Int Ed Engl 42:4815-4818.

[51] Goldberg RN, Tewari YB. 1995. Thermodynamics of enzyme-catalyzed reactions: part 4. Lyases. J Phys Chem Ref Data 24:1669-1698.

[52] Goldberg RN, Tewari YB, Bhat TN. 2004. Thermodynamics of enzyme-catalyzed reactions - a database for quantitative biochemistry. Bioinformatics 20:2874-2877.

[53] Granström TB, Takata G, Morimoto K, Leisola M, Izumori K. 2005. L-Xylose and L-lyxose production from xylitol using *Alcaligenes* 701B strain and immobilized L-rhamnose isomerase enzyme. Enzyme Microb Tech 36:976-981.

[54] Greenberg WA, Varvak A, Hanson SR, Wong K, Huang HJ, Chen P, Burk MJ. 2004. Development of an efficient, scalable, aldolase-catalyzed process for enantioselective synthesis of statin intermediates. Proc Natl Acad Sci USA 101:5788-5793.

[55] Grill CA, Miller L, Yan TQ. 2004. Resolution of a racemic pharmaceutical intermediate - A comparison of preparative HPLC, steady state recycling, and simulated moving bed. J Chromatogr A 1026:101-108.

[56] Grund A, Shapiro J, Fennewald M, Bacha P, Leahy J, Markbreiter K, Nieder M, Toepfer M. 1975. Regulation of alkane oxidation in *Pseudomonas putida*. J Bacteriol 123:546-556.

[57] Gustavsson B, Betner I. 1990. Fully automated amino acid analysis for protein and peptide hydrolysates by precolumn derivatization with 9-fluorenyl methylchloroformate and 1-aminoadamantane. J Chromatogr 507:67-77.

[58] Harder MPF, Sanders EA, Wingender E, Deckwer WD. 1994. Production of human parathyroid hormone by recombinant *Escherichia coli* TG1 on synthetic medium. J Biotechnol 32:157-164.

[59] Hashimoto K, Adachi S, Noujima H, Ueda Y. 1983. A new process combining adsorption and enzyme reaction for producing higher-fructose syrup. Biotechnol Bioeng 25:2371-2393.

[60] Häusler H, Stütz AE. 2001. D-xylose (D-glucose) isomerase and related enzymes in carbohydrate synthesis. Top Curr Chem 215:77-114.

[61] Helfferich FG. 1995. Ion Exchange. New York: Dover Publications INC.

[62] Hellmuth K, Korz DJ, Sanders EA, Deckwer WD. 1994. Effect of growth rate on stability and gene expression of recombinant plasmids during continuous and high cell density cultivation of *Escherichia coli* TG1. J Biotechnol 32:289-298.

[63] Hermann T. 2003. Industrial production of amino acids by coryneform bacteria. J Biotechnol 104:155-172.

[64] Horn U, Strittmatter W, Krebber A, Knupfer U, Kujau M, Wenderoth R, Muller K, Matzku S, Pluckthun A, Riesenberg D. 1996. High volumetric yields of functional dimeric miniantibodies in *Escherichia coli*, using an optimized expression vector and high-cell-density fermentation under non-limited growth conditions. Appl Microbiol Biotechnol 46:524-532.

[65] Howard AJ, Carta G, Byers CH. 1988. Separation of sugars by continuous annular chromatography. Ind Eng Chem Res 27:1873-1882.

[66] Itoh H, Sato T, Takeuchi T, Khan AR, Izumori K. 1995. Preparation of D-sorbose from D-tagatose by immobilized D-tagatose 3-epimerase. J Ferment Bioeng 79:184-185.

[67] Jackson BG, Pedersen SW, Fisher JW, Misner JW, Gardner JP, Staszak MA, Doecke C, Rizzo J, Aikins J, Farkas E and others. 2000. Enantioselective syntheses of 1-carbacephalosporins from chemoenzymically derived β-hydroxy-α-amino acids: Applications to the total synthesis of carbacephem antibiotic Loracarbef. Tetrahedron 56:5667-5677.

[68] Jana S, Deb JK. 2005. Strategies for efficient production of heterologous proteins in *Escherichia coli*. Appl Microbiol Biotechnol 67:289-298.

[69] Jensen EB, Carlsen S. 1990. Production of recombinant human growth-hormone in *Escherichia coli*: expression of different precursors and physiological effects of glucose, acetate, and salts. Biotechnol Bioeng 36:1-11.

[70] Juza M, Mazzotti M, Morbidelli M. 2000. Simulated moving-bed chromatography and its application to chirotechnology. Trends Biotechnol 18:108-118.

[71] Keasling JD. 1999. Gene-expression tools for the metabolic engineering of bacteria. Trends Biotechnol 17:452-460.

[72] Khlebnikov A, Risa O, Skaug T, Carrier TA, Keasling JD. 2000. Regulatable arabinose-inducible gene expression system with consistent control in all cells of a culture. J Bacteriol 182:7029-7034.

[73] Khlebnikov A, Datsenko KA, Skaug T, Wanner BL, Keasling JD. 2001. Homogeneous expression of the P-BAD promoter in *Escherichia coli* by constitutive expression of the low-affinity high-capacity AraE transporter. Microbiology 147:3241-3247.

[74] Khlebnikov A, Keasling JD. 2002. Effect of lacY expression on homogeneity of induction from the P-tac and P-trc promoters by natural and synthetic inducers. Biotechnol Prog 18:672-674.

[75] Khmelnitsky YL, Mozhaev VV, Belova AB, Sergeeva MV, Martinek K. 1991. Denaturation capacity: a new quantitative criterion for selection of organic solvents as reaction media in biocatalysis. Eur J Biochem 198:31-41.

[76] Kim H-J, Ryu S-A, Kim PS, Oh D-K. 2003. A feasible enzymatic process for D-tagatose production by an immobilized thermostable L-arabinose isomerase in a packed-bed bioreactor. Biotechnol Progr 19:400-404.

[77] Kim MJ, Hennen WJ, Sweers HM, Wong CH. 1988. Enzymes in carbohydrate synthesis: *N*-acetylneuraminic acid aldolase catalyzed reactions and preparation of *N*-acetyl-2-deoxy-D-neuraminic acid derivatives. J Am Chem Soc 110:6481-6486.

[78] Kimura T, Vassilev VP, Shen G-J, Wong C-H. 1997. Enzymatic synthesis of β-hydroxy-α-amino acids based on recombinant D- and L-threonine aldolases. J Am Chem Soc 119:11734-11742.

[79] Kitakawa A, Yamanishi Y, Yonemoto T, Tadaki T. 1995. Modeling and simulation of continuous rotating annular ion-exchange chromatography for separation of amino acids. Sep Sci Technol 30:3089-3110.

[80] Klibanov AM. 2001. Improving enzymes by using them in organic solvents. Nature 409:241-246.

[81] Kok M, Oldenhuis R, van der Linden MP, Raatjes P, Kingma J, van Lelyveld PH, Witholt B. 1989. The Pseudomonas oleovorans alkane hydroxylase gene: Sequence and expression. J Biol Chem 264:5435-41.

[82] Korz DJ, Rinas U, Hellmuth K, Sanders EA, Deckwer WD. 1995. Simple fed-batch technique for high cell density cultivation of *Escherichia coli*. J Biotechnol 39:59-65.

[83] Kragl U, Niedermeyer U, Kula MR, Wandrey C. 1990. Engineering aspects of enzyme engineering - continuous asymmetric C-C bond formation in an enzyme-membrane-reactor. Ann NY Acad Sc 613:167-175.

[84] Kragl U, Gygax D, Ghisalba O, Wandrey C. 1991. Enzymatic two-step synthesis of *N*-acetylneuraminic acid in the enzyme membrane reactor. Angew Chem Int Ed Engl 30:827-828.

[85] Kragl U, Kruse W, Hummel W, Wandrey C. 1996. Enzyme engineering aspects of biocatalysis: Cofactor regeneration as example. Biotechnol Bioeng 52:309-319.

[86] Kragl U, Eckstein M, Kaftzik N. 2002. Enzyme catalysis in ionic liquids. Curr Opin Biotechnol 13:565-571.

[87] Kreuzman AJ, Zock JM, Dotzlaf JE, Vicenzi JT, Queener SW, Yeh WK. 1997. Enzymatic synthesis of diastereospecific carbacephem intermediates using serine hydroxymethyltransferase. J Ind Microbiol Biotechnol 19:369-77.

[88] Kyslik P, Dobisova M, Maresova H, Sobotkova L. 1993. Plasmid burden in chemostat culture of *Escherichia coli* - its effect on the selection for overproducers of host enzymes. Biotechnol Bioeng 41:325-329.

[89] Lee SB, Bailey JE. 1984. Analysis of growth rate effects on productivity of recombinant *Escherichia coli* populations using molecular mechanism models. Biotechnol Bioeng 26:66-73.

[90] Lee SK, Keasling JD. 2005. A propionate-inducible expression system for enteric bacteria. Appl Environ Microbiol 71:6856-6862.

[91] Lee SK, Newman JD, Keasling JD. 2005. Catabolite repression of the propionate catabolic genes in *Escherichia coli* and *Salmonella enterica*: Evidence for involvement of the cyclic AMP receptor protein. J Bacteriol 187:2793-2800.

[92] Lee SY. 1996. High cell-density culture of *Escherichia coli*. Trends Biotechnol 14:98-105.

[93] Leuchtenberger W, Huthmacher K, Drauz K. 2005. Biotechnological production of amino acids and derivatives: current status and prospects. Appl Microbiol Biotechnol 69:1-8.

[94] Liese A, Karutz M, Kamphuis J, Wandrey C, Kragl U. 1996. Enzymatic resolution of 1-phenyl-1,2-ethanediol by enantioselective oxidation: Overcoming product inhibition by continuous extraction. Biotechnol Bioeng 51:544-550.

[95] Liese A. 2002. Replacing Chemical Steps by Biotransformations: Industrial Application and Processes Using Biocatalysis. In: Drauz K, Waldmann H, editors. Enzyme Catalysis in Organic Synthesis. Weinheim: Wiley-VCH. p 1419-1459.

[96] Liese A, Seelbach K, Wandrey C. 2006. Industrial biotransformation. Weinheim: Wiley-VCH.

[97] Liu J-Q, Odani M, Dairi T, Itoh N, Shimizu S, Yamada H. 1999. A new route to L-*threo*-3-[4-(methylthio)phenylserine], a key intermediate for the synthesis of antibiotics: recombinant low-specificity D-threonine aldolase-catalyzed stereospecific resolution. Appl Microbiol Biotechnol 51:586-591.

[98] Liu J-Q, Dairi T, Itoh N, Kataoka M, Shimizu K, Yamada H. 2000. Diversity of microbial threonine aldolases and their application. J Mol Catal B: Enz 10:107-115.

[99] Liu JQ, Odani M, Yasuoka T, Dairi T, Itoh N, Kataoka M, Shimizu S, Yamada H. 2000. Gene cloning and overproduction of low-specificity D-threonine aldolase from *Alcaligenes xylosoxidans* and its application for production of a key intermediate for parkinsonism drug. Appl Microbiol Biotechnol 54:44-51.

[100] Lode F, Houmard M, Migliorini C, Mazzotti M, Morbidelli M. 2001. Continuous reactive chromatography. Chem Eng Sci 56:269-291.

[101] Looser V, Hammes F, Keller M, Berney M, Kovar K, Egli T. 2005. Flow-cytometric detection of changes in the physiological state of *E. coli* expressing a heterologous membrane protein during carbon-limited fedbatch cultivation. Biotechnol Bioeng 92:69-78.

[102] Lorenz P, Eck J. 2005. Metagenomics and industrial applications. Nature Rev Microbiol 3:510-516.

[103] Lozano P, deDiego T, Iborra JL. 1996. Influence of water-miscible aprotic solvents on α-chymotrypsin stability. Biotechnol Prog 12:488-493.

[104] Ludemann-Hombourger O, Nicoud RM, Bailly M. 2000. The "VARICOL" process: A new multicolumn continuous chromatographic process. Sep Sci Technol 35:1829-1862.

[105] Lye GJ, Woodley JM. 1999. Application of *in situ* product-removal techniques to biocatalytic processes. Trends Biotechnol 17:395-402.

[106] Machajewski TD, Wong CH. 2000. The catalytic asymmetric aldol reaction. Angew Chem Int Ed Engl 39:1352-1374.

[107] Mahmoudian M, Noble D, Drake CS, Middleton RF, Montgomery DS, Piercey JE, Ramlakhan D, Todd M, Dawson MJ. 1997. An efficient process for production of *N*-acetylneuraminic acid using *N*-acetylneuraminic acid aldolase. Enzyme Microb Technol 20:393-400.

[108] Majors RE. 2004. Developments in preparative-scale chromatography - Columns and accessories. LCGC Eur 17:630-638.

[109] Marquardt W. 2005. Model-based experimental analysis of kinetic phenomena in multi-phase reactive systems. Chem Eng Res Des 83:561-573.

[110] May O, Verseck S, Bommarius A, Drauz K. 2002. Development of dynamic kinetic resolution processes for biocatalytic production of natural and nonnatural L-amino acids. Org Process Res Dev 6:452-457.

[111] Mazzotti M, Storti G, Morbidelli M. 1997. Optimal operation of simulated moving bed units for nonlinear chromatographic separations. J Chromatogr A 769:3-24.

[112] Means GE, Feeney RE. 1995. Reductive alkylation of proteins. Anal Biochem 224:1-16.

[113] Meissner JP, Carta G. 2002. Continuous regioselective enzymatic esterification in a simulated moving bed reactor. Ind Eng Chem Res 41:4722-4732.

[114] Mensah P, Gainer JL, Carta G. 1998. Adsorptive control of water in esterification with immobilized enzymes: I. Batch reactor behavior. Biotechnol Bioeng 60:434-444.

[115] Mensah P, Carta G. 1999. Adsorptive control of water in esterification with immobilized enzymes. Continuous operation in a periodic counter-current reactor. Biotechnol Bioeng 66:137-146.

[116] Menzella HG, Gramajo HC. 2004. Recombinant protein production in high cell density cultures of *Escherichia coli* with galactose as a gratuitous inducer. Biotechnol Prog 20:1263-1266.

[117] Miller L, Grill C, Yan T, Dapremont O, Huthmann E, Juza M. 2003. Batch and simulated moving bed chromatographic resolution of a pharmaceutical racemate. J Chromatogr A 1006:267-280.

[118] Neubauer P, Winter J. 2001. Expression and fermentation strategies for recombinant protein production in *Escherichia coli*. In: Merten O-W, Mattanovich D, Lang C, Larsson G, Neubauer P, Porro D, Postma P, Teixeira de Mattos J, Cole JA, editors. Recombinant protein production with prokaryotic and eukaryotic cells: Kluwer Academic Publishers.

[119] Nicoud RM. 1992. The simulated moving bed: A powerful chromatographic process. LC-GC Intl 5:43-47.

[120] Nicoud RM. 1999. The separation of optical isomers by simulated moving bed chromatography. Part II. Pharm Technol Eur 11:28-34.

[121] Nicoud RM. 2000. Simulated moving-bed chromatography for biomolecules. In: Ahuja S, editor. Handbook of bioseparations: Academic Press. p 475-509.

[122] Oh M-K, Liao JC. 2000. DNA microarray detection of metabolic repsonses to protein overproduction in *Escherichia coli*. Metab Eng 2:201-209.

[123] Otto K, Hofstetter K, Rothlisberger M, Witholt B, Schmid A. 2004. Biochemical characterization of StyAB from Pseudomonas sp strain VLB120 as a two-component flavin-diffusible monooxygenase. J Bacteriol 186:5292-5302.

[124] Ozbudak EM, Thattai M, Lim HN, Shraiman BI, van Oudenaarden A. 2004. Multistability in the lactose utilization network of *Escherichia coli*. Nature 427:737-740.

[125] Pais LS, Loureiro JM, Rodrigues AE. 1998. Modeling strategies for enantiomers separation by SMB chromatography. AIChE J 44:561-569.

[126] Panke S, Meyer A, Huber CM, Witholt B, Wubbolts MG. 1999. An alkane-responsive expression system for the production of fine chemicals. Appl Environ Microbiol 65:2324-2332.

[127] Panke S, Wubbolts MG, Schmid A, Witholt B. 2000. Production of enantiopure styrene oxide by recombinant *Escherichia coli* synthesizing a two-component styrene monooxygenase. Biotechnol Bioeng 69:91-100.

[128] Panke S, Wubbolts M. 2005. Advances in biocatalytic synthesis of pharmaceutical intermediates. Curr Op Chem Biol 9:188-194.

[129] Pedeferri M, Zenoni G, Mazzotti M, Morbidelli M. 1999. Experimental analysis of a chiral separation through simulated moving bed chromatography. Chem Eng Sci 54:3735-3748.

[130] Pietrzyk DJ, Cahill WJ, Stodola JD. 1982. Preparative liquid chromatographic separation of amino acids and peptides on Amberlite XAD-4. J Liq Chromatogr 5:443-461.

[131] Pynnonen B. 1998. Simulated moving bed processing: escape from the high-cost box. J Chromatogr A 827:143-160.

[132] Reetz MT. 2001. Combinatorial and evolution-based methods in the creation of enantioselective catalysts. Angew Chem Int Ed Engl 40:284-310.

[133] Reiling HE, Laurila H, Fiechter A. 1985. Mass culture of *Escherichia coli*: medium development for low and high density cultivation of *Escherichia coli* B/r in minimal and complex media. J Biotechnol 2:191-206.

[134] Riesenberg D, Menzel K, Schulz V, Schumann K, Veith G, Zuber G, Knorre WA. 1990. High cell density fermentation of recombinant *Escherichia coli* expressing human interferon alpha-1. Appl Microbiol Biotechnol 34:77-82.

[135] Roels JA. 1983. energetics and kinetics in biotechnology: Elsevier Biomedical Press.

[136] Rothen SA, Sauer M, Sonnleitner B, Witholt B. 1998. Growth characteristics of *Escherichia coli* HB101 pGEc47 on defined medium. Biotechnol Bioeng 58:92-100.

[137] Saeed A, Young DW. 1992. Synthesis of L-β-hydroxyaminoacids using serine hydroxymethyltransferase. Tetrahedron 48:2507-2514.

[138] Salagnad C, Godde A, Ernst B, Kragl U. 1997. Enzymatic large-scale production of 2-keto-3-deoxy-D-glycero-D-galacto-nonopyranulosonic acid in enzyme membrane reactors. Biotechnol Prog 13:810-813.

[139] Sambrook J, Russell DW. 2001. Molecular cloning: a laboratory manual. Cold Spring Harbor, N.Y.: Cold Spring Harbor Laboratory.

[140] Samland AK, Sprenger GA. 2006. Microbial aldolases as C-C bonding enzymes - unknown treasures and new developments. Appl Microbiol Biotechnol 71:253-264.

[141] Sanden AM, Larsson G. 2001. Control and optimisation of cellular bottlenecks in recombinant protein production. In: Merten O-W, Mattanovich D, Lang C, Larsson G, Neubauer P, Porro D, Postma P, Teixeira de Mattos J, Cole JA, editors. Recombinant protein production with prokaryotic and eukaryotic cells: Kluwer Academic Publishers. p 189-194.

[142] Sanden AM, Prytz I, Tubulekas I, Forberg C, Le H, Hektor A, Neubauer P, Pragai Z, Harwood C, Ward A and others. 2003. Limiting factors in *Escherichia coli* fed-batch production of recombinant proteins. Biotechnol Bioeng 81:158-166.

[143] Schirch L. 1982. Serine hydroxymethyltransferase. Adv Enzymol Relat Areas Mol Biol 53:83-112.

[144] Schirch V, Hopkins S, Villar E, Angelaccio S. 1985. Serine hydroxymethyltransferase from *Escherichia coli*: purification and properties. J Bacteriol 163:1-7.

[145] Schmid A, Dordick JS, Hauer B, Kiener A, Wubbolts M, Witholt B. 2001. Industrial biocatalysis today and tomorrow. Nature 409:258-268.

[146] Schnell B, Faber K, Kroutil W. 2003. Enzymatic racemisation and its application to synthetic biotransformations. Adv Synth Catal 345:653-666.

[147] Schoemaker HE, Mink D, Wubbolts MG. 2003. Dispelling the myths - Biocatalysis in industrial synthesis. Science 299:1694-1697.

[148] Schramm H, Kaspereit M, Kienle A, Seidel-Morgenstern A. 2003. Simulated moving bed process with cyclic modulation of the feed concentration. J Chromatogr A 1006:77-86.

[149] Schulte M, Britsch L, Strube J. 2000. Continuous preparative liquid chromatography in the downstream processing of biotechnological products. Acta Biotechnol 20:3-15.

[150] Sheldon RA. 1993. Chirotechnology: Industrial synthesis of optically active compounds. New York: Marcel Dekker, INC.

[151] Shieh MT, Barker PE. 1995. Saccharification of modified starch to maltose in a semicontinuous countercurrent chromatographic reactor-separator (SCCR-S). J Chem Technol Biotechnol 63:125-134.

[152] Shieh MT, Barker PE. 1996. Combined bioreaction and separation in a simulated counter-current chromatographic bioreactor-separator for the hydrolysis of lactose. J Chem Technol Biotechnol 66:265-278.

[153] Shin CS, Hong MS, Bae CS, Lee J. 1997. Enhanced production of human mini-proinsulin in fed-batch cultures at high cell density of *Escherichia coli* BL21(DE3) [pET-3aT2M2]. Biotechnol Prog 13:249-257.

[154] Siegele DA, Hu JC. 1997. Gene expression from plasmids containing the araBAD promoter at subsaturating inducer concentrations represents mixed populations. Proc Natl Acad Sci USA 94:8168-8172.

[155] Silvestri MG, Desantis G, Mitchell M, Wong CH. 2003. Asymmetric aldol reactions using aldolases. Top Stereochem 23:267-342.

[156] Smits THM, Seeger MA, Witholt B, van Beilen JB. 2001. New alkane-responsive expression vectors for *Escherichia coli* and *Pseudomonas*. Plasmid 46:16-24.

[157] Staijen IE, Marcionelli R, Witholt B. 1999. The $P_{alkBFGHJKL}$ promoter is under carbon catabolite repression control in *Pseudomonas oleovorans* but not in *Escherichia coli* *alk*$^{+}$ recombinants. J Bacteriol 181:1610-1616.

[158] Stampfer W, Kosjek B, Moitzi C, Kroutil W, Faber K. 2002. Biocatalytic asymmetric hydrogen transfer. Angew Chem Int Ed Engl 41:1014-1017.

[159] Sticher P, Jaspers MCM, Stemmler K, Harms H, Zehnder AJB, van der Meer JR. 1997. Development and characterization of a whole-cell bioluminescent sensor for bioavailable middle-chain alkanes in contaminated groundwater samples. Appl Environ Microbiol 63:4053-4060.

[160] Straathof AJJ. 2001. Development of a computer program for analysis of enzyme kinetics by progress curve fitting. J Mol Catal B-Enzym 11:991-998.

[161] Straathof AJJ, Panke S, Schmid A. 2002. The production of fine chemicals by biotransformations. Curr Opin Biotechnol 13:548-556.

[162] Ströhlein G, Mazzotti M, Morbidelli M. 2005. Optimal operation of simulated-moving-bed reactors for nonlinear adsorption isotherms and equilibrium reactions. Chem Eng Sci 60:1525-1533.

[163] Strube J, Haumreisser S, Schmidt-Traub H, Schulte M, Ditz R. 1998. Comparison of batch elution and continuous simulated moving bed chromatography. Org Process Res Dev 2:305-319.

[164] Strube J, Schmidt-Traub H, Schulte M. 1998. Design, operation, and economics of chromatographic separations. Chem Ing Tech 70:1271-1279.

[165] Studier FW, Rosenberg AH, Dunn JJ, Dubendorff JW. 1990. Use of T7 Rna-Polymerase to Direct Expression of Cloned Genes. Methods Enzymol 185:60-89.

[166] Stulke J, Hillen W. 1999. Carbon catabolite repression in bacteria. Curr Opin Microbiol 2:195-201.

[167] Summers DK, Sherratt DJ. 1984. Multimerization of High Copy Number Plasmids Causes Instability - Cole1 Encodes a Determinant Essential for Plasmid Monomerization and Stability. Cell 36:1097-1103.

[168] Tachibana K, Ohnishi A. 2001. Reversed-phase liquid chromatographic separation of enantiomers on polysaccharide type chiral stationary phases. J Chromatogr A 906:127-154.

[169] Takeshita K, Suga A, Takada G, Izumori K. 2000. Mass production of D-psicose from D-fructose by a continuous bioreactor system using immobilized D-tagatose 3-epimerase. J Biosci Bioeng 90:453-455.

[170] Turner NJ. 2000. Applications of transketolases in organic synthesis. Curr Opin Biotechnol 11:527-531.

[171] Ulevitch RJ, Kallen RG. 1977. Purification and characterization of pyridoxal 5'-phosphate dependent serine hydroxymethylase from lamb liver and its action upon β-phenylserines. Biochemistry 16:5342-5350.

[172] van Beilen JB, Wubbolts M, Witholt B. 1994. Genetics of alkane oxidation by *Pseudomonas oleovorans*. Biodegradation 5:161-174.

[173] van Beilen JB, Panke S, Lucchini S, Franchini AG, Rothlisberger M, Witholt B. 2001. Analysis of *Pseudomonas putida* alkane-degradation gene clusters and flanking insertion sequences: evolution and regulation of the *alk* genes. Microbiology 147:1621-1630.

[174] van Rantwijk F, Oosterom MWV, Sheldon RA. 1999. Glycosidase-catalysed synthesis of alkyl glycosides. J Mol Catal B: Enzym 6:511-532.

[175] Venter JC, Remington K, Heidelberg JF, Halpern AL, Rusch D, Eisen JA, Wu DY, Paulsen IT, Nelson KE, Nelson WC and others. 2004. Environmental genome shotgun sequencing of the Sargasso Sea. Science 304:66-74.

[176] Vic G, Crout DHG. 1995. Synthesis of allyl and benzyl β-D-glucopyranosides, and allyl β-D-galactopyranoside from D-glucose or D-galactose and the corresponding alcohol using almond β-D-glucosidase. Carbohyd Res 279:315-319.

[177] Wandrey C, Liese A, Kihumbu D. 2000. Industrial biocatalysis: Past, present, and future. Org Process Res Dev 4:286-290.

[178] Wegman MA, Janssen MHA, van Rantwijk F, Sheldon RA. 2001. Towards biocatalytic synthesis of β-lactam antibiotics. Adv Synth Catal 343:559-576.

[179] Weiss J. 2004. Handbook of ion chromatography. Weinheim: Wiley-VCH.

[180] Welstein H, Sauer C. 1984. Separation of glucose and fructose: effects of resin characteristics on separation. In: Naden D, Streat M, editors. Ion Exchange Technology. Chichester: Ellis Horwood Limited. p 463-471.

[181] Wichmann R, Wandrey C, Buckmann AF, Kula MR. 1981. Continuous enzymatic transformation in an enzyme membrane reactor with simultaneous NAD(H) regeneration. Biotechnol Bioeng 23:2789-2802.

[182] Wöltinger J, Drauz K, Bommarius AS. 2001. The membrane reactor in the fine chemicals industry. Appl Catal A - General 221:171-185.

[183] Wöltinger J, Karau A, Leuchtenberger W, Drauz K. 2005. Membrane reactors at Degussa. Adv Biochem Eng/Biotechnol 92:289-316.

[184] Wong C-H; Scripps Research Institute, assignee. 1998. Method for synthesiszing 2-ketoaldonic acids patent US 5.759.825.

[185] Woodhall T, Williams G, Berry A, Nelson A. 2005. Creation of a tailored aldolase for the parallel synthesis of sialic acid mimetics. Angew Chem Int Ed Engl 44:2109-2112.

[186] Wu DJ, Xie Y, Ma Z, Wang NHL. 1998. Design of simulated moving bed chromatography for amino acid separations. Ind Eng Chem Res 37:4023-4035.

[187] Xiao TL, Armstrong DW. 2003. Enantiomeric separations by HPLC using macrocyclic glycopetide-based stationary phases. In: Gübitz G, Schmid MG, editors. Chiral Separations: Methods and Protocols. Totowa, NJ: Humana Press. p 113-170.

[188] Xie Y, Wu DJ, Ma ZD, Wang NHL. 2000. Extended standing wave design method for simulated moving bed chromatography: linear systems. Ind Eng Chem Res 39:1993-2005.

[189] Yang YJ, Lee CH, Koo YM. 2004. Separation of amino acids by simulated moving bed using competitive Langmuir isotherm. Biotechnol Bioprocess Eng 9:331-338.

[190] Yildirim S, Zezula J, Hudlicky T, Witholt B, Schmid A. 2004. Asymmetric dihydroxylation of cinnamonitrile to trans-3-[(5S,6R)-5,6-dihydroxycyclohexa-1,3-dienyl]-acrylonitrile using chlorobenzene dioxygenase in Escherichia coli (pTEZ30). Adv Synth Catal 346:933-942.

[191] Yildirim S, Franko TT, Wohlgemuth R, Kohler HPE, Witholt B, Schmid A. 2005. Recombinant chlorobenzene dioxygenase from Pseudomonas sp P51: A biocatalyst for regioselective oxidation of aromatic nitriles. Adv Synth Catal 347:1060-1072.

[192] Yu Q, Yang J, Wang NHL. 1987. Multicomponent ion-exchange chromatography for separating amino acid mixtures. React Polym 6:33-44.

[193] Yun HS, Hong J, Lim HC. 1991. Analysis of functioning ribosome content in *Escherichia coli* at different growth rates. Biotechnol Tech 5:471-474.

[194] Yun HS, Hong J, Lim HC. 1996. Regulation of ribosome synthesis in *Escherichia coli*: effects of temperature and dilution rate changes. Biotechnol Bioeng 52:615-624.

[195] Yuste L, Canosa I, Rojo F. 1998. Carbon-source-dependent expression of the *PalkB* promoter from the *Pseudomonas oleovorans* alkane degradation pathway. J Bacteriol 180:5218-5226.

[196] Zabriskie DW, Arcuri EJ. 1986. Factors Influencing Productivity of Fermentations Employing Recombinant Microorganisms. Enzyme Microb Technol 8:706-717.

[197] Zhang T, Kientzy C, Franco P, Ohnishi A, Kagamihara Y, Kurosawa H. 2005. Solvent versatility of immobilized 3,5-dimethylphenylcarbamate of amylose in enantiomeric separations by HPLC. J Chromatogr A 1075:65-75.

[198] Zhang ZY, Mazzotti M, Morbidelli M. 2003. PowerFeed operation of simulated moving bed units: changing flow-rates during the switching interval. J Chromatogr A 1006:87-99.

Curriculum Vitae

Stefan Klaus Makart

Born:	30.12.1973 in Luzern, Switzerland
Citizen:	Gempen (SO), Switzerland
Marital status:	Single

Education:

1980-1986	Primary school, Emmenbrücke, Switzerland
1986-1993	Kantonsschule Reussbühl, Luzern, Switzerland Matura Typus B
1994-2000	Studies in biology, University of Zurich, Zurich, Switzerland graduation as Dipl. Bot.
2002-2007	PhD student in the group of Prof. Dr. Sven Panke, ETH Zurich, Switzerland

Acknowledgements

First of all I would like to thank Prof. Dr. Sven Panke for supervising my work. I am very grateful to him for his support and many interesting discussions, and especially for giving me the opportunity to take part in building up the Bioprocess Lab.

Many thanks to Prof. Dr. Marco Mazzotti and Prof. Dr. John M. Woodley to take the time and effort acting as co-referees of my thesis.

Special thanks go to Matthias Bechtold, who also worked on the integration of SMB and biotransformation in his doctoral thesis. He helped me a lot in modelling and chromatography issues. Thanks Matthias, and it was a pleasure to share the office with you.

André, Dominique, Gian Andri, Carlos and Martin were students who contributed to the success of this thesis and I like to thank all of them for the effort they have put in their work.

I like to thank all the people of the BPL-group for their advice and helpful discussions, and of course for all the diverting chats in the lab. So, thanks to Agnes, Alex, Andy, Anne, Eve, Frauke, Giorgia, Giovanni, Laetitia, Marcel, Maria, Marta, Martin, Matthias H., Michael, Oliver, Patrick, René, Silvia and Simone.

I would like to thank Arvind, Galatea and Stefanie from the SPL group for the helpful discussions on packing chromatography columns and on SMB.

Finally I thank all my colleagues at IPE for making my time at ETH a very enjoyable and interesting experience.

Many thanks go to my parents who supported and encouraged me during the – long – time of my studies.